Universidade de Aveiro Departamento de Engenharia Mecânica
2019

João Henrique Gamito Trindade Carvalho Cachão

Performance of a capacitive monitoring system for instrumented bone implants

Desempenho de sistema de monitorização capacitivo em implante ósseo instrumentado

Universidade de Aveiro Departamento de Engenharia Mecânica
2019

João Henrique Gamito Trindade Carvalho Cachão

Performance of a capacitive monitoring system for instrumented bone implants

Desempenho de sistema de monitorização capacitivo em implante ósseo instrumentado

Dissertação apresentada à Universidade de Aveiro para cumprimento dos requisitos necessários à obtenção do grau de Mestre em Engenharia Mecânica, realizada sob orientação científica do Doutor Marco Paulo Soares dos Santos, Professor Auxiliar Convidado do Departamento de Engenharia Mecânica da Universidade de Aveiro e do Doutor António Manuel de Amaral Monteiro Ramos, Professor Auxiliar do Departamento de Engenharia Mecânica da Universidade de Aveiro.

This work was funded by Portuguese Foundation for Science and Technology (grant reference SFRH/BPD/117475/2016, project reference POCI-01-0145-FEDER-031132 and POCI-01-0145-FEDER-032486). It was also supported by the Centre for Mechanical Technology & Automation (UID/EMS/00481/2019-FCT and CENTRO-01-0145-FEDER-022083).

o júri / the jury

presidente / president

Prof. Doutor Miguel Armando Riem de Oliveira
Professor Auxiliar da Universidade de Aveiro

Doutor José António de Oliveira Simões
Equiparado a Professor Coordenador c/ Agregação da Escola Superior de Artes e Design de Matosinhos

Prof. Doutor Marco Paulo Soares dos Santos
Professor Auxiliar Convidado da Universidade de Aveiro (orientador)

agradecimentos / acknowledgements

My Family. For always supporting me and making sure I had everything I needed, for providing and giving me the opportunity to pursue what I want. The ones in the south margin. For always being there, ready to listen and support.
The northern ones. For welcoming me and making me feel at home.

Special thanks to my advisor Marco Soares dos Santos and co-advisor António Ramos for the guidance, help and insight provided along these months. For providing comments and suggestions, support and encouragement.

Thanks to António Festas for manufactoring the needed parts, Paulo Martins for the fabrication of the printed circuit and Rui Heitor for the help with the sensor assembly and other works. Also, my appreciation to the Department of Electronics, Telecommunications and Informatics (DETI) from University of Aveiro for their disposition in the fabrication of the printed circuits. Lastly, thanks to Bom Talho for providing the bone specimens.

keywords Bioelectronic device, Instrumented implant, Bone-implant interface, Capacitive technology, Osseointegration

abstract Musculoskeletal disorders are becoming an ever-growing societal burden and, as a result, millions of bone replacements surgeries are performed per year worldwide. Although total joint replacements are recognized among the most successful surgeries of the last century, implant failure rates exceeding 10% are still reported. These numbers highlight the necessity of technologies to provide an accurate monitoring of the bone-implant interface state. This work aims to identify the performance of an instrumented implant to monitor implant stability using a planar capacitive technology. A 5x10x0.8 mm printed circuit with two 5x2 mm electrodes was fabricated to be integrated in an implantable device, with the objective of assessing the effect of a fully implantation into a biological specimen. The implant was fabricated with a conic geometry, to achieve a press-fit fixation, with 55 mm of length and a minimum/maximum diameters of 12 and 15 mm, respectively. After implantation, the system was put under compression and decompression cycles, so the bone-implant interface could be altered. In the compression cycle, the observed capacitance values decreased, indicating the sensor was moving away from the bone; and contrarily, in the decompression cycle, the capacitance increased with the progressive unloading. Values were obtained in intervals of [2.2090; 3.0764] pF for the compression and [1.9806; 3.1841] pF for the decompression. The mean percentage of capacitance change for the compression cycle was 3.67% and 5.06% for the decompression, indicating a greater change rate in the decompression cycle. Additional tests were carried where the implant and the sensor were rotated 90 and 180°, to show the influence of different interfaces in the measured capacitance. The latter tests allowed to support the results obtained without rotation, as different sensor positions provided different behaviors of the capacitance change. Further development is still needed related to the experimental setup, more specifically the *in vitro* specimens fixation and the environment control of the experiment room. In addition, energy harvesting to create self powering systems to avoid exernal links or finite-life alternatives are also a necessity for future instrumented implants. This work further demonstrated the potential of capacitive technologies to monitor the bone-implant fixation. Therefore, it also contributed towards the design of a new era of high-sophisticated implantable medical devices.

palavras-chave

Dispositivo bioelectrónico, Implantes instrumentados, Interface osso-implante, Tecnologias capacitivas, Osseointegração

resumo

Distúrbios musculares estão a tornar-se um fardo cada vez maior para a sociedade atual, e, como resultado, milhões de artroplastias são realizadas anualmente por todo o mundo. Apesar da artroplastia estar reconhecida entre os procedimentos mais bem sucedidos do último século, ainda se observa uma taxa de falha em implantes de cerca de 10%. Estes números realçam a necessidade das tecnologias conseguirem fornecer um diagnóstico preciso da interface osso-implante, podendo reduzir significativamente a necessidade de cirurgias de revisão. Este trabalho tem como objetivo avaliar o desempenho de um implante instrumentado para monitorizar a estabilidade em implantes, utilizando uma tecnologia capacitiva planar. De forma a verificar o efeito de uma inserção completa em espécimes biológicos, um circuito impresso de dimensões 5x10x0.8 mm com dois elétrodos de 5x2 mm foi fabricado com o objetivo de ser integrado dentro de um implante. O implante foi projetado com uma geometria cónica, de forma a obter uma fixação *press-fit*, com diâmetros mínimo/máximo de 12 e 15 mm, respetivamente, e um comprimento de 55 mm. Depois de implantado, o sistema foi posto sobre ciclos de compressão e de descompressão de forma a alterar a interface osso-implante. Nos ciclos de compressão, os valores observados da capacidade decresceram, indicando que o sensor se estava a afastar do osso; contrariamente, nos ciclos de descompressão, a capacidade tendia a aumentar com o descarregamento. Os valores foram obtidos no intervalo de [2.2090; 3.0764] pF para os ciclos de compressão e de [1.9806; 3.1841] pF para a descompressão. A percentagem média de variação da capacidade para os ciclos de compressão foi de 3.67% e de 5.06% para os de descompressão, indicando uma maior taxa de variação nos ciclos de descompressão. Adicionalmente, foram realizados testes em que o implante e o sensor foram rodados 90 e 180° de forma a verificar o efeito de interfaces diferentes na capacidade medida. Estes últimos testes permitiram também corroborar a validade dos testes de compressão e descompressão, visto que orientações diferentes do sensor deveriam dar tendências diferentes nas curvas de capacidade. No entanto ainda é necessário um desenvolvimento adicional relativamente ao *setup* experimental, mais concretamente na fixação dos espécimes biológicos durante os ensaios *in vitro*, assim como no controlo das condições ambiente do laboratório. Adicionalmente, o desenvolvimento de sistemas de *energy harvesting* são uma necessidade para o futuro dos implantes instrumentados de forma a ter um sistema auto-sustentável, evitando ligações com o exterior ou soluções de vida limitada. Este trabalho permitiu comprovar o potencial de tecnologias capacitivas para a monitorização do estado da interface osso-implante. Assim, também contribuiu para o desenvolvimento de uma nova era de dispositivos médicos implantáveis altamente sofisticados.

List of publications

The current work resulted in the following publication: J. H. Cachão, M. P. Soares, R. Bernardo, A. Ramos, R. Bader, J. A. F. Ferreira, A. T. Marques, and J. A. O. Simões, "*Altering the course of technologies to monitor loosening states of endoprosthetic implants*'', Sensors, accepted for publication.

"Nobody ever figures out what life is all about, and it doesn't matter. Explore the world. Nearly everything is really interesting if you go into it deeply enough"
- Richard P. Feynman

Contents

List of Tables

Intentionally blank page.

List of Figures

Intentionally blank page.

List of Abbreviations

AE	Acoustic Emission
CT	Computed Tomography
EIS	Electrical Impedance Spectroscopy
MRI	Magnetic Resonance Imaging
NJR	National Joint Registry
PCB	Printed Circuit Board
PET	Positron Emission Tomography
SPECT	Single-photon Emission Computed Tomography
THA	Total Hip Arthroplasty
TJR	Total Joint Replacement
TKA	Total Knee Arthroplasty
WHO	World Health Organization

Intentionally blank page.

Part I

Introduction and Literature Review

Chapter 1

Introduction

Joint replacement is considered one of the biggest revolutionary and most important surgical procedures of the last two centuries. The surgery consists in replacing the damaged joint for an artificial one. It was first introduced in Germany, late 19^{th} century, by Professor Themistocles Gluck who implanted an artificial knee joint [1]. He also made an hip implant made of ivory to replace the femoral head of patients with tuberculosis. Soon after, the French surgeon Jules-Émile Pean, implanted the first reported artificial shoulder joint made of natural biological materials [2]. While the idea of using prosthetics was proposed in the 19^{th} century, the greatest development occurred in the mid-late 20^{th} century, when, in the early 60's, the surgeon Sir John Charnley designed a hip replacement component which the modern components still resemble in principle [3]. Regarding the knee joint, around the same period, two models were proposed and further developed in the following decades [4].

With the increase of longevity in the overall population and the necessity of remaining active, bone related diseases are becoming more frequent and the need of joint replacements is expected to rise in the following years [5]. Presently, it's considered a successful surgery and an effective way to restore the joint mobility of patients, thus improving their lifestyle. However, every implant has a risk of failure that will potentially lead to a revision surgery, a more aggressive and invasive procedure in which the old implant is usually replaced.

1.1 Joint replacement

The necessity of total joint replacement is steadily growing. According to a study conducted by Kurtz *et al*, the increase in demand for both knee and hip replacements, in the US, will be 673% and 174%, respectively, by 2030 [6]. Another group confirmed that tendency using a different method and taking into account the ageing of population [5].

The greater cause for the surgery is osteoarthritis and it is one of the most common musculoskeletal diseases worldwide [7, 8]. It is a degenerative condition, which wears down the cartilage, eventually leading to inflammation and pain. In the earlier stages of this condition, it's possible to relieve the symptoms with medication and some other precautions. However, in the late stages, the symptoms may become disabling, conditioning the patient's mobility and life, ultimately leading to the necessity of surgery. This condition tends to worsen with the ageing and it's often associated with sedentary lifestyles and obesity, hence is a more common condition in developed countries opposed

to developing ones. According to 2010 World Health Organization (WHO) Global Burden of Disease Study, this disease affects nearly 3.8% of the population worldwide in case of the knee and 0.85% in case of the hip [9].

Joint replacement surgery was first meant for the elderly and the implant would generally last for the rest of the patient's life. This was done under the assumption that patient's life-expectancy was less than of the implant itself. By this way the revision rates were kept to a minimum. However, in another study, Kurtz *et al* [10] found an increasing trend in younger patients (< 65 years old) undergoing joint replacement surgery. They predict that, by 2030, the primary Total Hip Arthroplasty (THA) demand to be 52% for patients less than 65 years old and 55 to 62% for the Total Knee Arthroplasty (TKA). The increase in younger patients can also bring a rise in the revision surgery rates. This can be explained by their more active life, when compared to the elderly, which promotes the implant wear and failure, mainly if implant technology is not designed to ensure long-term fixations.

1.2 Failure in implants

In spite of being a successful procedure, there are still reports of failure in Total Joint Replacement (TJR). Recent data show there is a 10% risk of revision 10 years post-operatively for TKA. Considering the predicted growth of surgery demand, these can potentially be a major burden for patients and healthcare systems [11]. McGrory, Etkin and Lewallen [12] evaluated the National Joint Registry (NJR) of five healthcare systems, focusing on revision burden (ratio of implant revisions to the total number of arthroplasties) during a given period. For the THA the mean revision rate between 2011 and 2014 was 11.7%. Regarding the TKA during the same period, the mean revision rate was 7.0%.

Currently, aseptic loosening is the main cause for implant failure. Khan *et al* [11] performed a major study, cross referencing results from five NJR and some individual study groups worldwide for TKA. The group pooled the NJR data together and concluded that aseptic loosening accounts for 29.8% of all revision surgeries. Infection and pain are the second and third reasons, being 14.8% and 9.5%, respectively. By analyzing the reports

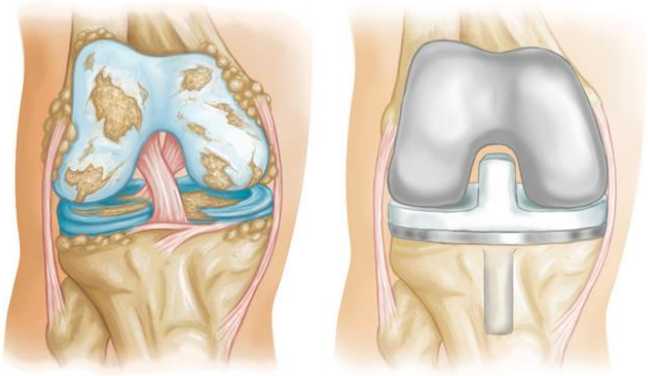

Figure 1.1: Example of damaged cartilage in the knee and subsequent knee joint replacement (from *OrthoInfo.org*).

of individual groups referring to THA, the Australian Registry [13] reported, in 2018, the most common causes for implant failure as: aseptic loosening (26.2%), dislocation (20.3%) and infection (18.6%). The latest report from the National Joint Registry [14], which encompasses England, Wales, Northern Ireland and Isle of Man, reports the most common causes as aseptic loosening (24.3%), dislocation/subluxation (17.1%) and infection (14.5%). They also stated that aseptic loosening and pain probability increase with time from surgery. In 2017, the Swedish Hip Arthroplasty Registry [15], reviewed the failure causes and concluded that the most common reasons for revision are aseptic loosening (44.6%), infection (25.6%) and dislocation (13.6%).

1.3 Current diagnosis methods

Currently, the standard medical diagnosis of the implants state is performed using imaging methods. These medical images can be acquired from a range of different techniques and each one can be defined by its characteristics, cost and ease of usage.

The analysis with X-rays is more common, partially because of its low cost and for being a non-invasive technique. Usually, the potential loosening of the implant is detected by the existence of radiolucencies present in the bone-implant interface (Figure 1.3 a). Zhang *et al* [16] tested the accuracy of this method, reaching an 88% detection rate for radiolucencies of 0.7 mm. The potential for detecting smaller radiolucencies decreases quickly, making it a difficult technique to predict implant loosening at early stages. Temmerman *et al* [17] also reviewed this method and reported an 82% sensitivity for plain radiography. Magnetic Resonance Imaging (MRI) can also be used for the diagnostic of implant's state. This method uses strong magnetic fields to generate images of the body. In response to the magnetic field, some atoms will emit radio frequency waves which can then be detected externally through an antenna. Cooper *et al* [18] showed the potential of this method for THA implant's early loosening assessment, although they did not give any specific values of the method's effectiveness. One method capable of processing multiple X-ray images is Computed Tomography (CT). Furthermore, CT can be used to generate a three-dimensional model by obtaining various images from different angles, around one axis of rotation which allows it to be recognized as a powerful diagnostic tool [19]. Figure 1.3 b shows the final three-dimensional image obtained

Figure 1.2: Hip implant components and implantation location (from *OrthoInfo.org*).

by using CT. Two other types of CT are Positron Emission Tomography (PET) and Single-photon Emission Computed Tomography (SPECT). These have the disadvantage of requiring the injection of radioisotopes into the patients' body.

Arthrography is an invasive method in which a contrast agent is injected into the joint and can be visualized through fluoroscopy, MRI or CT, although it is usually used in combination with the latter. The resulting image can be improved by using subtraction arthrography, in which the contrast is increased [21]. Temmerman *et al* [22] found a sensitivity of 86% for aseptic loosening detection [17] and 89% for a loose acetabular component, relative to subtraction arthrography. One other invasive method is scintigraphy. Distinctively, the injected agents are radioactive isotopes that can be observed through a gamma camera, providing a two dimensional image. Claassen *et al* [23] tested the method's sensitivity on 46 patients and reached a value of 76%, for aseptic loosening detection. The combination of the two previous methods is called nuclear arthrography. This method requires that the patient is injected with a radionuclide contrast agent. The joint can be further analyzed with radiographic contrast arthrography and afterwards with a gamma camera. Oyen *et al* [24] reported a better sensitivity for the detection of cemented femoral components loosening in comparison to uncemented loosed components (92% and 65%, respectively), for the latter method, having studied it on 105

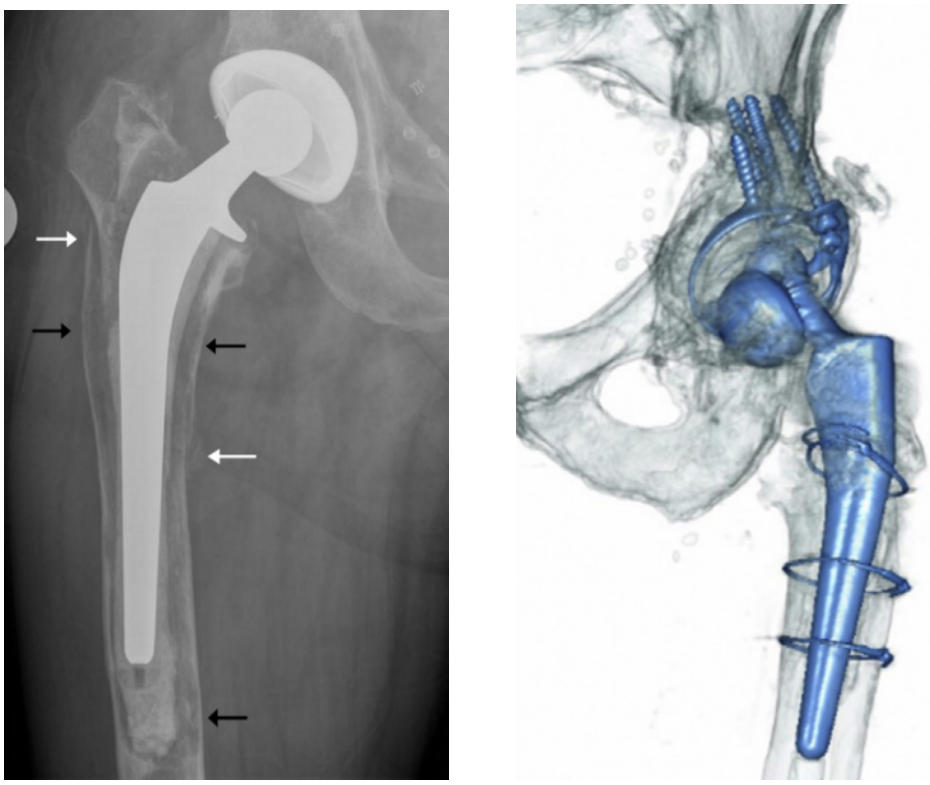

(a) (b)

Figure 1.3: (a) Radiography showing radiolucencies which may be indicative of mechanical loosening in the cement-bone interface [20]. (b) CT scan of a hip implant showing the resulting three-dimensional image [19].

patients. Despite these low numbers, the group still finds that nuclear arthrography presents a relatively better performance when compared to other methods (scintigraphy and radiographic arthrography).

As seen in the literature, these methods present good results, although one may conclude that these cannot be considered ideal technologies for assessing the implant-bone interface state. Although these methods are considered accurate techniques to detect loosening states of both cementless and cemented implants, the clinical follow-up can only be carried out in clinical laboratories, and thus the monitoring cannot be established throughout the daily life of patients.

1.4 Types of implants

One possibility to overcome the imaging technologies limitations is to design an implant with ability to perform the implant stability assessment: an instrumented implant incorporating a monitoring system to follow-up implant loosening states. The idea of designing instrumented implants is becoming more concrete with recent technological advances. Thus, for the present work, it is important to differentiate the traditional implant of the instrumented one.

1.4.1 Non-instrumented implants

This type of implants is the standard implant, their only objective is to restore joint function. There are multiple differences across all implants, either the geometry, the materials or fixation method. Their fixation can be achieved through bone cement or osseointegration. The use of bone cement has a clear advantage in the way that it provides immediate fixation post-operation once the cement is curated. However, it is very susceptible to fatigue failure, thus its use is discouraged in younger patients with a more active lifestyle and is usually used in older patients with low mobility. Figure 1.4 a shows the common hip implant used for cemented fixation. Cementless implants rely on the ability to provide osseointegration. One of the most common methods to attain osseointegration is to coat the implant surface with a bioactive material named hydroxyapatite. Bone-metal interactions are promoted due to the similar nature between hydroxyapatite and the mineral phase of the bone [25]. Another alternative is to cover the implant with a porous coating to allow for bone growth, as illustrated in Figure 1.4 b. Since the fixation of the implant requires a strong enough interaction between bone and implant, the post-operation recovery of patients takes longer than using cemented fixations. Stress-shielding is also frequently observed in cementless implants, which eventually leads to a decrease in local bone density.

There is no consensus about the better method to attain fixation, although cementless implants are more commonly used. Troelsen *et al.* [26] conducted a review to registries with more than five years of data collection to assess the prevalence of the uncemented fixations in THA. The Two Scandinavian countries were the lowest with Sweden (15%) and Norway (25%). The others were England-Wales (43%), New Zealand (51%), Australia (65%), Denmark (68%) and Canada (82%). The United States present the largest rate with 86%. These numbers can be indicative of an increasing trend in the use of uncemented fixations.

(a) (b)

Figure 1.4: (a) Typical hip implant with a clear surface, intended for cementing (from *medicalexpo.com*). (b) Porous coating in the implant's surface, allowing for osseointegration (from *bonesmart.org*).

1.4.2 Instrumented implants

An instrumented implant can be characterized by having an integrated system able to provide information about a physical quantity of the implant and/or the surrounding tissues. The concept was first tested by Rydell [27] in 1966 with the integration of strain gauges to measure the loads and moments over the neck of the implants. More recently, some groups designed architectures which incorporate reading and telemetry systems, in order to provide wireless monitoring operations. Bergmann *et al* [28] studied the hip joint interface temperature to assess the risk of thermally induced necrosis, which can cause subsequent implant failure. The electronic system could be powered externally through an inductive coil inside the implant (implant-sensor system displayed in Figure 1.5). Arami *et al* [29] focused on measuring forces and the kinematic motion of the knee joint. They installed a magnetic system to predict the joint orientation and strain gauges to estimate the applied force. This system is also powered inductively through a coil placed externally and the reading can be carried out without wires.

Instrumented implants hold potential to improve the lifestyle of patients by decreasing the risk of revision surgeries and implant failure. These implants can be classified by two categories: passive or active implants.

Passive implants

A passive implant has the ability of acquiring information regarding the peri-implant state. So far, all proposed implant technologies described above are passive, as those described in sub-section 1.4.2. Earlier studies regarding instrumented implants were mainly focused on the measurement of temperature and forces [28, 30–32], although there are many researchers who are currently directing their study towards implant stability [33, 34].

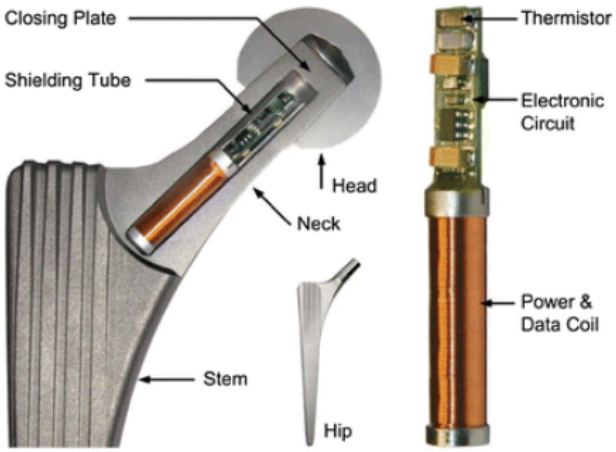

Figure 1.5: Illustration of an instrumented implant with the electronic system housed in the implant's head and neck. From Bergmann *et al.* [28].

Active implants

The concept of instrumented active implants was introduced by Soares dos Santos *et al.* [35]. In addition to the monitoring, an instrumented active implant is distinguished by its ability to stimulate bone growth around the implants. It's been observed that bone cells respond to electric stimuli, improving bone remodeling (by enhancing bone proliferation, differentiation and mineralization) and thus instrumented implants can be used to deliver future personalized therapies to the surrounding tissues. Ideally, an instrumented active implant would have the ability to monitor the implant fixation while being able to provide controlled and local stimuli to promote bone-implant integration.

Soares dos Santos *et al* [35] proposed five key points that an instrumented active implant must fulfill: (a) monitoring systems providing real-time data regarding the physiological states of surrounding tissues; (b) real-time processing systems to assess potential failure; (c) actuation systems, to provide the delivery of personalized therapies when loosened regions are detected; (d) telemetry system for external communication; and (e) self-supply electrical system for powering the components under operation, while preserving an autonomous operation.

1.5 Objectives

This work follows a previous research work focused on the performance identification of a capacitive system to monitor different bone-implant interfaces [36], which in turn was proposed by Soares dos Santos. In the previous work, the working principle based on a planar architecture was observed. By using the bone as a dielectric promising results were achieved, showing changes in the electric capacitance according to different distances between bone and sensor. Although, Soares dos Santos *et al.* [37] also proposed other geometrical arrangements for the capacitive technology, this work will focus only on the stripped architecture.

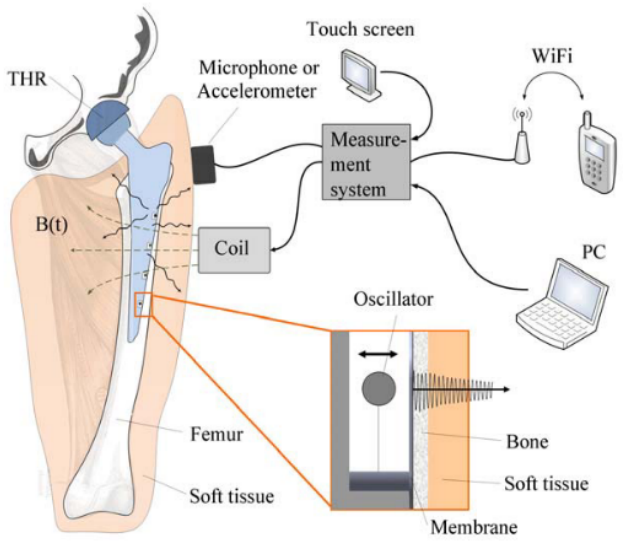

Figure 1.6: Sensors, telemetry and network system for implant monitoring and control. A scheme provided by Ruther *et al.* [38].

This work aims to further develop and improve this technology towards a more real and suitable monitoring system, revolutionizing the course of instrumented implants and implant stability monitoring. The proposed goals are as follows:

1. Development of an implant to integrate inside a femoral head;
2. Development of the capacitive planar architectures and their integration in the implant;
3. Development of an *in vitro* experimental setup to integrate the bone-implant-sensing technology components;
4. *In vitro* experiment to analyze the performance of the monitoring technology through the measuring of the capacitance.

Chapter 2

Bone properties and physiology

The skeleton is one of the primary body structures, having 206 bones which provide for mobility, give protection for the internal organs, among other functions. Its functioning and composition are some of the most important characteristics in the biomechanical and orthopedic fields, so understanding the bone structure is highly relevant for the present work. Bone is one of the hardest structures in the human body, nevertheless is one of the most dynamic and metabolic active tissues. It is highly vascularized and receives 10% of the cardiac pumping each minute, has a self-regeneration and adaptation ability to local mechanical loading [39].

Bone tissue is primarily composed of inorganic matter (mineral salts), accounting for 50 to 70% of the total constitution. The organic matrix, 20 to 40%, gives to bone structure its flexibility and elasticity, while the inorganic part offers the rigidity. The remaining percentages are water and lipids. Bone composition varies according to its anatomic location, age and metabolism.

2.1 Types of bone

Bone structure is arranged in different ways, creating layers of bone with distinguishable properties. The external layer is called cortical bone and the internal is the cancellous or trabecular bone (Figure 2.1). Their distribution is not uniform throughout the bone. Long bones are characterized by a greater concentration of cancellous bone in the distal and proximal areas, near the joints. Cortical bone has a dense structure that gives the rigidity for supporting and protection and it accounts for 80% of the total bone

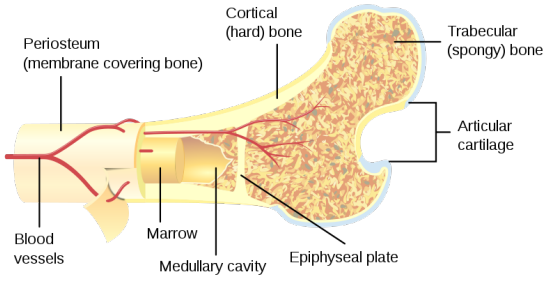

Figure 2.1: Arrangement of cortical and trabecular bone (from *differencebetween.com*).

mass. Its remodeling rate is lower than cancellous, around 3% per year. Cancellous bone is composed by a mesh of trabeculae, creating a less dense structure with a higher remodeling rate than cortical bone (around 25% per year). This lower density makes it more flexible than cortical bone, but also less rigid. Its "spongy" structure makes it good for absorbing impact, thus its greater concentration near the joints area. The trabeculae orientation varies according to physical loading, changing the structure's local mechanical properties (Figure 2.2).

2.2 Bone remodeling and modeling

Bone remodeling is a process used for producing and maintaining bone tissue. Throughout life, the body is continually subjected to cyclic loads, which progressively deteriorate the bone tissue. Bone remodeling allows to replace or renew the tissue by constantly absorbing and creating it, ensuring the structure's integrity [40]. In bone modeling (or adaptation), the distinction is made in that the bone resorption and formation are not balanced, meaning resorption can occur and not be followed by bone formation. This can result in changes to the bone structure, mass or shape [39]. Both these processes consist in constant bone formation and resorption which are performed mainly by two types of cells: osteoblasts and osteoclasts [39], respectively (Figure 2.3). Other types of cells are osteocytes. It is hypothesized that these are sensible to mechanical stimuli and are the responsible for triggering the bone remodeling activity [41]. Bone tissue has the ability of adapting itself to mechanical loading and this process is achievable due to the skeleton's modeling and remodeling. Harold Frost tried to describe this event in his Mechanostat theory in which, according to the magnitude of the load in the tissue, local bone density can increase or decrease.

These phenomena are of great importance for implantable prosthetics that rely on osseointegration to achieve stability. Usually, the implant is made of a material more rigid than the bone itself, resulting in a non-suitable load transfer from the bone to the implant. This decrease in load will cause local bone resorption, which may compromise implant's stability. It is usually referred to as stress shielding [42].

Figure 2.2: Trabeculae distinct orientations at the femoral head [43].

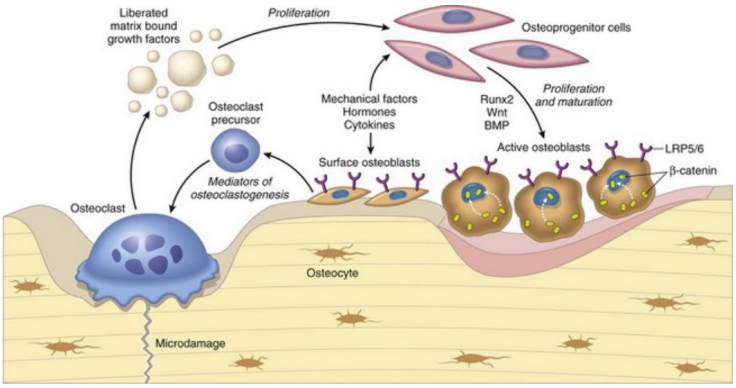

Figure 2.3: Schematic of bone remodeling illustrating the acting cells. Osteoblasts responsible for the formation of bone and osteoclasts, responsible for bone resorption (from Kumar V., Abbas AK., Fausto N. *et al*: *Robbins & Cotran pathologic basis of disease*, ed 8, Philadelphia, 2009, Saunders).

2.3 Mechanical properties

Characterization of bone tissue is important to understand bone responses to implants, as well as the effect of bone-related diseases.

As mentioned, bone tissue has the ability of adapting itself according to local physical stimuli, thus its mechanical properties also vary accordingly. The load location and type, its direction and velocity are some of the factors that influence their behavior. Moreover, patient-related characteristics like age, health and metabolism also impact this structure's heterogeneity. The unique and individual properties make it hard to define a high-precision model for bone mechanical properties, which may explain why literature results may differ. Nevertheless, cortical and cancellous bone can be clearly distinguished and present very dissimilar stress-strain curves, which can be easily related to their difference in Young's modulus.

Bone structure is arranged in multiple directions and so, its properties vary depending on the direction of the load, making it an anisotropic material. Besides the direction, the type of loading also influences the bone behavior. Cortical bone has a high resistance to flexion and torsion, bearing more load but absorbing less deformation energy, making it more fragile. Differently, cancellous bone works best with compressive loads and has a higher capability of absorbing deformation energy, which can be explained by its porous structure. Both types of bone present a lower resistance under traction loads.

2.4 Electrical properties

The complex structures of organic and inorganic elements of bones makes them hard to be characterized. Dielectric properties of biological tissue are dependent of the analyzed frequency and so, its behavior can be divided into three main relaxation regions: α, β, γ corresponding to low, medium and high frequencies [44]. It's possible to define each of these relaxation zones with expression 2.1, referring to the complex relative permittivity ($\hat{\varepsilon}$), function of a time constant (τ) and the angular velocity (ω). ε_∞ is the permittivity

at frequencies where $\omega\tau \gg 1$ and ε_s the permittivity at $\omega\tau \ll 1$.

$$\hat{\varepsilon} = \varepsilon_\infty + \frac{\varepsilon_s - \varepsilon_\infty}{1 + j\omega\tau} \tag{2.1}$$

The latter expression is further described with a Cole-Cole equation that accounts for the broadening of the dispersion due to the high complexity of bone tissue's properties, resulting in equation 2.2. The added parameters correspond to: the conductivity (σ_i); permittivity in vacuum (ε_0); and a distribution parameter (α), which measures the broadening of the dispersion. Expression 2.2 allows to predict the tissue's dielectric behavior relative to the frequency. Gabriel, Lau and Gabriel [44] used this analytical model to predict the cortical and cancellous bone conductivity and permittivity curves, among other tissues. Parameters values and bode plots can be found in Annex A, Figure A.1.

$$\hat{\varepsilon}(\omega) = \varepsilon_\infty + \sum_n \frac{\Delta\varepsilon_n}{1 + (j\omega\tau_n)^{(1-\alpha_n)}} + \frac{\sigma_i}{j\omega\varepsilon_0} \tag{2.2}$$

Chapter 3

Monitoring of loosening states of bone implants

In this chapter, a literature review of the existing monitoring technologies is presented. Technologies were considered relevant according to the following criteria: (1) Monitoring technologies not requiring medical imaging methods; (2) Intracorporeal and extracorporeal adjuvant technologies with ability to monitor implant loosening (including those technologies incorporated within instrumented bone implants); (3) Monitoring technologies to monitor the implant–bone interface with *in vitro* or *in vivo* validation; and (4) Monitoring technologies for both cementless and cemented implants fixations.

This review is focused on the recent findings related to monitoring of biointegration and stability on joint implants. Six different methodologies were discerned and a total of thirty-nine technologies were developed [45].

3.1 Categorization and features of monitoring technologies

To facilitate the comparison between technologies, each monitoring method was inserted into a category according to its features. Apart from the categorization, specific characteristics relative to the system's architecture and functionality were considered important to highlight. These are: (i) type of excitation necessary for the system's operation (system input); (ii) outcome related to the bone-implant (or implant-cement-bone) interface state (system output); (iii) components comprising the system and their location in the analyzed body; (iv) characteristics of the output signal that allow distinction between interface states; (v) *in vivo* and *in vitro* tests validating the technology.

3.2 The vibrometric approach to monitor implant loosening states

Monitoring methods and technologies for cementless fixations

Three methods and ten technologies were already proposed (Table A.1, Appendix A): Method 1: Extracorporeal mechanical excitation/extracorporeal mechanical signal. Eight technologies implemented this method:

(T1-L1) Georgiou and Cunningham [46] designed a noninvasive technology to diagnose loosening of total hip replacements (stem and acetabular component). They use an extracorporeal shaker (excitations up to 1000 Hz) located in the knee (or near the distal femur condyle) and an extracorporeal accelerometer on the hip. The stability assessment of total hip replacements is performed by monitoring the waveform distortion (presence of harmonics) of the output acceleration signals. Only secure loose states can be detected. Loose implants are detected in three scenarios: (i) five or more harmonics, (ii) harmonics with amplitude higher than 50% of the fundamental frequency, and (iii) two or more resonant frequencies. The bone–implant integration failures are noticed in a large frequency range (up to 2000 Hz), and harmonics can emerge exceeding 100 Hz apart from the fundamental frequency.

(T1-L2) Alshuhri *et al.* [47, 48] also proposed a totally noninvasive technology to detect loosening of the acetabular component in total hip replacements. An extracorporeal shaker, in the femoral lateral condyle, and two extracorporeal accelerometers, in the iliac crest and greater trochanter, are required to monitor acetabular cup loosening, which is analyzed by computing the harmonic ratios (relative magnitude of the first harmonic to the fundamental frequency) in the output signal. The mechanical excitation is delivered in the 100 to 1500 Hz range and acetabular loosening is detected if any harmonic ratio is observed. Different fixation scenarios can be identified (authors analyzed two loosening states), as they are correlated to different harmonic ratios. The loosening is distinguished in a large frequency range (up to 1000 Hz) and harmonics can be more than 100 Hz apart from the fundamental frequency. This technology is illustrated in Figure 3.1.

(T1-L3) Rieger *et al.* [49] proposed a technology to detect failed implant integration of total hip replacements (femoral stem and acetabular cup) by delivering mechanical excitation on the knee, by an extracorporeal shaker (100–2000 Hz), and subsequent identification of shifts in the resulting resonance frequency of the output vibrations measured by three accelerometers (medial condyle, greater trochanter, and iliac crest) extracorporeally localized. Failures are detectable at frequencies below 1000 Hz, but

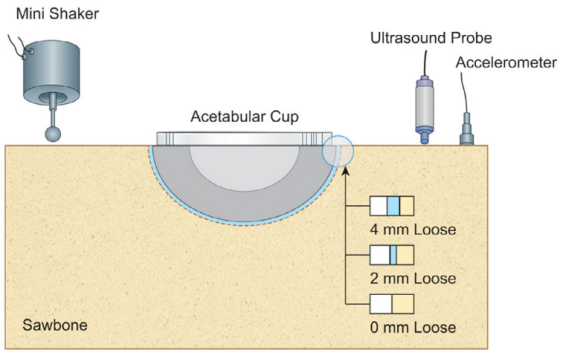

Figure 3.1: Depiction of the technology T1-L2 of the 1st method of uncemented fixations for both vibrometric and acoustic approaches, illustrating a mini-shaker providing the input excitation signal, the reading components (ultrasound probe and accelerometer), and the acetabular cup. Reprinted from [47] with permission from Elsevier

.

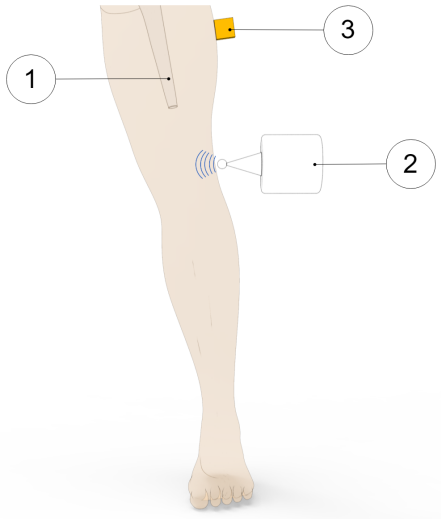

Figure 3.2: Illustration of the 1st method (extracorporeal mechanical excitation/extracorporeal mechanical signal) for vibrometric cemented and cementless fixations: (1) implant, (2) vibrator providing the input excitation, and (3) extracorporeal accelerometer measuring the resulting vibration from the implant–bone system (or implant–cement–bone). Figure depicting a hip implant case.

the frequency shifts are in the 2 to 111 Hz range, even though the larger the resonance frequency the larger the frequency shifts. The measures in the ilium only provided frequency shifts (3-22 Hz) for excitations of 200 Hz. This technology only reports two integration states (secure or loose), although it allows to differentiate states of stem-cup combinations.

(T1-L4) The research team of Rieger *et al.* [50] also developed an alternative technology to detect loosening of hip endoprostheses. The mechanical excitation is extracorporeally provided by an array of piezoelectric actuators arranged on a spherical cap to drive shock waves (characterized by an approximation to a Dirac delta function: short rise time, high amplitude, and short pulse width around few μs). The mechanical pulses are delivered from the lateral knee condyle, the greater trochanter, and the iliac crest. These are the same locations where three accelerometers were extracorporeally allocated to allow analyses to shifts in the resonance frequency. This technology allowed to determine significant shifts in the 4 to 847 Hz range (most of them higher than 100 Hz) between 386 Hz and 847 Hz, and can be used to distinguish different states of stem-cup combinations, but only differentiate secure or loose integration levels.

(T1-L5) Lannocca *et al.* [51] and Varini *et al.* [52] engineered a medical device customized to measure stability intraoperatively. It is attached to the implant system and comprises an extracorporeal piezoelectric system (piezoelectric cantilever vibrator based on a ceramic multilayer bender) to provide excitations in the 1200 to 2000 Hz range. An extracorporeal accelerometer located on the greater trochanter is also required to analyze the primary stability, performed by monitoring shifts in the resonance frequency. The identified threshold for differentiating between stable and quasi-stable

implants is a frequency shift of 5 Hz. Different shifts provide data concerning different primary stabilities. The technology of Varini *et al.* is represented in Figure 3.3.

(T1-L6) Lannocca *et al.* [51] and Varini *et al.* [52], using the same medical device to deliver the mechanical excitation, proposed to include a displacement transducer (LVDT) to track the primary stability by measuring implant–bone micromotions. Micromotions higher than 150 μm are an intraoperative indication of implant instability. Different micromotions are used to distinguish different primary stabilities.

(T1-L7) Pastrav *et al.* [53] also contributed towards the perioperative monitoring of fixation of total hip endoprostheses. A shaker and a mechanical impedance head are attached to the prosthetic neck. They found frequency response patterns shifted to the right, and sustained increases as a function of the stiffness increase between successive insertion stages.

(T1-L8) Jiang, Lee, and Yuan [54] tested a noninvasive technology to distinguish between failed (by wear and malalignment) and normal total knee replacements. An isokinetic dynamometer is used to impose extracorporeally excitations based on knee flexion–extension motions (up to 67°/s), as well as an accelerometer positioned on the skin covering the patella. Early and late stages of failure can be identified by analyzing the spectral power ratios of dominant poles of a transfer function representing the vibration signals. The physiological patellofemoral crepitus signals are also able to detect wear of knee components. A threshold, using the average spectral power ratio of dominant poles, was found to identify implant failures. Besides, interface failures are detected by spectral power ratio decreases for frequencies lower than 100 Hz.

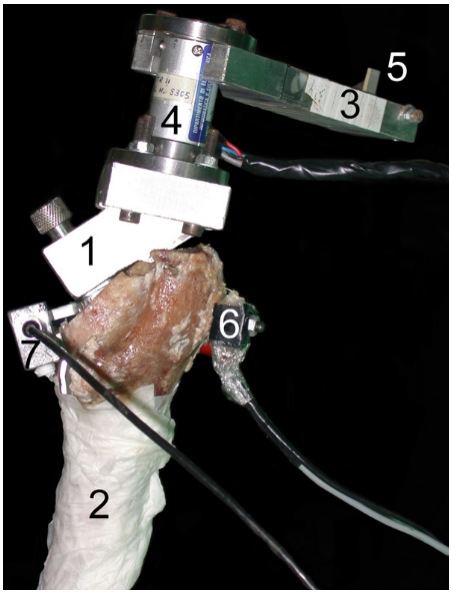

Figure 3.3: Illustration of the intraoperative technology developed by Varini *et al.* (T1-L5 of the cementless fixations for vibrometric.) Described by the authors as (1) stem holder, (2) femur, (3) handle to deliver the torque, (4) load cell, (5) component providing the system excitation, and (6) the accelerometer. Reprinted from [52] with permission from Elsevier.

Method 2: Extracorporeal magnetic induction/extracorporeal mechanical signal. Only a single technology established this method:

(T2-L1) Ruther *et al.* [38,55] provided an innovative technology based on intracorporeal mechanical excitation driven by extracorporeal magnetic induction and extracorporeal acceleration sensing (depicted in Figure 3.4). They developed an oscillator–implant system in which one or more magnetic spherical oscillators, attached to a flat spring, are embedded into the implant near the stem walls for detection of loosening features in several endoprosthetic devices (including total hip and knee replacements). The vibrational excitation is inductively provided by a coil extracorporeally, producing a magnetic field that imposes collisions of the oscillators with the implant walls, which causes the propagation of vibrations along the adjacent tissues surrounding the implant that can be measured by an accelerometer externally located at the skin surface. The measurement of the resulting accelerations signals and subsequent computation of the frequency shift in the output signal, as well as the central frequency in the resultant spectrum, allows prediction of the differing loosening locations and stages (press fit, slight loosening, and significant loosening). Shifted frequencies around 300 Hz and 400 Hz allow the detection of slight loosening and significant loosening, respectively, although better results were achieved using the central frequency as an indicator, as these frequencies always varied more than 1000 Hz for any loosed scenario under analyses. These authors also demonstrated an effective change in the central frequencies (exceeding 500 Hz) for different measurement locations, apart from a geometric reference in the range extended from the 5 to 124 mm range (distance in the three-dimensional space). Besides, they found longer transient periods for unstable fixations.

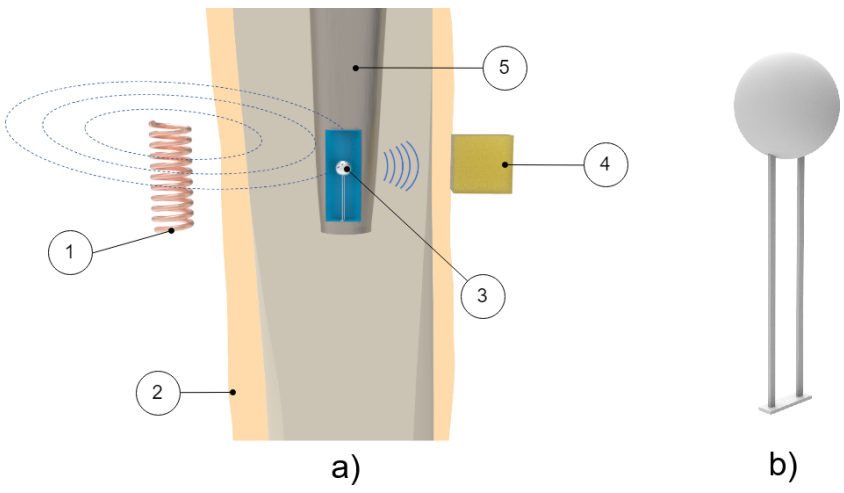

Figure 3.4: Depiction of the magnetic oscillator method (T2-L1 of cementless fixation of vibrometric technologies). (a) Schematic of components: (1) Extracorporeal coil providing movement to the oscillator; (2) Human tissue; (3) Oscillator housed inside the implant; (4) Extracorporeal accelerometer used to measure the resulting vibration from the oscillator's impact; (5) Implant. (b) Detailed illustration of the oscillators.

Method 3: Intracorporeal mechanical excitation/extracorporeal mechanical signal. Only a single technology established this method:

(T3-L1) Glaser *et al.* [56] developed a noninvasive technology to monitor the performance of hip joint implants within the bone–implant interface. An intracorporeal excitation is delivered by the implant displacement during dynamic movements of patients. Mechanical vibration can be detected by placing two accelerometers: one at the greater trochanter and the other on the anterior superior iliac spine. The acetabulum–femur separation is identified by a high-frequency sound, which is originated by the impact caused when the femoral head slid back into the acetabular component.

The proposed methods were specifically designed for medical analyses related to hip and knee joint implants, although they hold potential for implementation in other bone implants. A deeper analysis of these methods and technologies reveals significant findings, as follows. The most explored method was the one requiring extracorporeal mechanical excitation and extracorporeal mechanical signal (eight technologies out of ten). Most methods (nine out of ten) established the use of extracorporeal excitation systems to monitor bone–implant integration; among them, most technologies (eight out of ten) require a mechanical excitation to drive the monitoring system. The mechanical excitation was neither undervalued by Ruther *et al.* [38] nor by Glaser *et al.* [56]; instead, such an excitation was used as an intermediate process between the primary excitation and measured outcome. Harmonic excitations are delivered by six technologies, but shock waves and magnetic induction were also used. Note that eight of the technologies perform monitoring operations using extracorporeal accelerometers. Concerning the interface monitoring of total hip implants, note that technologies were developed for the detection of both femoral stem and acetabular cup loosening. Note that three technologies (out of nine) are able to identify different loosening stages, and six of them are limited to a monitoring operation on the no-loosening-loosening basis; however, no technology was designed to analyze bone–implant integration states along distinct bone-implant locations, even though theoretical analyses were already conducted towards the design of instrumented implants with such ability [57]. Concerning technologies for total knee systems, their operation was focused on the detection of interface failures. Another relevant matter concerns the effective monitoring period: most monitoring systems (seven out of ten) were designed for postoperative sensing, and only three technologies were customized for intraoperative monitoring operations. Data processing operations were mainly conducted by analyzing the resulting shifts in the resonance frequency, but analyses of the waveform distortions, harmonic ratios, central frequencies, bone–implant micromotions, spectral power ratios, and transient periods were also considered. The sensitive band was usually found in the 1500 to 2500 Hz range [58]. The vibrometric approach was validated both *in vitro* and *in vivo*, although some technologies (six out of ten) have not yet been validated *in vivo*. Furthermore, their performance was not measured in terms of measure accuracy.

Monitoring methods and technologies for cemented fixations

Two methods and eight technologies were already proposed (Table A.2, Appendix A), as follows.

Method 1: Extracorporeal mechanical excitation/extracorporeal mechanical signal. Five technologies implemented this method:

(T1-C1) Li, Jones, and Gregg [59] developed a similar technology to T1-L1 (Georgiou and Cunningham [46]), but for cement–bone–implant interfaces. They used a shaker to deliver extracorporeal mechanical vibrations (100 to 1200 Hz) at the distal femur and monitored the output vibration by two extracorporeal accelerometers at the distal and proximal femur. The output signal was analyzed in the same frequency bandwidth as the extracorporeal excitation. Implant loosening was detected by distortion analyses of the output acceleration waveforms, as well as using the number of resonance frequencies (two or more). The authors tested three fixation states: secure, early loosening, and late loosening. Loose implants are characterized by highlighting more than two resonance frequencies and present a distorted output signal in several excitation frequencies. Contrarily, early implant loosening fixation states are not clearly distinguished from the secure state.

(T1-C2) Similarly to Li, Jones, and Gregg [59], Rosenstein *et al.* [60] developed a method to assess the stability of cemented hip implants. They applied a mechanical excitation provided by an extracorporeal shaker (100 to 1000 Hz) at the lateral condyle while measuring the resulting output vibration, in the same bandwidth, with an extracorporeal accelerometer on the greater trochanter. The tests were only performed with fixed and loosened cemented implants (two loosening states). The loosening was correlated with harmonics in the output acceleration signals, although no specific frequency values were reported.

(T1-C3) The research team of Rowlands, Duck, and Cunningham [61] also developed a method to monitor hip implant loosening. Using an extracorporeal shaker to provide input mechanical vibrations (100 to 1500 Hz) in the distal femur, they monitored response vibrations on the greater trochanter using an extracorporeal accelerometer. Although four fixations states were analyzed (a loosened state, as well as three fixed states), only the results regarding the loose implant were reported. Loosening is observed by analyzing the output signal resonance frequency. The most sensitive band for the driving frequency was found between 100 and 450 Hz. Apart from the loose implant results, no additional data was provided.

(T1-C4) Leuridan *et al.* [62] developed a technology to assess the fixation state of tibial knee implants. Distinct tests were conducted by varying the measurement region (tibia surface and tibial plate) and using extracorporeal accelerometers to measure the output signals in the 50 to 4500 Hz frequency band. Mechanical excitation was provided by an impact hammer at the tibial plate surface. Four different cement–bone–implant interface scenarios were reported: secure, peripheral loosening, medial loosening, and lateral loosening. The authors used two criteria to process the resonance frequency results: the Modal Assurance Criterion and the Frequency Assurance Criterion; fixation states could be distinguished by the different values given by each criteria. The most sensitive band was found to be above 1500 Hz.

(T1-C5) Arami *et al.* [63] also provided a technology to detect loosening states of tibial knee implants. An extracorporeal shaker located below the patella (100 mm) was used to deliver mechanical excitations in the 30 to 3000 Hz frequency range. Three

extracorporeal accelerometers were used: one was fixed in the vibrator tip, such that the output frequencies can be analyzed in the same range as the input, and the remaining two accelerometers were used to assess the vibration propagation to the tibial implant and were placed in the tibial plate. They assessed two interface states: well-fixed (cemented) and completely loose. Implant loosening is characterized with a new peak emerging in the 750 to 900 Hz range, when compared to a baseline result taken from the well-fixed case. Furthermore, peak shifts of 53.1 ± 13.7 Hz (in the 700 to 1200 Hz range) and 66.2 ± 9.0 Hz (in the 1200 to 2200 Hz range) can be observed. A graphical example of these two loosening indicators can be seen in Figure 3.5 b.

Method 2: Extracorporeal mechanical excitation/intracorporeal mechanical signal. This method was established by three technologies:

(T2-C1) Puers *et al.* [34] also designed an instrumented hip prosthesis but, differently, housing an acceleration sensor and some additional electronics in the implant head. The implant loosening detection is observed by analyzing the waveform distortion of the output acceleration signal (Figure 3.5 a) when extracorporeal vibrations (100 to 200 Hz) are driven by a shaker placed on the distal end of the femoral bone. Loosened implants are detected by observational verification of non-similarity between the excitation signal and the measured acceleration outcome. Two interface states distinction were reported: secure or loose.

(T2-C2) Marschner *et al.* [64] incorporated a two-axis accelerometer and supporting electronics inside an instrumented hip implant (distal end of stem) to measure shifts in the resonance frequency of the output vibrations when an extracorporeal shaker

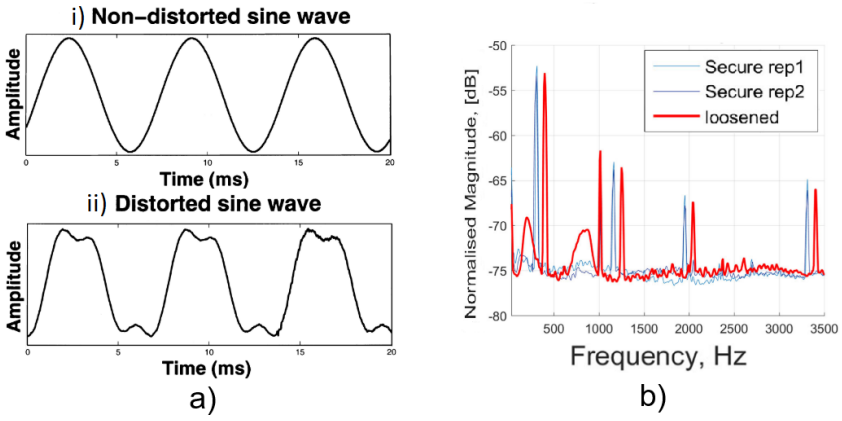

Figure 3.5: (a) Graphic showing the distinction of waveform in the cases of loose and fixed implants. The fixed case output signal (i) resembles the input frequency driving the system. In contrast, for the loose case (ii), signal distortion can be observed. Adapted from the work in [34] with permission from Elsevier. (b) Graphic showing the effect of a loose implant in a frequency analysis. The loose implant (in red) can be characterized (by comparison with the fixed, in blue) by an increase in the resonance frequency and by the appearance of harmonics in the output signal. Adapted from the work in [63] under the Creative Commons Attribution 4.0 International License: http://creativecommons.org/licenses/by/4.0/.

delivers a mechanical excitation (500 to 2500 Hz) on the distal femur condyle. This technology to detect loosening of total hip replacements also includes the ability to perform wireless monitoring and to be inductively powered. Two loosening states (proximally loose and proximally secure) can be distinguished in a band within the 1500 to 2500 Hz range. The shift threshold can exceed 300 Hz.

(T2-C3) Sauer *et al.* [65] developed a similar technology to Marschner *et al.* [64] by incorporating a three-axis acceleration sensor in the implant head (and some additional electronics) and delivering extracorporeally mechanical excitations (500 to 2500 Hz), and, using a shaker placed at the central part of the femur, the implant loosening detection is observed by identifying shifts in the resonance frequency of accelerations measured inside the implant. Three loosening states were detected in the 500 to 1500 Hz range: maximum, medium, and minimum loosening. These states could be distinguished according to frequency shifts up to 100 Hz (approximately in the 20 to 100 Hz range).

As observed, for uncemented fixations, the proposed methods were specifically developed for hip and knee joint implants. Most technologies (five out of eight) were developed employing extracorporeal excitation and extracorporeal sensing (Method 1). The less explored method concerns three technologies (out of eight) with a higher level of sophistication by incorporating sensors within the bone implant (Figure 3.6 schematizes these technologies). A common feature found in all technologies is the requirement for extracorporeal mechanical excitation. Nevertheless, the intracorporeal components of instrumented implants require inductive powering via extracorporeal coils. Regarding the interface monitoring, six technologies (out of eight) only identified two loosening states (secure or loose), whereas the other two technologies identified several loosening stages (up to three). Similarly to the uncemented technologies, none of these technologies were designed to assess loosening in different locations, and their operation is limited to laboratory testing, hardly adaptable for continuous operation throughout the daily life of patients. The loosening detection is mainly computed by analyzing shifts in the output resonance frequency. However, sensing was also performed by evaluating the harmonic ratio and number of harmonics defining the output signal and also by observing the non-similarity between the input excitation and output measured acceleration. All the established methods were validated *in vitro*, and only one of them was validated both *in vivo* and *in vitro*. No measure accuracy was provided to further analyze the technology performance.

Limitations of vibrometric monitoring technologies

A general limitation of vibrometric methods is the patient-dependent output vibration due to the strong influence of soft tissues surrounding implants on mechanical wave propagation [61]. It is pertinent to emphasize that most of the proposed methods are specifically designed for hip and knee joint implants. The ability of the vibrational approach to monitor the fixation state in hip implants was computationally analyzed (using the finite element method) by Qi, Mouchon, and Tan [58] for cemented fixations and by Pérez and Seral-García [66] for uncemented fixations. Regarding the first model, only reliable loosening detection of cemented hip fixations can be obtained for failure sizes exceeding one-third of the stem length, although some inconclusive data can be provided

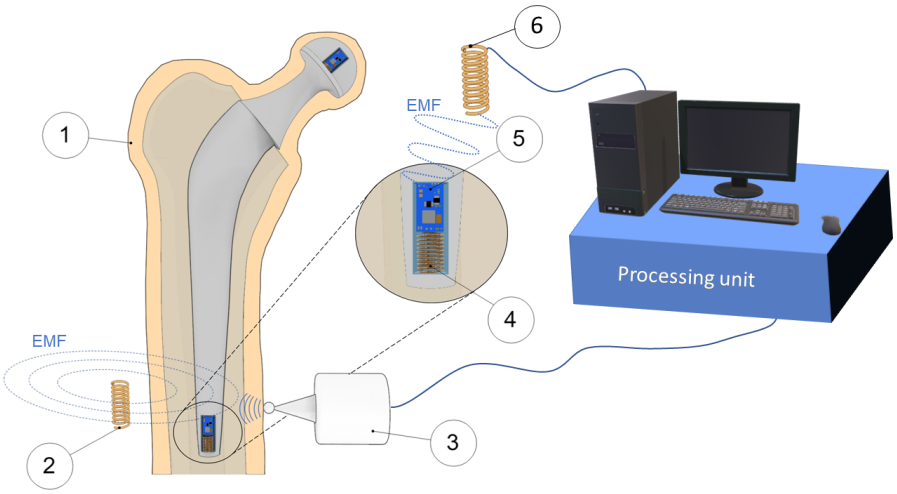

Figure 3.6: Illustration of the 2nd method (extracorporeal mechanical excitation/intracorporeal mechanical signal) for vibrometric cemented fixations: (1) Human tissue; (2) Extracorporeal coil required to power the system through electromagnetic induction; (3) Extracorporeal shaker providing the input mechanical excitation; (4) Intracorporeal coil used to power the system; (5) Intracorporeal monitoring system. (6) An extracorporeal coil was used to acquire data from the sensor through magnetic induction; afterwards, the data is sent to a processing unit (EMF: electromagnetic field).

for failure sizes greater than one-fifth of the stem length. Although effective identification of different states of uncemented fixations can be provided, Pérez and Seral-García [66] only managed to detect differences in the resonance frequency for input frequencies greater than 2400 Hz. In addition, Leuridan *et al.* [62] also developed a computational model to predict failures on cemented knee implants, namely, to detect loosening of the tibial component. Failure states can be detected when more than 15% of the implant surface is loose on the lateral and medial side.

Concerning the first monitoring method (input: extracorporeal mechanical excitation; output: extracorporeal mechanical signal) for both uncemented and cemented fixations, as extracorporeal technology is required, two mutually exclusive scenarios may occur: (i) the nonstop tracking of fixation states requires the attachment of technologies to the patient's body, which is uncomfortable and troubles the activities of the patients, or (ii) the circumstantial monitoring implies the inability to obtain effective monitoring data throughout the daily living of patients. Indeed, this issue could be overcome if the monitoring technologies could be designed to be incorporated inside instrumented implants. Nevertheless, the overall components were not designed to be housed within the implants, but only the acceleration sensors and processing systems (as carried out by technologies developed for cemented fixations using the 2nd method). The ability of this noninvasive method to detect where loosening failures are occurring was not demonstrated. Still, the loosening location cannot be accurately detected due to the diffusivity nature of the mechanical excitation, which makes the delivery of different excitations to much closed target regions quite hard to achieve [67]. Most technologies are only able to detect if the implant is loose or the opposite. Five technologies successfully provide more than two levels of detection. Regarding the medical devices engineered to analyze

the intraoperative implant stability [52, 53], an overall analysis to the bone–implant interlocking (primary stability) along the implant surface cannot be obtained. Besides, as low-frequency shifts are required to identify the stable–unstable threshold, precision and expansive electronic systems are required. Note that only four (out of seventeen) technologies were validated *in vivo*. Interestingly, an additional technology was reported by Rieger *et al.* [49] using laser vibrometry, but it is not suitable for clinical practice.

Concerning the second monitoring method (input: extracorporeal magnetic induction; output: extracorporeal mechanical signal) for uncemented fixations, mechanical systems (magnetic oscillators and springs) must be embedded within the instrumented implant to provide an intracorporeal excitation, even if an extracorporeal excitation system is required, similarly to the technologies designed by Puers *et al.* [34], Marschner *et al.* [64], and Sauer *et al.* [65]. This limitation troubles an effective biointegration monitoring throughout the daily living of patients. The use of magnetic induction to provide the primary excitation also demands complex extracorporeal systems to deliver different excitations to different intracorporeal oscillators, and thus a personalized monitoring of target regions along the implant surface will be hard to achieve [67]. The experimental results using the technology developed by Ruther *et al.* [38] highlight the difficulty to distinguish between different loosening states by analyzing the resonance frequency shifts. Nevertheless, a significant technological breakthrough was also performed by Ruther *et al.* [57], as they designed an instrumented hip implant to measure several loosening locations, although no experimental results (neither *in vitro* nor *in vivo*) were provided. Finally, *in vivo* tests need to be conducted to demonstrate the clinical potential of technologies from the second monitoring method.

Concerning the second monitoring method for cemented fixations, some components of the technologies developed by Puers *et al.* [34], Marschner *et al.* [64], and Sauer *et al.* [65] must operate extracorporeally, namely, to generate and drive the excitation signals. The miniaturization of the excitation source could be carried out to house the overall technology inside the implant; nevertheless, this technology upgrade would not be enough to accurately identify the regions where varying bone–implant integrations occur. The alternative would be to design extracorporeal mechanical vibration systems much more complex, such that they would be able to deliver excitations to much closed target regions. Although the instrumented implants were designed to incorporate acceleration sensors, microcontrollers, and additional electronics to support sensing and telemetric link, the data processing is extracorporeally conducted. Intracorporeal processing capability will require precise electronics and powerful processing units, as low-frequency shifts must be automatically detected, which will certainly impose a more complex and expensive manufacturing of the instrumented implants. Detection reliability requires the use of additional analyses to measured outcomes (such as the computation of the central frequency, as proposed by Ruther *et al.* [38]), which, in turn, demands additional processing capability. No results were reported related to loosening states in different regions along the implant surface. Besides, neither technologies comprising electromechanical components incorporated inside the implants were validated *in vivo*, nor measure accuracies were provided.

The single technology proposed in the third method presents some limitations as well. The need for extracorporeal components makes harder for continuous monitoring. One possibility for overcoming that limitation is attaching the components to the patient, although that makes patient movement cumbersome. Another possibility is to integrate

the components (accelerometers) in the implant itself, which will in turn require for a miniaturization of the technology. Despite these scenarios, some difficulties in the measurements may arise. Unwanted noises from different movements or even arising from muscular activity can make the analysis troublesome. Furthermore, different implant materials highly influence the output signal, as shown by the authors. This highlights the necessity of studying each individual combination of types of implants and their materials with the objective of recording the different results, aiming to have a comparable data set of the different frequency patterns.

3.3 The acoustic approach to monitor implant loosening states

Monitoring methods and technologies for cementless fixations

Three methods and five technologies were already proposed (Table A.3, Appendix A), as follows.
Method 1: Extracorporeal mechanical excitation/extracorporeal acoustic signal. Three technologies implemented this method:

(T1-L1) Unger *et al.* [68] developed a noninvasive technology to assess the hip implant stability. The extracorporeal excitation was provided by hand hitting the implant with a metallic device. The produced sound was monitored with an extracorporeal microphone attached to the lateral condyle. The implant loosening is distinguished by the response frequency: the resonance frequency increases as stability increases (authors observed increases from 400 to 800 Hz). Different fixation scenarios can also be identified by damping analyses: increasing dampened outputs were observed for increasing stabilities.

(T1-L2) The research team of Alshuhri *et al.* [47,48] reported an alternative technology to the one previously described in the vibrometric approach to detect the acetabular component loosening for uncemented fixation, also depicted in Figure 3.1. The only difference concerns the use of an extracorporeal ultrasound probe instead of an accelerometer. Loosening is identified by analyzing harmonic ratios in the output signal. Different loosening scenarios (authors analyzed two loosening states) can be correlated to different harmonic ratios. The ultrasound measurements were performed in the 200 to 1500 Hz range, although the most sensitive excitation frequency was observed in the 200 to 950 Hz range. Note that the output signal presented higher harmonic ratios when compared to the monitoring data obtained using the accelerometer. The ultrasound results are shown in Figure 3.7.

(T1-L3) Goossens *et al.* [69] engineered a custom-made technology to monitor the fixation states of the acetabular component of hip implants. The driving excitation input was provided by an extracorporeal hammer by hitting a metal rod connected to the simulated acetabular component. The acoustic outcomes were measured using an extracorporeal microphone, suspended above the experimental setup (approximately 20 cm) (Figure 3.8). The authors tested several fixation levels which could be distinguished by analyzing shifts in the output resonance frequency. The tests showed differences in the output frequency according to the different components (artificial

and cadaveric pelvis) and the shifts were observed ranging from 9 to 248 Hz, which are bone model-dependent.

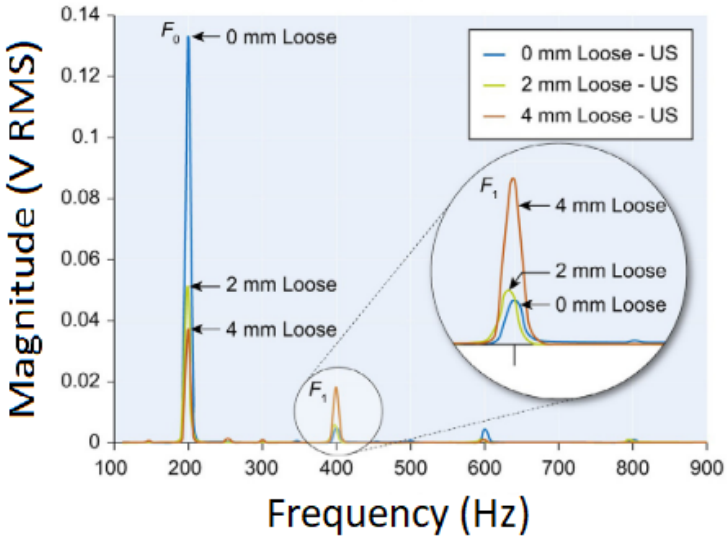

Figure 3.7: Illustration of the distinction between three implant fixation states: fixed, 2mm loose, and 4mm loose. An increase in the harmonics magnitude can be observed with increasing acetabular cup loosening. Adapted from the work in [47] with permission from Elsevier.

Figure 3.8: Example of *in vitro* testing of the T1-L3 technology for uncemented fixations of the acoustic approach. The following components are included; artificial pelvis, microphone (suspended above the artificial pelvis), the metal rod (connected to the acetabular cup), and the hammer (used to drive the system). Reprinted from [69] with permission from Elsevier.

Method 2: Intracorporeal mechanical excitation/extracorporeal acoustic signal. A single technology implemented this method:

(T2-L1) Glaser *et al.* [56, 70] developed an alternative technology to analyze the output of the previous T3-L1 technology for uncemented fixations in the vibrometric approach. The difference concerns the analysis of the resulting sound emissions from the intracorporeal implant displacement, instead of the mechanical vibrations. Acoustic emissions were recorded with an extracorporeal sound transducer attached on the skin surface in the closest distance to the hip joint interface. High correlation was observed between the data obtained by the sound transducer and the accelerometers.

Method 3: Extracorporeal magnetic induction/extracorporeal acoustic signal. A single technology implemented this method:

(T3-L1) Ewald *et al.* [71,72] developed an innovative technology using a similar method to the one proposed by Ruther *et al.* (technology T2-L1 for uncemented fixations using the vibrometric approach). Similarly to Ruther *et al.* [71,72], they also incorporated spherical oscillators inside the implant, near the stem wall, attached to a flat spring, which are driven by magnetic induction excitations provided by extracorporeal coils (Figure 3.9). Unlike Ruther *et al.* [71,72], they used an extracorporeal microphone to record the resulting sound emission originated by collisions of the oscillators with the implant walls. The output sound emission was recorded on a wide frequency range, namely between 0 and 20 kHz. Different fixation scenarios can be detected (the authors identified up to four) by observing shifts in the output resonance frequency. The resonance frequency of the fixed and loose scenarios is up to 10 kHz apart.

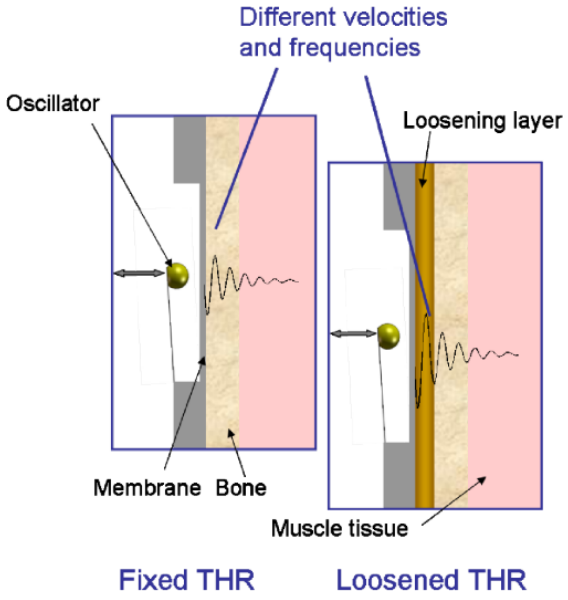

Figure 3.9: Schematic of the principle behind Ewald *et al.* and Ruther *et al.* oscillator loosening detection system. It clearly demonstrates the effect of a loose implant in the output signal frequency and intensity [72]. Figure registered under ©2011 IEEE.

Relative to the system's input, four out of the five technologies require an extracorporeal stimuli, namely, mechanical vibration or magnetic induction; in contrast, a single technology was developed to record the acoustic emissions originated from the implant's own motion. Note that all the described studies use extracorporeal sensors to monitor the implant–bone interface state. One may also highlight that two methods minimize patient's discomfort and contact by using a technology requiring magnetic induction as excitation, or by using a technology that does not require extracorporeal excitation. Similarly to the vibrometric approach, the loosening detection was mainly computed by analyzing shifts in the output frequency (three out of five), although harmonic ratios and the analysis of the amplitude and frequency of the output signal were also assessed. None of the presented technologies are able to identify the regions where loosening occur; however, all the technologies managed to distinguish more than one loosening stage. Regarding the experimental validation, four out of the five technologies only validated their methods *in vitro* while the remaining one only performed *in vivo* validation. A common feature shared by all technologies is their inability to provide sensing data throughout the daily living of patients (monitoring limited to laboratory facilities).

Monitoring methods and technologies for cemented fixations

Four methods and ten technologies were already proposed (Table A.4, Appendix A), as follows.

Method 1: Extracorporeal mechanical excitation/extracorporeal acoustic signal. Three technologies implemented this method:

(T1-C1) Rowlands, Duck, and Cunningham [61] engineered a technology similar to T1-C3 technology using the vibrometric approach. The only difference concerns the use of an extracorporeal ultrasound transducer to monitor acoustic signals in the proximal femur. Similar results to the ones provided using extracorporeal accelerometers were observed, although higher magnitude signals can be obtained. Same as before, they only provided results for the loose implant.

(T1-C2) The technology developed by Unger *et al.* [68] for uncemented fixations (T1-L2) can also be applied in cemented fixations. The driving excitation is provided by hitting the femoral condyle with hammer strikes, and the extracorporeal microphone is attached to the hip. The implant stability is assessed by analyzing shifts in the resonance frequency. At least three distinct loosening scenarios are distinguished: secure, fissured (in the cement), and loose. The detection algorithm includes the analyses to harmonics and damping of the sound outcome, as resonance frequencies and damping increases for increasing stabilities. Different fixation scenarios can also be identified by observing resonance frequencies below 1000 Hz. An *in vivo* experiment showing the technology operation is illustrated in Figure 3.10 a.

(T1-C3) Dahl *et al.* [73] developed a technology to quantify different levels of osteointegration of the talar component of total ankle prosthesis (Figure 3.10 b). An extracorporeal actuator (ankle foot orthosis), located around the ankle, drives a mechanical excitation to impose motion to the talar component. The resulted vibration is detected by an ultrasound probe in the skin's surface. Loose and fixed states are analyzed by computing the ratio of magnitudes of harmonics with the driving frequency: this ratio decreases as the fixations state is improved.

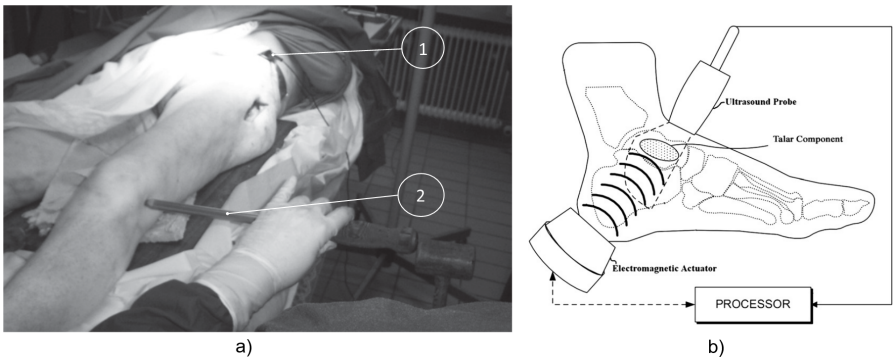

Figure 3.10: (a) Cadaver test performed in the development of T1-C2 technology for cemented fixations of the acoustic approach. In which one can observe (1) the microphone placed on the hip to measure the resulting vibration provided by (2) the impact hammer. Adapted from the work in [68] under the Creative Commons Attribution 4.0 International License: http://creativecommons.org/licenses/by/4.0/. (b) Schematic of T1-C3 technology for cemented fixations of the acoustic approach. Reprinted from [73] with permission from Elsevier.

Method 2: Intracorporeal mechanical excitation/extracorporeal acoustic signal. Five technologies implemented this method:

(T2-C1) Davies, Tse, and Harris *et al.* [74] developed a monitoring technology to assess the cement–stem interface condition after hip arthroplasty. The analysis was focused on monitoring acoustic emissions generated by the cement–metal interface debonding or by cement cracks when the femur is physiologically loaded. An extracorporeal acoustic emission transducer attached to the femur's mid-surface is required to monitor the acoustic emissions. Different interface stages can be observed by analyzing varying acoustic intensities and waveforms. However, this technology is not able to distinguish acoustic emissions between debonding of interfaces (without cement cracks) and cracks in the cement mantle.

(T2-C2) Roques *et al.* [75] developed a technology to monitor the fatigue-related cement failures in the bone–cement interface. Two extracorporeal acoustic sensors, up to 70 mm away from each other on the top surface of the cemented device, were used to detect differing acoustic patterns due to crack propagation after static and dynamic loading. Progressive failure is distinguished by analyzing the energy and duration of the acoustic signal output: both increase with the fatigue crack growth. Interestingly, this technology is able to detect the crack location by analyzing the arrival time of the acoustic waves.

(T2-C3) Qi *et al.* [76] developed a technology to assess cement failures in hip implants using eight extracorporeal acoustic emission sensors, attached along the medial–proximal femoral surface, and dynamically loading the femur. Crack locations can also be detected by measuring the arrival time of the acoustic waves. This monitoring system is able to distinguish the progress of crack formation based on the arrival times, number of events, signal energy, amplitude, and their location distribution. An *in vitro* test showing the experimental setup is depicted in Figure 3.11 b.

(T2-C4) Gueiral and Nogueira [77] designed a similar monitoring system to Qi *et al.* [76] (T2-C3) to monitor cement deterioration, but only used three acoustic transducers arranged in a cylindrical disposition at the femur surface. Acoustic events were characterized by their energy, amplitude, and arrival time. Their location can be predicted as well. The authors used the following parameters to characterize the acoustic emissions; amplitude, duration, and number of threshold crossings, although no concrete values were given.

(T2-C5) Mavrogordato *et al.* [78] also proposed a technology to monitor cement deterioration in hip implants but including the ability to operate with surrounding soft tissues. The excitation is provided by delivering dynamic loading to the hip stem. Four acoustic sensors are externally mounted on the cement mantle along the stem length. The chosen criteria to find relevant acoustic events was based on the energy and rise time of the output signal. This technology is also able to predict the crack location by measuring the arrival time across different sensors. Components and materials used by the authors in the *in vitro* test can be seen in Figure 3.11 a.

Method 3: Intracorporeal mechanical excitation/intracorporeal acoustic signal. Only a single technology was designed using this method:

(T3-C1) Mavrogordato *et al.* [78] also engineered a technology using intracorporeal acoustic sensors to monitor the cement–implant interface of hip implants. This method is similar to the previous T2-C5, but the sensors are embedded within the implant stem. The results regarding the intracorporeal sensors showed higher sensi-

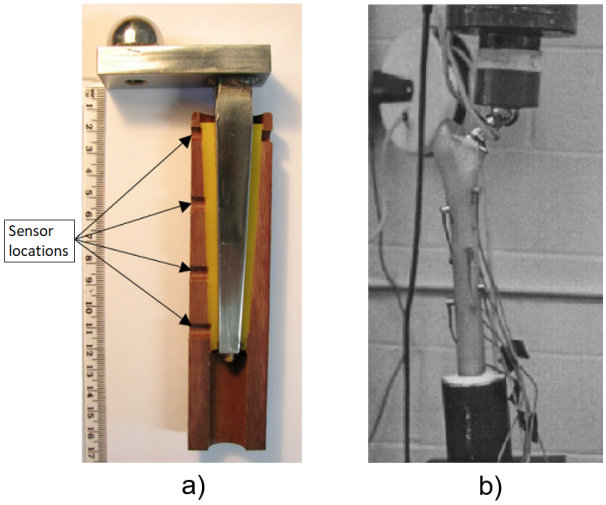

Figure 3.11: (a) Example of *in vitro* testing of the T2-C5 technology for cemented fixations of the acoustic approach. The used implant, cement, and Tufnol tubing can be observed. Adapted from the work in [78] with permission from Elsevier. (b) Experimental set-up used by Qi *et al.* in the development of T2-C3 technology for cemented fixations of the acoustic approach; the figure shows the implant inserted in the artificial femur, the acoustic emission sensors placed at the femur's surface, and the loading machine [76]. Figure registered under ©2004 Wiley Periodicals, Inc.

tivity in detecting acoustic events when compared to the extracorporeal sensors, as well as minor influence from ambient noise.

Method 4: Extracorporeal acoustic emission/extracorporeal acoustic signal. Only a single technology was tested using this method:

(T4-C1) Davies, Tse, and Harris [79] developed an active acoustic emission technology to assess the cement–implant interface state. The same extracorporeal device—an ultrasonic pulser/receiver—is attached to the femur's surface. The interface bonding state was identified by emitting an ultrasonic wave through the cement and implant and consequent analyzes to the reflected acoustic signal outcome, namely, the amplitude and arrival time. A bonded interface is characterized by detecting a secondary signal corresponding to the reflection of the wave in the metal surface. In contrast, with a debonded surface, only the primary signal can be observed. Only two interface states were distinguished: bonded and debonded. A scheme illustrating the principle behind the emitter/receiver and the wave reflection is displayed in Figure 3.12.

Most of the described technologies were developed for hip implants (nine out of ten); only one research group focused their research on the fixation monitoring of an ankle implant. The most explored method requires extracorporeal acoustic emission sensors to monitor the cement mantle integrity (five out of ten): note that most of the proposed technologies, with the exception of one, used extracorporeal sensors to measure the output signal. A wide variety of analysis was conducted to conclude about the interface state. The second and third methods were established by computing the loosening detection by analyzing the acoustic magnitudes, waveform, duration, energy, and rise time. The first method presents similarities, with many of the previously described requiring both extracorporeal excitation and extracorporeal sensors; therefore, stability assessment can be carried out by analyzing harmonic ratios and shifts in the output resonance frequency. In a distinct way, the fourth method analyzed the reflected wave's magnitude and time of arrival to monitor the cement mantle bonding state. Regarding the interface state monitoring ability, only five (out of ten) technologies can predict the location of acoustic events. Seven (out of the ten) technologies can distinguish between more than two interface states; the other three technologies only managed to distinguish between loose or secure interfaces. All the technologies were validated *in vitro*, but no *in vivo* validations were carried out.

Limitations of acoustic monitoring technologies

Similarly to the vibrometric approach, for both cemented and cementless implants, acoustic technologies present a patient-dependent general limitation, due to the influence of the surrounding soft tissues on wave propagation. Another similarity is related to their application: most of the proposed technologies were engineered for hip implants, although some of them were also targeted for knee and ankle implants. Progressive monitoring of the cement integrity was computationally modeled by Qi *et al.* [76]. Their model was used to assess the 3D locations of the cracks, as well as their dynamic emergence. Although progressive crack monitoring was achieved, the group noted a lack of accuracy in computing the data regarding the crack's location due to the high sampling rate. A technology resembling the second method (acoustic methodology) for both

cemented and cementless fixations was also developed [80, 81]. Their technology was implemented for hip implants, such that it comprises four acoustic emission sensors to detect acoustic events originated from the implant's motion. By progressively monitoring the implant and computing the acoustic emissions, it is possible to detect sounds which can be indicative of the implant's wear and damage. Although they showed the sensors working principle, a clear correlation between the interface state and the output signal was not reported.

It is pertinent to emphasize that all the proposed acoustic technologies require extracorporeal reading units. This is a significant limitation that shrinks the applicability range and the possibility for continuous interface monitoring, as the electromechanical components attached to the patient's body cause discomfort and troubles in their daily life, which, excluding the latter possibility, limits the technology's operation to the laboratory environment, and in turn disregards the interface state dynamics and does not allow timely delivery of therapeutic stimulation [37]. Mavrogordato *et al.* [78] were the only authors that aimed towards a more sophisticated monitoring system by housing the sensors within the implant's stem, although their technology also requires external units. The driving mechanism also plays an important role in patient's comfort and method versatility. Using extracorporeal excitation units, constrains even further the possibility of turning the technology portable. Miniaturization of components could be a feasible solution; nevertheless, the need to carry more than one component attached to the patient's body imposes an even greater burden. Concerning this matter, the second method (applied to both cemented and cementless technologies) presents an advantage because it does not demand input excitation components, as the driving signals are generated intracorporeally, either from the cement mantle or from the implant's motion. Furthermore, the use of shakers or hammers may cause pain and discomfort for the patient, although this effect is frequency-related. In addition, by using non-contact excitation systems, such as magnetic induction input sources, the mechanical contact with the patient's body is minimized, reducing the risk of infections.

Regarding the second method for cementless and cemented fixations, as well as the third method for cemented fixations, a general limitation is shared by the developed technologies: the susceptibility to undesirable or not expected noises. Either from the surrounding tissues or from ambient background sources, there is a number of environ-

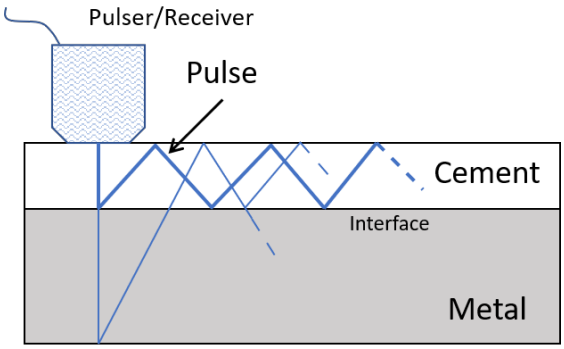

Figure 3.12: Schematic of the T4-C1 technology for cemented fixations of the acoustic approach. The effect of a bonded/debonded surface on the reflection of the wave and its time of arrival are clearly demonstrated. Based on the work in [79].

mental factors that may compromise the effectiveness of this method. Ambient noises can be avoided by providing a controlled space, although this scenario excludes the possibility of continuous monitoring, which is a requirement for technologies assessing the progressive damage in cement. Other acoustic signals arising from unwanted internal sources can be avoided by using databases of known noises. A research group [80] resorted to using patients with natural hips to provide a baseline of ambient noise characteristics and unwanted vibrations due to the implant motion.

Concerning the fourth cemented method, the estimation of the wave's reflection will most likely be hard to achieve due to topological nonlinearities of the interface. The authors also stated that the smallest detectable area was half the diameter of the transducer. Furthermore, as this technology only comprises extracorporeal components, it will have the associated limitations as previously explained.

3.4 The bioelectric impedance approach to monitor implant loosening states

Monitoring methods and technologies for cementless fixations

One method and one technology were already proposed (Table A.5, Appendix A), as follows.

Method 1: Extracorporeal electrical current/extracorporeal electric potential difference. A single technology established this method:

(T1-L1) Arpaia and Clemente *et al.* [82, 83] used electrical impedance spectroscopy to assess bone–implant integration states. This technology requires two extracorporeal electrodes, which are used to deliver a variable current at the skin's surface and measure the voltage drop between them (Figure 3.13). The resulting impedance is correlated to the interface state: the impedance increases for decreasing levels of integration. Furthermore, no information concerning the location of less stable regions is provided.

This technology exclusively utilizes extracorporeal components and thus its use is limited to a laboratory environment. As described, the interface state can be assessed by computing the resulting electrical impedance, and different interface states can be correlated to different impedance values. The identification of areas with lesser bone–implant integration levels was not achieved. Concerning validation, *in vitro* and *in vivo* tests were made, although the latter was performed with percutaneous implants.

Limitations of bioelectric impedance monitoring technologies

Analyzing the single proposed technology, the use of extracorporeal components limits its monitoring ability, because its use is limited to a specific environment (laboratory). Another important limitation is the influence of patient physiology. As this technology relies directly on the tissues response to electrical stimuli, the output signal will vary accordingly to the tissues composition. A possibility to overcome this limitation is to create a database with the typical impedance values according to the patient's physical characteristics. Even so, due to the complexity of the human's tissue, this technology may prove difficult to be applied.

3.5 The magnetic induction approach to monitor implant loosening states

Monitoring methods and technologies for cementless fixations

One method and two technologies were already proposed (Table A.6, Appendix A), as follows.
Method 1: Extracorporeal magnetic induction/extracorporeal magnetic induction. Two technologies implemented this method:

(T1-L1) Ewald *et al.* [71] developed a piezo-acoustic method to monitor implant loosening states. The technology comprises a piezo crystal (Figure 3.14) incorporated within the implant, which vibrates when it is driven by a magnetic field provided by an extracorporeal coil. According to the state of the bone–implant interface, the crystal's vibration presents different dampening characteristics, which can be measured inductively, throughout an extracorporeal coil. Different interface states can be distinguished by analyzing the output signal amplitude for excitations with a constant frequency (the authors reported a frequency of 83 kHz).

(T1-L2) With a similar technology to T2-L1 of the cementless vibrometric method, Ruther *et al.* [84] used a different approach to measure the output signal. The same oscillators are driven through magnetic induction provided by an extracorporeal coil, and, instead of reading a resulting mechanical vibration, an extracorporeal coil is used to measure the resultant oscillator velocity caused by the impact. By placing the oscillators in a magnetic field, their displacement induces a current in the extracorporeal coil, which is proportional to their velocity. Different loosening states can be distinguished by computing the oscillator's velocity after impact.

Both the proposed technologies drive the systems through magnetic induction; moreover, both assessed the output signal also via magnetic induction. The components used for both the excitation and monitoring were extracorporeally positioned. Regarding the

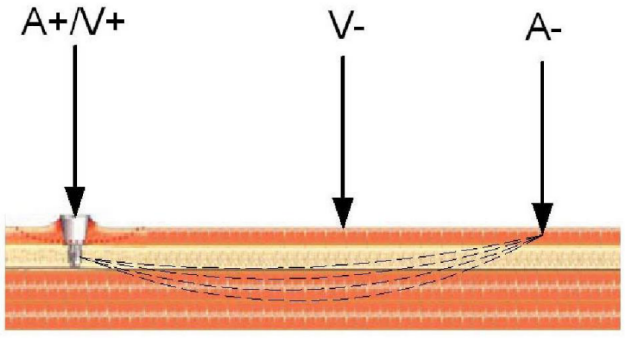

Figure 3.13: Illustration of the working principle of the single proposed technology in the bioelectric impedance approach. One can see the electrodes placed on the skin surface to generate an alternate current (A+/A−), resulting in a voltage drop (V−) that can be directly correlated to the impedance [83]. Figure registered under ©2007 IEEE.

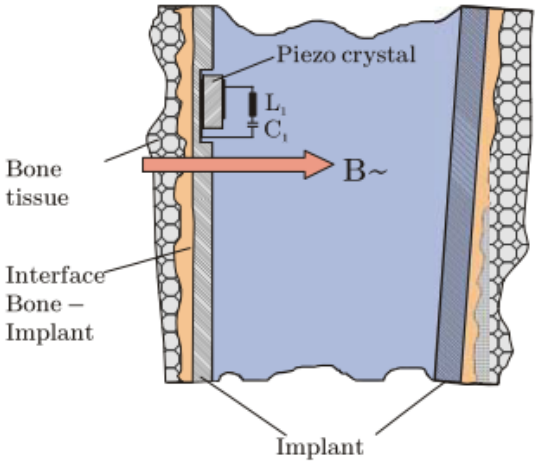

Figure 3.14: Illustration of the working principle and architecture of the piezo-acoustic method. The crystal is integrated inside the implant's walls and driven by a magnetic field. The crystal's vibration dampening is affected by the surrounding tissues [71]. Figure registered under ©2011 IEEE.

detection algorithm, the amplitude of the output signal and velocity of the magnetic oscillators are used. Similarly, both technologies were limited to laboratory analysis and were only validated *in vitro*.

Limitations of magnetic induction monitoring technologies

The use of magnetic induction to measure the bone–implant integration requires the use of non-magnetic materials in the interface. This issue can indeed be inconvenient, as the design of multimaterial implants must be considered. Regarding the components, the use of extracorporeal coils limits the application of these methods to a laboratory environment, excluding the possibility for continuous monitoring. Furthermore, the risk of electromagnetic interference emphasizes the need for a controlled testing apparatus. In both technologies, the monitoring ability is limited to the proximity between components. To perform monitoring operation in various regions, several components must be incorporated within the implants along, and near to, the implant's walls. This feature requires miniaturized components to avoid compromising the implant's physical integrity.

In a similar way as the vibrometric and acoustic methodologies, this method also relies on the patient-dependent dampening strongly influenced by the tissues condition.

3.6 The strain approach to monitor implant loosening states

Monitoring methods and technologies for cementless fixations

Two methods and two technologies were already proposed (Table A.7, Appendix A), as follows.

Method 1: Intracorporeal mechanical loads/intracorporeal bone deformation. A single technology implemented this method:

(T1-L1) Burton, Sun, and Lynch [85] developed a strain sensor to measure bone growth. The technology comprises two cosurface circuits: one for measuring the axial strain, and the other for the radial strain (Figure 3.15 a). Each circuit was connected to a parallel-plate capacitor whose dielectric changes according to strain variations; the second is further connected to a titanium fuse which yields according to a set threshold of radial deformation. Powering and signal reading were achieved through extracorporeal magnetic induction. The changing capacitance values are assessed by monitoring shifts in the output resonance frequency: increasing strains shift the resonance frequency to lower values. This technology is meant to operate in contact with the bone tissue, wrapped around the bone structure.

Method 2: Intracorporeal mechanical loads/intracorporeal fixation plate deformation. A single technology implemented this method:

(T2-L1) McGilvray *et al.* [86] developed a biocompatible, microelectromechanical technology to track the fracture healing in implantable fixation plates (Figure 3.15b). It comprises intracorporeal planar capacitors and a resonance circuit incorporated in the implant to monitor variations in physical loading. Changes in the capacitance cause shifts in the resonance response frequency: a decrease in loading increases the resonance frequency. The technology is powered inductively through an extracorporeal antenna which also performs as the receiver of the sensor's signal.

Both of the proposed technologies in the strain methodology are both driven by mechanical loading, provided by the body's own weight. Similarly, both technologies output strain is measured through differences in the system's capacitance, by analyzing the resonance frequency. Regarding the monitoring potential, the technologies managed

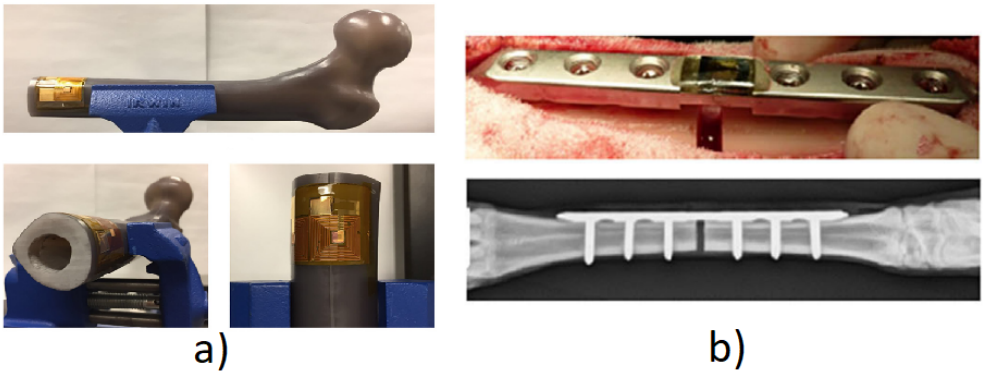

Figure 3.15: (a) Illustration of the flexible capacitive circuit for strain monitoring. The sensors can visibly adapt to the bone tissue structure [85]. Reprinted by Permission of SAGE Publications, Ltd. Copyright ©2019, ©SAGE Publications. (b) Fixation plate integrated with the capacitive and resonating sensor (in the middle) [86]. Figure registered under ©2015 Orthopaedic Research Society and published by Wiley Periodicals, Inc.

to distinguish a secure state and several degrees of loosening. Both technologies were validated *in vitro*, although only one was validated *in vivo*.

Limitations of strain monitoring technologies

Both of the proposed technologies require extracorporeal powering, which limits the method's applicability. One solution is to incorporate an intracorporeal power source or attached powering components to the patient's body, although the latter can be a burden. Furthermore, the reading operation is performed by analyzing the technology response frequency, through magnetic induction, with extracorporeal components. This emphasizes the need for a controlled environment, as electromagnetic noise can interfere with the results. Regarding the first method's technology, as the circuit is meant to operate in contact with the bone, it can also act as an obstacle for bone integration. Although the technology developed by McGilvray *et al.* [86] (T2-L1) was designed for fixation plates, the same technology can be applied in other implant technologies requiring bone implant integration.

3.7 The capacitive approach to monitor implant loosening states

Monitoring methods and technologies for cementless fixations

A single method and technology were already proposed (Table A.8, Appendix A), as follows.
Method 1: Intracorporeal voltage excitation/intracorporeal electric capacitance. A single technology implemented this method:

(T1-L1) Luis Henriques [36] investigated a novel technology to measure bone-implant interface changes. By using an intracorporeal stripped architecture composed by four planar electrodes, intracorporeal electric capacitance changes are measured when an intracorporeal voltage excitation is provided (Figure 3.16 a,b). The assessing of the bone-implant interface is achieved by monitoring the overall system's capacitance, in which the dielectric also comprises the bone sample. The closer bone tissue is, the higher the electric capacitance. Up to date, the powering was only achieved through wires. This technology was further tested *in vitro* using different bone samples. Promising results were obtained relating the capacitance with the distance between the stripped sensor architecture and the bone samples.

By measuring the output capacitance, this technology can assess dielectric changes when the bone-implant interface is changed. Regarding the monitoring ability, this system can distinguish several levels of bone-implant fixation, including the secure state. The technology was only validated *in vitro*.

In the *in vitro* testing, four types of tests were conducted: approximation and contact; decompression and separation; fatigue; and repeatability. The achieved results can be seen in Figures 3.17 a,b, 3.18 and 3.19, respectively.

From Figure 3.17 a one can observe an increase in the capacitance as the bone sample gets closer to the sensor interface; differently, during the decompression and separation phase (Figure 3.17 b), the capacitance decreases as the sample is withdrawn from the

sensor interface. These results evidence the sensitivity and potential of capacitive technologies in assessing bone-implant interface states, managing to distinguish differences in biointegration with slight displacements. Figure 3.18 shows the effect of successively compressing the bone samples, leading to an increase in the general capacitance.

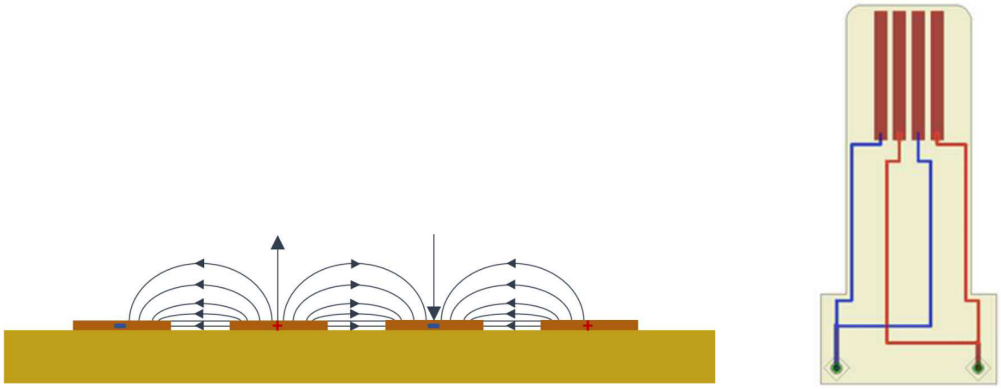

(a) (b)

Figure 3.16: (a) Scheme and representation of the electric field lines produced by a planar capacitance system composed by four stripped electrodes. (b) Final PCB schematic related to the planar capacitance system taken from the software *EAGLE*. From Henriques [36].

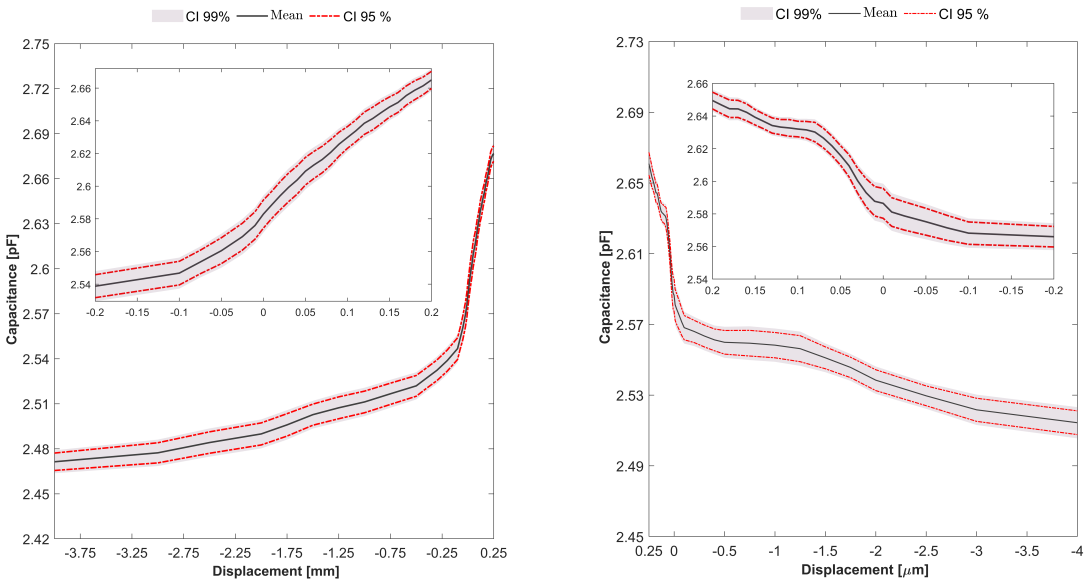

(a) (b)

Figure 3.17: (a) Approximation and contact test. (b) Decompression and separation. Adapted from Henriques [36].

Limitations of capacitive monitoring technologies

The proposed technology was only powered through wires, limiting its applicability. However, since it is a monitoring system with low power consumption, an intracorporeal supply (based on energy harvesting systems) or even an extracorporeal inductive link will most likely be an effective powering solution. Also, the system's reliability on electric fields assessment can be another difficult factor to overcome, as external interference can influence the output capacitive readings. Nevertheless, the incorporation of this

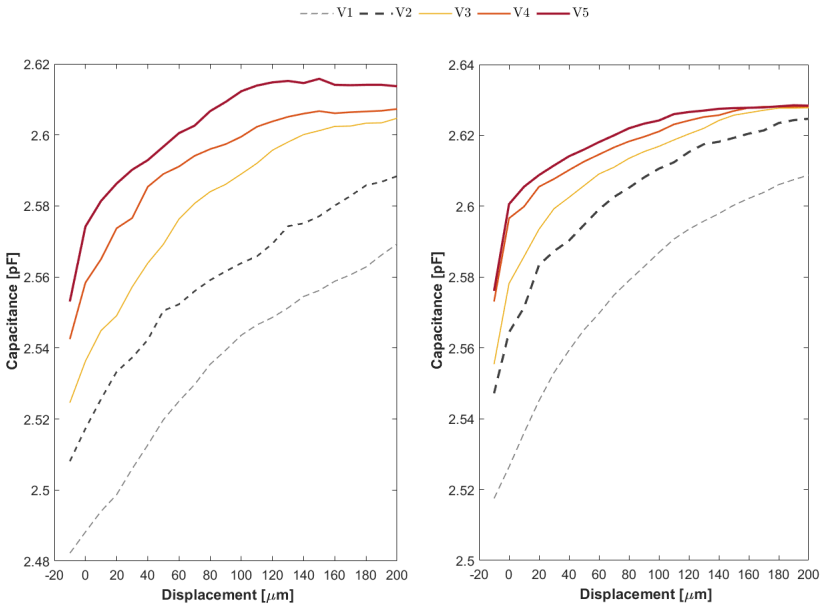

Figure 3.18: *In vitro* fatigue test performed by Henriques. The plots refer to five fatigue tests stages for two separate samples. Adapted from Henriques [36].

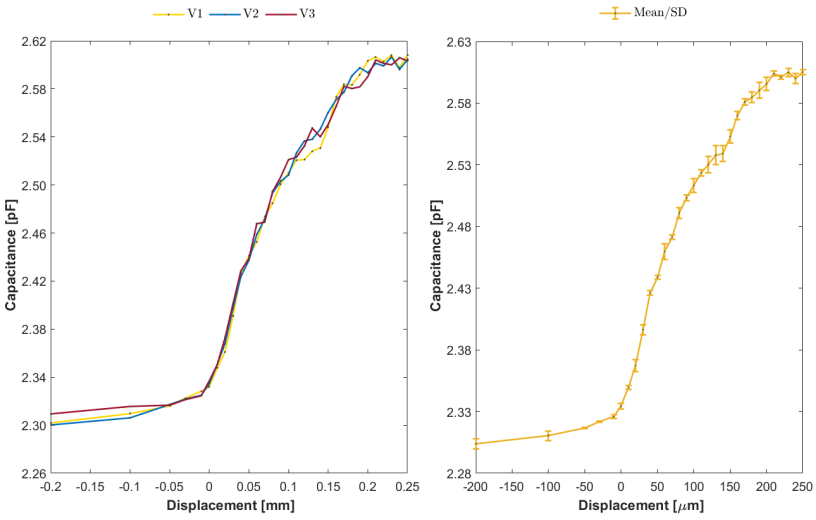

Figure 3.19: *In vitro* repeatability test performed by Henriques. Adapted from Henriques [36].

monitoring system into the implant, will decrease the interference impact, although this must be further tested. Another relevant aspect is the implant's material, since metallic elements greatly influence electric and magnetic fields, the implant will require a non-metallic surface (electrically neutral as possible).

Intentionally blank page.

Part II

Materials and Methods

Chapter 4

Materials

4.1 Sensing technology

Capacitive sensing technologies have the ability of detecting changes in its surroundings induced by variations in the dielectric. These variations can be observed as a change in the sensor's capacitance. In his work, Henriques [36] used a cosurface capacitor, arranged in a planar architecture (Section 3.7). This author projected it aiming to cover key aspects with the objective of making it suitable for instrumented implants. Regarding architecture and power aspects, this system provides low power consumption, cheap fabrication and the possibility of achieving miniaturized dimensions. Due to its planar arrangement, the electric field lines are not limited to the lines perpendicular to the electrodes. Furthermore, the bone structure can be used to define the dielectric which will affect the system's capacitance when changes in the bone occur, such as its positioning related to the electrodes. All these characteristics facilitate the integration of this technology in an implant, which can be placed near the implant's surface, close enough to bone-implant interface, and allow a controlled monitoring.

Following the works of Henriques [36], a similar circuit was used. Although, with the objective of facilitating its integration, a smaller scale printed circuit was developed using the software EAGLE (v9.3.2, Autodesk). The circuit's arrangement and disposition can be seen in Figure 4.1 a. Its fabrication was performed by the Department of Electronics, Telecommunications and Informatics (DETI) from University of Aveiro and the final physical circuit is shown in Figure 4.2. Both electrodes are electrically excited independently to achieve capacitive coupling. Regarding the dimensions, the number of electrodes (n) of the newer circuit is reduced, as well as its length. By referring to Figure 4.1 b, related to the architecture used by Henriques [36], parameters w and g of the newer circuit stayed the same ($g = 0.5\ mm, w = 1\ mm$); while l and the number of electrodes were reduced to half ($l = 5\ mm$, $n = 2$).

4.2 Implant design

A personalized implant was developed to house the sensing technology and to be implanted into a biological organism. The implant was developed using the 3D drawing software Solidworks (v2018-2019, Dassault Systèmes) and the final computer product can be seen in Figure 4.3 a,b. It was manufactured in the Department of Mechanical

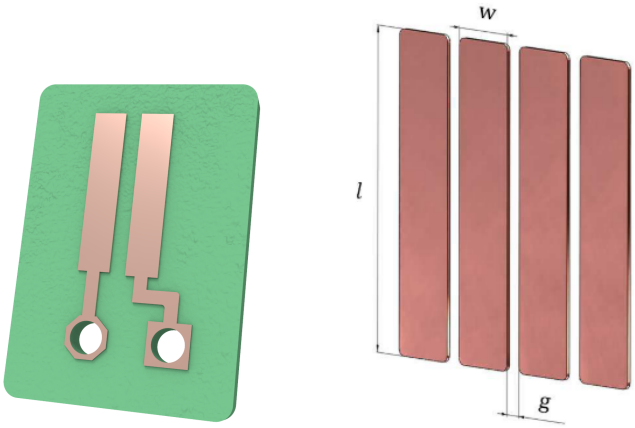

(a) (b)

Figure 4.1: (a) New sensing technology composed of two planar electrodes. (b) Schematic of the planar architecture of the capacitive system used by Henriques [36].

Engineering (DEM) from the University of Aveiro using acrylic as the raw material. The final prototype is shown in Figure 4.3 c and the corresponding technical drawing is in Appendix C, Figure C.1. The material choice presented as decisive, as metallic materials significantly influence the dielectric properties (higher electric conductivity and higher electric permittivity would be obtained), which will negatively influence the results. Hence, the material was required to be as electrically neutral as possible.

As seen in Figure 4.3 a, the implant can house two circuits, placed in distinct areas. These circuits were placed as far from each other as possible to avoid possible electrical interactions between both circuits. As such, their disposition along the implant longitudinal axis aimed to increase the distance between them, opposed to a disposition along the implant radial surface which allowed them to interact through the implant itself. To ensure sensor-bone contact, the implant was developed with a conic geometry so the insertion was performed by press-fit fixation.

To apply the loads, the implant was designed with an extension in the proximal side.

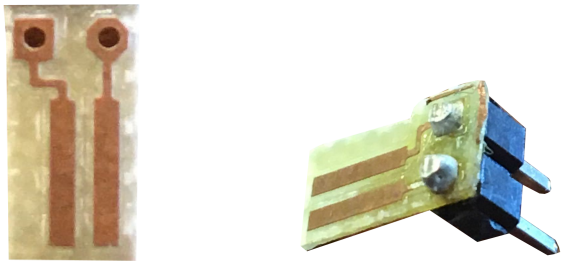

(a) (b)

Figure 4.2: (a) Front view of the new sensing technology showing the copper pads and drill holes. (b) Lateral view showing the soldered connectors.

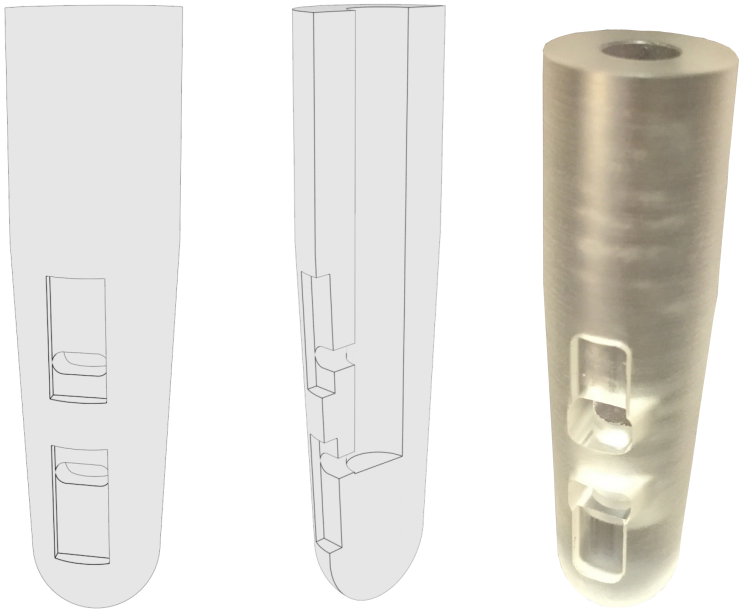

(a) (b) (c)

Figure 4.3: Final computer product of the developed implant displaying the circuits placement locations in (a) and its inner structure, where the wires are housed in (b). Real machined part made in acrylic represented in (c).

The monitoring system was externally powered by using wires (inside of the implant) to connect the sensors to the reading board (implant inner structure shown in Figure 4.3 b).

4.3 Specimens

All experimental tests were performed using biological specimens. Criteria used for the samples choice were the ones presented as follows: (i) bone structure resembling as close as possible a human structure; (ii) accessibility of the specimens; (iii) intact bone with sufficient volume such that the implant can be inserted without compromising the structural integrity of the bone; and (iv) fresh samples with an intact bone structure. Following these specifications, complete porcine femurs were chosen. The specimens were ceded by a butcher's shop, Bom Talho, and were immediately frozen after their acquirement.

4.4 Specimen support platform

In order to integrate the bone-implant-sensor system in the experimental setup, a test apparatus was developed. This apparatus was designed with two parts: a bottom slab and a U-shaped plate (Figure 4.4).

The bottom slab (Figure 4.4 a) provides fixation to the test machine as well as support

to the bone specimen. To adapt to the non-similarity found among the femur specimens, an adjustable setup was required in order to ensure that the mechanical load is applied in the same place across all experiments. Two sliders were then added to provide up to 30 mm adjustment. Since the femoral head has a slight deviation from its longitudinal axis, a 10 mm hole was projected to fixate the specimen in a non-centered position (40 mm from the center). The chosen material was Aluminum and the corresponding technical drawing is shown in Appendix C, Figure C.2.

Additionally, a U-shaped plate was added to the setup, as shown in Figure 4.4 b (technical drawing in Appendix C, Figure C.3). This profile was attached to the bottom slab by a M5 screw and includes a M10 hole to house the same screw as the one projected for the bottom slab (final assembly in Figure 4.4 c). For further fixation, adjustable plastic clamps were used alongside the U-plate and around the mid-femur section. By using this test apparatus, the femur was locked in the direction of the bending moment originated from the applied load.

4.5 Data acquisition and processing

Data was acquired using the AD7746 Evaluation Board (Analog Devices) [87]. This setup is a capacitive-to-digital converter with a high resolution, up to 21 bits, high linearity (0.01%), high accuracy (±4 fF) and operates in a range of ±4 pF. The communication between the board and the sensor was accomplished by using the Evaluation Software (v2.2, Analog Devices) and using an USB port. The board electrically supplied the capacitive sensor with a square wave with an amplitude of 5 V and a frequency of 32 kHz. The board was connected to each planar electrode using the channels C1N+ (positive polarization) and EXCB (negative polarization). Data was acquired at 50 Hz rate and the input set to single-ended.

After the data acquisition, data was exported to a Microsoft Excel (Microsoft Office 365) datasheet. Afterwards, a script from Matlab (v9.6, R2019a, MathWorks) was used for data processing, namely to compute the mean, the standard deviation and the confidence interval.

Standard deviation and the confidence interval were calculated using equations 4.1

(a) (b) (c)

Figure 4.4: Platform designed to hold the biological specimens in the experiment: (a) bottom slab showing the two holes and sliders; (b) the U-shaped part for further fixation; and (c) the complete assembly.

and 4.2, respectively. N and n refer to the number of observations (represented differently due to convention) and $\bar{x}$ to the mean. The variable z^* is related to the chosen confidence interval and the type of distribution.

$$\sigma^2 = \frac{1}{N-1}\sum_{i=1}^{N}(x_i - \bar{x})^2 \tag{4.1}$$

$$CI = (\bar{x} - z^*\frac{\sigma}{\sqrt{n}}, \bar{x} + z^*\frac{\sigma}{\sqrt{n}}) \tag{4.2}$$

4.6 Test machine

The experiment was carried out using a loading machine AGS-X 10 kN (Shimadzu), located in the Department of Mechanical Engineering (University of Aveiro), with a precision of 0.001 μm. It is controlled by the software Trapezium X (Shimadzu). In the validation tests this machine was used to progressively move the bone samples downward, followed by the loading. In the load tests it was used to apply the loading to the implant's distal segment.

Intentionally blank page.

Chapter 5

Methods

5.1 Validation tests using a previous test apparatus

5.1.1 Experimental procedure

The monitoring ability of the sensing technology to monitor different bone-implant interfaces in the femoral head was experimentally analyzed. The porcine bone samples, were cut as cubes with 10x10x10 mm. Furthermore, to facilitate the use of the sensor, some connectors were soldered to the board's cables, thus increasing the potential of parasitic capacitance.

Approximation and contact tests were performed (Figure 5.1): starting 4 mm apart from the sensor and reaching 0 mm, followed by the compression of the sample. The objective was to verify if the capacitive changes are similar to those obtained by Henriques [36]. The experimental procedure followed closely the protocol developed by Henriques, with an exception in the data acquisition software: instead of 200 capacitance values, 500 values were computed to minimize the impact of eventual outliers due to the sensors sensitivity.

As the environment can significantly alter the obtained capacitance values, similar temperature and humidity conditions were ensured in the laboratorial environment throughout the *in vitro* tests. By using a Testo 635-2 (Testo Co.) sensor to measure these variables, it was possible to keep the room at a temperature of approximately 22ºC and 50% humidity while conducting the experiments.

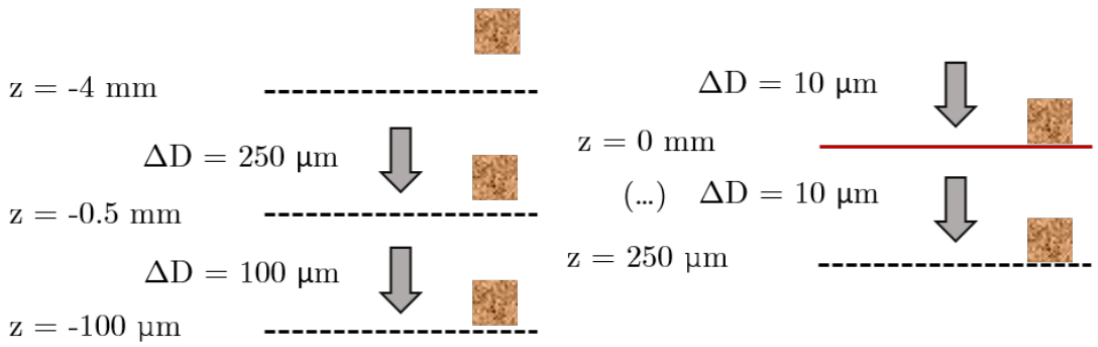

Figure 5.1: Scheme illustrating the approximation and contact tests for validation.

5.1.2 Analysis of results

Figure 5.2 presents the results regarding the new sensing technology and the results obtained by Henriques [36]. The circuit's capacitance increases with the approximation of the sample, agreeing with the data provided by Henriques' work. The initial behavior is characterized by smaller changes in the capacitance. When approaching the interface, the capacitance increases at a sharper rate, reaching the higher values when under compression. The range on which the values were obtained was [1.1516, 1.5475] pF, showing lower values of capacitance than the ones obtained by Henriques [36]. This might be explained by the reduced area and number of the newly developed electrodes.

Figure 5.3 illustrates the confidence interval for 95 and 99%, regarding the mean of the samples. The mean standard deviation is ±0.0983 pF and the maximum and minimum values are ±0.1200 pF and ±0.0852 pF, respectively. For the 99% interval the maximum variation band is ±0.0659 pF, while for the 95% it is ±0.0502 pF.

5.1.3 Sign test

To verify if the obtained results show significant differences in their tendency compared to the ones provided by Henriques [36], the sign test was employed.

This test analyzes the differences between two conditions for the same given situation. In each pair (x_i, y_i), with $i = 1, 2, 3..., n$, both values are compared. For the present case, the variables correspond to the capacitance values obtained by the new sensing technology and the ones obtained by Henriques. The test's distribution is binomial with parameters $p = 0.5$ and n, being n the number of non-equal values. X and Y refer to the full data-sets, P to the probability and T is the number of pairs for which $y_i - x_i > 0$.

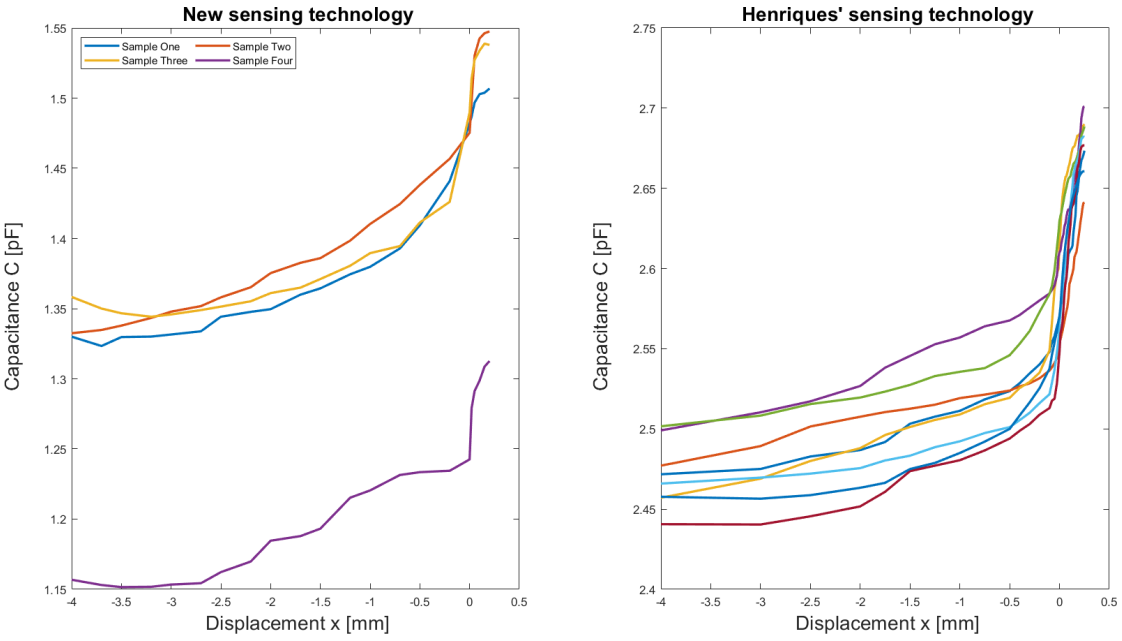

Figure 5.2: Values of the capacitance, comparing the results from the new sensing technology and the ones performed by Henriques [36] in eight distinct porcine samples.

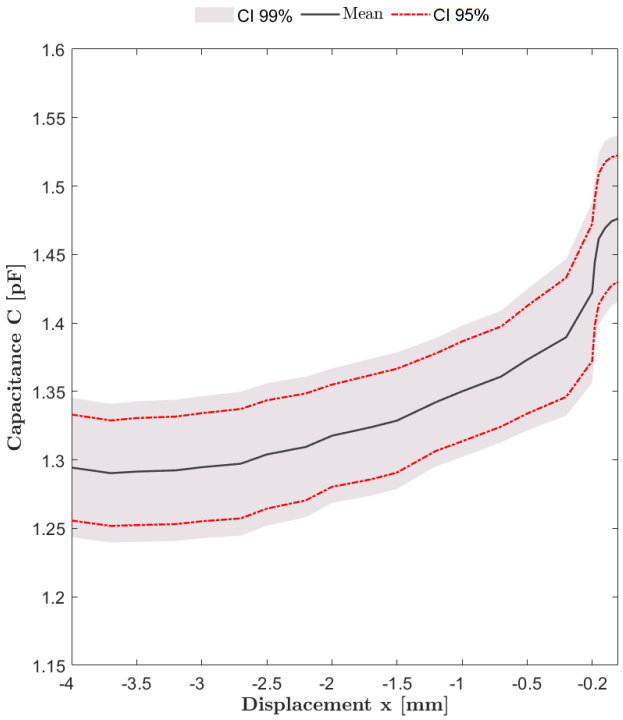

Figure 5.3: Confidence interval plot referring to the approximation and contact validation test of the newly developed sensing technology.

Then, $T \sim bin(n, 0.5)$ and the null and alternate hypothesis are, respectively:

$$H_0 : P(X > Y) = P(X < Y) \qquad vs. \qquad H_1 : P(X > Y) \neq P(X < Y) \tag{5.1}$$

Calculations were carried out with Matlab (v9.6, R2019a, MathWorks) using the Statistics and Machine Learning Toolbox. For a two-sided hypothesis test and exact computation: $p\text{-}value = 0.143$, and, thus, with a 95% confidence, both data have the same tendency and the null hypothesis is not rejected.

5.1.4 Limitations

The sensing system capacitance order of magnitude is *pico Faraday* ($10^{-12}F$) , which indicates the high sensitivity of the capacitive system. This can represent a problem as the electric capacitance is highly susceptible to environment factors (e.g. air drafts, temperature or humidity), posing a challenge to replicate the same conditions on each test. Therefore, similar results throughout different tests are hard to achieve.

5.2 Implantation tests

5.2.1 Sensor-Implant assembly

Two of the sensors were integrated into the implant. They were then electrically connected to the wires which came through the distal end of the implant (Figure 5.4 a),

which in turn provide electric connection to the AD7746 Evaluation Board. Before the system's implantation in the porcine specimens, it was wrapped in a commercially used cellophane film to avoid direct contact between the sensors and the bone. The cellophane film was previously tested to ensure it was permeable to the electric field.

5.2.2 Specimen preparation

A flat surface in the distal femur would simplify the fixation of the specimen and so the porcine condyles were removed. The cutting was performed with an electrical saw (E+P85 Minor, Eco + Plus), perpendicular to the femur longitudinal axis. To facilitate the implantation, the femoral head was partially cut along its longitudinal axis, such that a flat surface was obtained. Afterwards, a hole, with a diameter corresponding to the minor diameter of the implant (12 mm) was drilled to allow a press-fitting insertion (Figure 5.4 b). To fixate the specimen in the support platform, the bone marrow in the distal part was removed and a wedge was hammered into the bone press-fit (Figure 5.4 c).

During the tests the femur suffered a slight bending along its longitudinal axis (Figure 5.5 a). A bending moment (M) resulted from the applied excitation force (F), caused a decrease in displacement changes of the femoral head near the implant. To lessen this deflection, the cutting was performed in the metaphysis, leaving around 80 mm from the cut part to the top. After the preparation, the specimens were frozen.

(a) (b) (c)

Figure 5.4: (a) Sensor-Implant system assembly. Both the two sensors and the wires (throughout the inner structure and the distal part) can be observed. (b,c) Porcine specimen illustrating the drill hole in the femoral head, meant to house the sensor-implant system (front view) (b) and the wedge hammered into the distal part used to fixate the bone to the support platform (bottom view) (c).

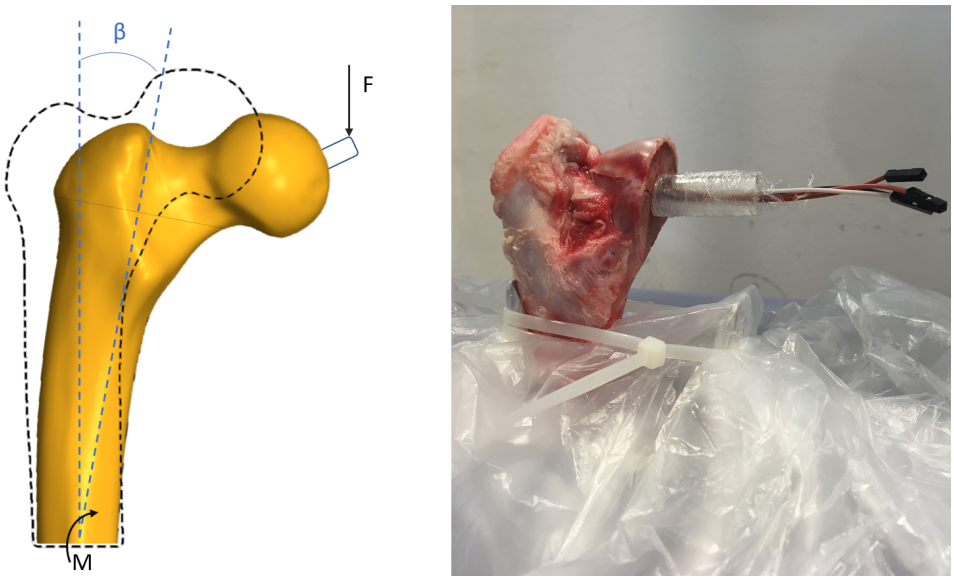

(a) (b)

Figure 5.5: (a) Schematic of the bending suffered by the specimens. Force F originates a moment M which causes the femur's deflection β in relation to its longitudinal axis. (b) Experimental setup used to carry out the experimental tests.

5.2.3 Stimulation and types of tests

Loads were applied to the proximal part of the implant such that implant displacements occur, causing capacitance changes as different bone-sensor interfaces are provided. The load was applied by an acrylic stem to press the implant's proximal area.

The nature of bone structure makes it very adaptable to compression loads. This constant adaptation renders the control by force an unreliable measure to track, as the load is never able to stabilize and tends to continually decrease. As a result, for the current procedure the tracked variable was the machine's displacement in the distal segment of the implant.

Compression and decompression: In order to assess the performance of the capacitive architecture when its surrounding is under change, a new series of tests were performed. Experimental tests consisted in the downward displacement of the implant's distal segment up to a certain stage, proceeded by the decompression back to the zero position (Figure 5.6). As such, displacement range was defined from 0 to 4 mm with step increments of 0.2 mm. The sensor was only used in position one, as defined in Figure 5.7.

Implant rotation: To verify the influence of the sensor orientation on the capacitive change, three tests (similar to the compression and decompression) with 90° distinct rotations were carried. The first test, defined as position one, was carried out using the sensor facing upwards. The next two orientations (positions 2 and 3) were rotated by 90° defined clockwise from the latter position, as described in Figure 5.7. Since the

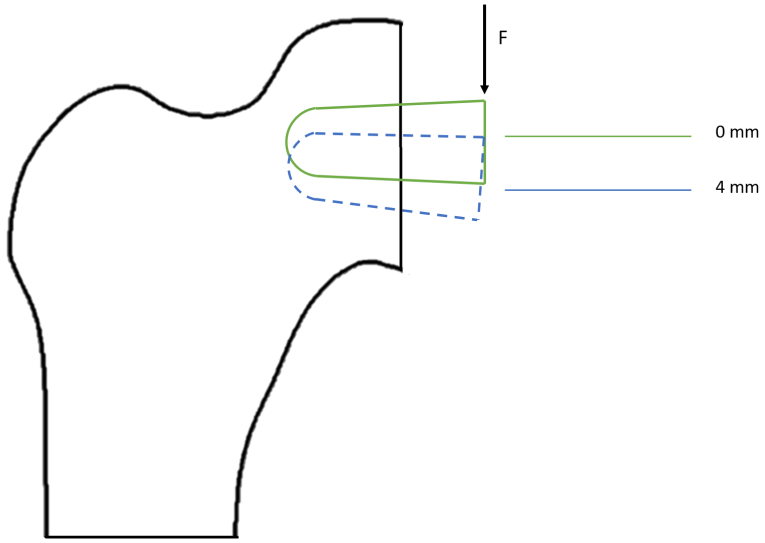

Figure 5.6: Schematic of the performed compression and decompression tests. The sensor's initial position (in green) is defined at 0 mm, followed by the progressive displacement of the test machine (increments of 0.2 mm) and up to the final position (in blue) defined at 4 mm. The process is inverted in the decompression cycle (from 4 to 0 mm).

direction of the load was always the same, these test allowed to verify the eligibility of the tests, as different sensor orientations should provide distinct results.

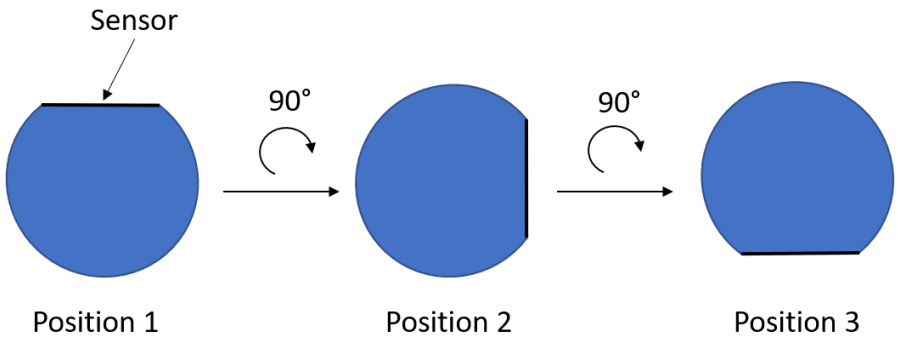

Figure 5.7: Illustration of the different orientations used to analyze the performance of the capacitive architecture. Only position 1 was used throughout compression and decompression tests.

5.2.4 Experimental procedure

After the sensor-implant assembly and specimen preparation, each test followed the following procedure:

- Defrost of the specimen for a duration of 90 minutes;
- Placement of the support platform in the loading machine;
- Isolation of the machine and the support platform with a plastic cloth, leaving only the screw uncovered, to avoid the contamination of the material;
- Insertion of the implant into the femoral head with a press-fit fixation;
- Fixation of the bone in the support platform by screwing the wedge in the M10 screw with a length of 50 mm;
- Tightening of the two plastic clamps around the femur;
- Initiation of the stimulation by defining the zero position when forces smaller then 0.05 N were observed.

5.2.5 Data processing and analysis

In order to minimize the effect of external conditions in the capacitance values and also to improve the comparison ability, a normalization of the data was carried. This way, data could assessed in the same dimensionless scale, independent of the capacitance measurement range. Besides, by normalizing the data, a clearer visualization of the curves tendency and behavior is achieved. Normalization was carried by dividing each data set by its corresponding maximum value. Another useful feature is the assessment of each curve percentage of capacitive change, in relation to its maximum value.

As such, the analyzed parameters can be summarized as:

- Capacitive measurements range - range on which the capacitance was measured;
- Percentage of capacitive change - defined as the difference between the maximum and minimum values of the normalized data;
- Confidence interval - 99 and 95% confidence interval.

Intentionally blank page.

Part III

Results and Discussion

Chapter 6

Results

6.1 Compression and decompression

A capacitance decrease was observed throughout the compression cycles, indicating that the bone is moving away from the sensor (Figure 6.1 a). Differently, the capacitance increased throughout the decompression cycle (Figure 6.1 b), supporting the results obtained in the previous compression cycle by demonstrating an inverse behavior. From this data, one can observe a capacitive changing trend that follows the trend already reported in section 5.1. Regarding the compression, the mean percentage of capacitive change was 3.67% while the maximum and minimum were 4.82% and 2.33%, respectively. The range on which the values were obtained was [2.209, 3.076] pF, corresponding to a difference of 0.867 pF between the maximum and minimum values. Concerning the decompression cycles, the percentage of capacitive change increased when compared to the latter measures. The mean percentage variation was 5.06% and the maximum and minimum variations were 6.77% and 2.59%. The observed range was [1.981, 3.184] pF corresponding to a difference of 1.203 pF. By analyzing the capacitance in function of the displacement, a mean of 0.0255 pF/mm for the compression and 0.0304 pF/mm for the decompression was measured. It is important to note that the mentioned displacements refer to the ones performed by the test machine and not those established in the sensor-implant interface.

The normalized results emphasize the capacitive changes trend, showing the increase and decrease in the capacitance as steeper patterns (Figure 6.2). Figures B.1 and B.2 in Appendix B, show the curve fitting regarding the compression and decompression mean. Both cycles were approximated by a third-degree polynomial model expressed by Equation 6.1 for both the compression and decompression (only the parameters differ). Regarding the coefficient of determination, the obtained values were $R^2 = 0.9993$ for the compression and $R^2 = 0.9994$ for the decompression, indicating a strong fit for both curves. Polynomial regression was achieved by using the *Curve Fitting* application from Matlab (v9.6, R2019a, Mathworks). The software also allowed to normalize the input data such that: $x_{norm} = (x - \mu)/\sigma$ with $\mu = 2$ and $\sigma = 1.241$, for the given interval of $0 \leq x \leq 4$ [mm].

$$C(x_{norm}) = \sum_{i=0}^{3} p_i \, x_{norm}^{i} \tag{6.1}$$

Compression:	$p_0 = 0.9812$	$p_1 = -0.01266$	$p_2 = 1.119 \times 10^{-4}$	$p_3 = 4.404 \times 10^{-4}$
Decompression:	$p_0 = 0.9758$	$p_1 = -0.01405$	$p_2 = 5.324 \times 10^{-4}$	$p_3 = -4.864 \times 10^{-4}$

Referring to the mean of the normalized data, the confidence intervals of both cycles are displayed in Figure 6.3 a,b for 95 and 99%. Both cycles present a *quasi*-linear behavior and as expected, decompression provides an increased percentage growth than those provided by compression. Regarding the compression cycle, the mean standard deviation was 0.7437%, while the maximum and minimum values were 0.9892% and 0.0028%, respectively. The greater variation band was 0.5332% and 0.4002% for the confidence intervals of 99% and 95%, respectively. A mean standard deviation of 0.7095% for decompression cycles, in which a maximum and minimum values of 1.3841% and 0.0117% were, respectively, observed. The greater variation band was 0.9281% for the 99% interval and 0.7420% for the 95%. Additionally, the confidence intervals regarding the mean of the absolute capacitance values are shown in Figure 6.4. Here, one can

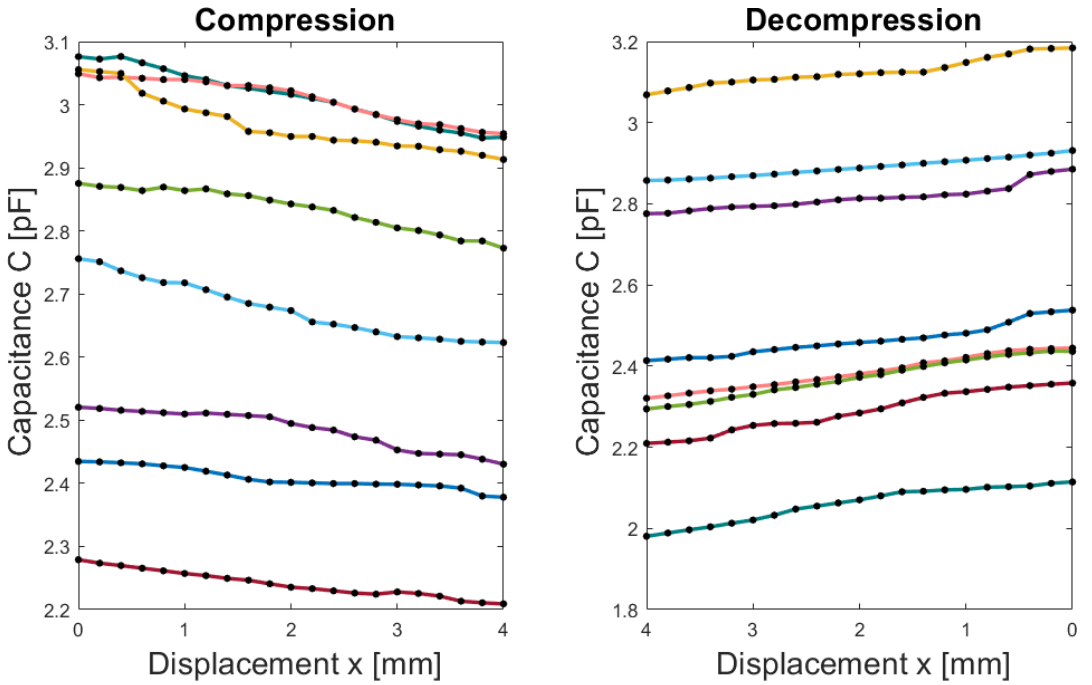

(a) (b)

Figure 6.1: Obtained curves from the compression and decompression tests. (a) Compression cycle curves, showing a tendency to decrease the capacitance along the experiment. (b) Decompression cycle curves, showing a tendency to increase the capacitance along the tests. Note: different colors refer to different tests. Furthermore there is not a connection between the colors of both plots.

clearly observe the effects of the great differences in the obtained values, as the confidence interval bands are fairly large. The mean standard deviation for the compression was 0.2992 pF while the maximum and minimum values were 0.3124 pF and 0.2886 pF, respectively. For the decompression, the mean standard deviation was 0.3573 pF and the maximum and minimum values were 0.3708 pF and 0.3449 pF, respectively.

6.2 Implant rotation

The data used for the analysis of the results corresponded to the normalized mean of all the tests (Figure 6.5). The normalized results concerning the first position refers to compression tests as expressed in Section 6.1: the capacitance clearly decreases with the implant displacement, indicating the progressive bone-sensor separation. The mean variation rate was 3.67%, as previously reported. The second position curve is characterized by a nearly constant behavior, indicating small changes in the bone-implant interface: the mean variation rate was 0.31%. Finally, for the third position, the capacitance presented an inverse behavior when compared to position 1, characterized by a mean variation rate of 4.08%. It is then possible to hypothesize that the contact between the bone and implant was increasing for position 3, supporting the evidence obtained in the previous experiments.

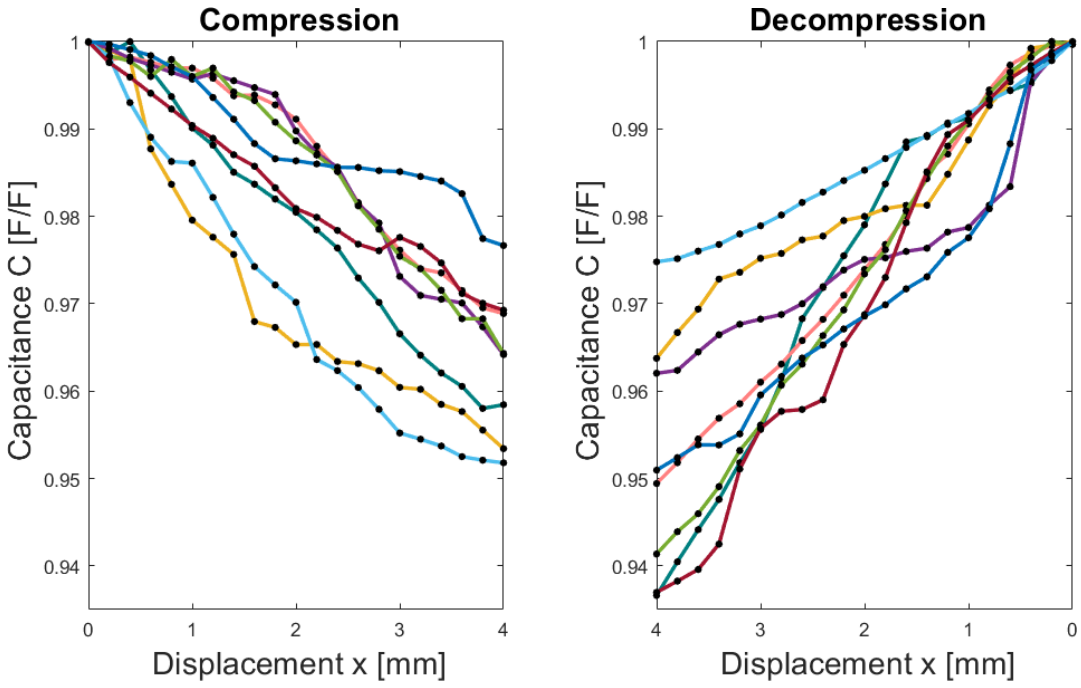

(a) (b)

Figure 6.2: Normalization of the capacitance data displayed in Figure 6.1 for both the compression (a) and decompression (b) cycles. Data normalization was achieved by dividing each data set by its corresponding maximum value. Note: different colors refer to different tests. Furthermore there is not a connection between the colors of both plots.

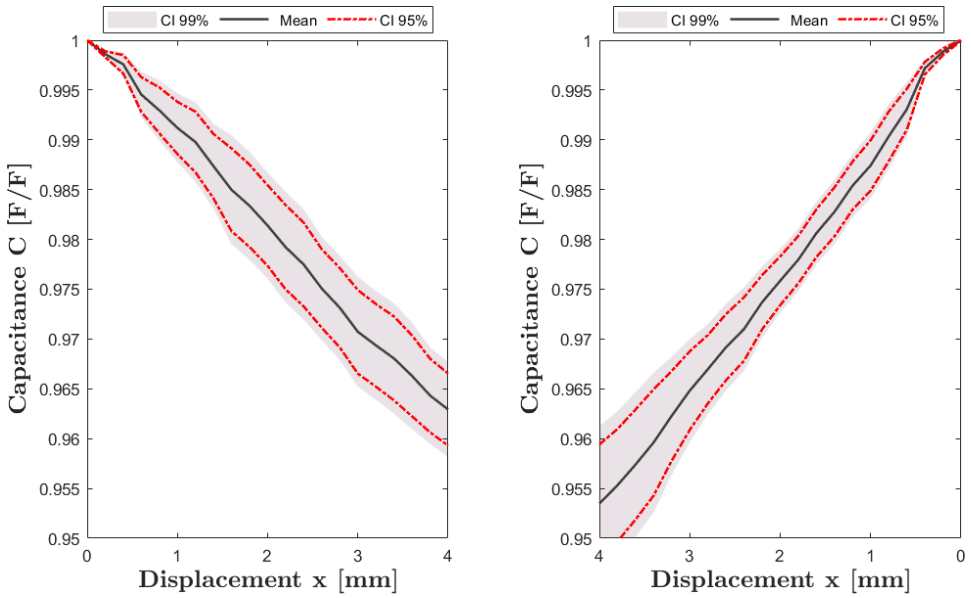

Figure 6.3: Confidence intervals of 99 and 95% regarding the normalized mean of the compression (a) and decompression (b) cycles.

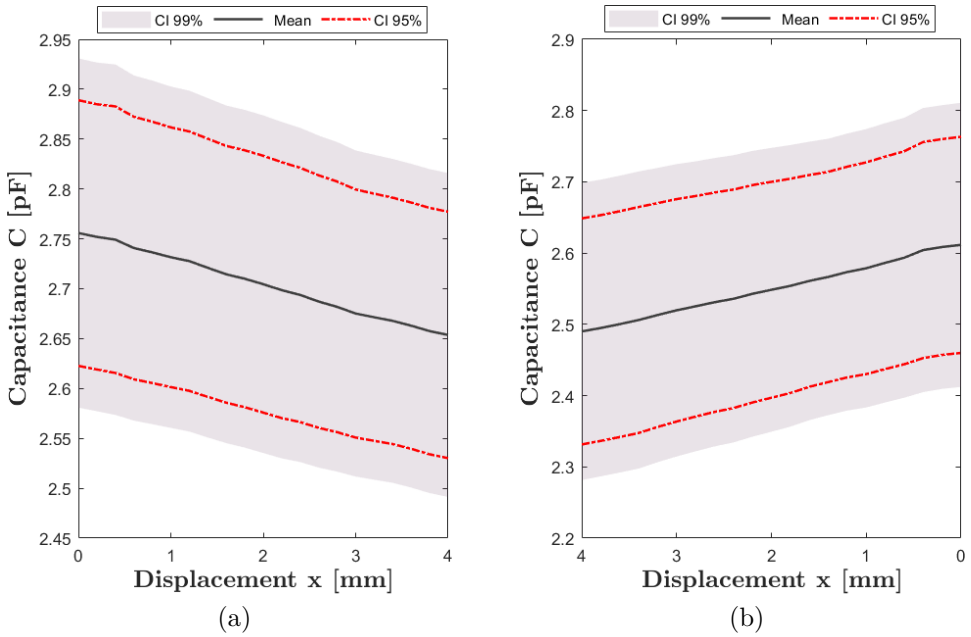

Figure 6.4: Confidence intervals of 99 and 95% of the absolute capacitance values. The large dispersion band highlights the difference in the measured values, emphasizing the difficulties in re-creating the same *in vitro* conditions across all performed tests. Decreasing tendency for the compression cycle (a) and an inverse behavior for the decompression (b), showing a tendency to increase the capacitance along the tests.

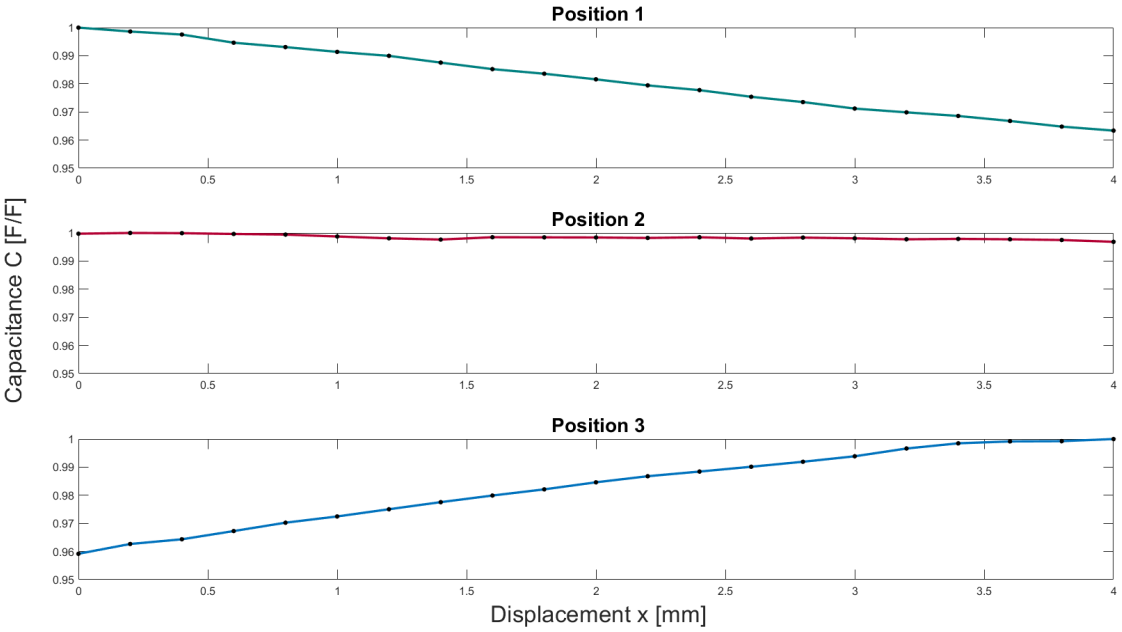

Figure 6.5: Mean of the normalized capacitive measurements related to different orientations of the capacitive architecture, used in the implant rotation tests. The compression and decompression tests were only performed for position 1. Orientations scheme in Figure 5.7.

Intentionally blank page.

Chapter 7

Discussion

In the literature review many technologies and monitoring methods were analyzed by assessing their ability to follow-up the stability of implants and the bone-implant interface states. Despite these scientific efforts, a suitable monitoring system has not yet been developed as all developed technologies present significant limitations. Indeed, an effective technology must fulfill the following criteria:

1. Operate non-invasively regarding peri-implants tissues;
2. Allow the integration inside implants;
3. Allow stretchable and flexible integration inside implants;
4. Allow their design with different topological structures and for different geometries of the bone-implant interface;
5. Enable controllable and personalized monitoring of target regions on the tissues;
6. Allow to follow-up the bone-implant interface state throughout the daily life of patients.

A comparative analysis of the ability of the monitoring methods (and related technologies) to fulfill these key points is introduced in Table 7.1. The vibrometric and acoustic methodologies present the widest variety of methods and technologies; in contrast, the bioelectric impedance approach only presents a single technology. Most technologies are able to operate noninvasively (only one technology, related to the strain approach, is not able of such ability). Besides, none of the technologies managed to monitor specific target regions.

Regarding the cementless technologies using the vibrometric approach, the second method fulfills the greatest number of requisites, being distinguished by its ability to be integrated inside the implant with flexible integration. On the other hand, this method has been developed to be integrated into hip implants and, then, it is unknown if it holds potential to be used in other implants. The other missing point is relative to the targeted monitoring of tissues. Although one technology was developed for such goal, its effectiveness was not explored [57]. The cemented technologies of the second method were developed to be incorporated inside the implants and to have the potential to adapt to different topological structures. Concerning the not fulfilled requirements,

targeted monitoring and flexible integration are hard to be achieved using the vibrometric approach.

The third method related to acoustic methodology for cementless fixations is the one fulfilling more requisites. Its limitations are similar to those described for the second method of the vibrometric methodology. The other methods were neither developed for integration inside of implants nor to monitor target tissue regions. As in the cemented methods, these methods all present similar limitations, although the third method is distinguished by its ability to be integrated inside implants and the fourth method by its inability to monitor different states of the bone–cement–implant interface. They all lack the flexibility and the potential for monitoring target regions.

The technology based on bioelectric impedance allows to monitor different interface states and ensures that different topological structures and geometries can be designed. Regarding the other features, the incorporation of the technology, as well as targeted monitoring, inside implants can be difficult.

Concerning the only proposed method for the magnetic induction approach, one may notice its inability to adapt to different topologies and geometries, and limitations related to targeted monitoring of tissues. Nevertheless, this method allow the incorporation of the technologies inside the implants, showing some degree of flexibility and the possibility to monitor different states of the implant–bone interface.

Methods developed for the strain approach were both developed as implantable systems, allowing for the conception of different topological designs and the ability to monitor different states of the bone–implant interface, although none of them managed to achieve monitoring of target tissue regions. Regarding the first method, the circuitry and design allow for a very flexible and stretchable integration. Nevertheless, the developed technology is invasive, as it must be attached in contact with bone tissues. The second method can be noninvasively applied ensuring flexibility and allowing a stretchable integration.

The capacitive technology here proposed presents a simple architecture, allowing flexible integration inside implants, different designs and adaptability to several geometries. The experimental results highlight its potential to monitor different bone-implant interface states that can occur throughout time. Besides, it does not require for an invasive operation.

Many of the proposed technologies were not validated *in vivo* to demonstrate their real potential when incorporated into functional biological systems. Furthermore, further research is required to overcome their current limitations. Technologies requiring extracorporeal components provide a limited monitoring capability, although their limitations can be overcome by miniaturizing and incorporating the components inside the implants. Indeed, an important capability that none of the technologies are able to provide (and just a few referred to) is the possibility to monitor targeted regions, such that the overall time-dependent loosening states along the implant interface can be accurately identified. As the more critically unstable regions are detected, locally preventive treatments can be timely provided, thus decreasing the risk for revision surgeries.

The work of Henriques [36], provided for the first time promising results concerning the performance of planar capacitive technologies for instrumented bone implants, which hold potential to overcome the limitations found in other technologies. This work represents a step forward in the development of a fully working capacitive system, as it was further tested *in vitro* by implanting the instrumented implant (comprising the

Table 7.1: Criteria used to define the potential of monitoring methods.[a]

Methodologies	Fixation	Methods	Requirements[b] (1)	(2)	(3)	(4)	(5)	(6)
Vibrometric	Cementless	Ext. mechanical excitation / Ext. mechanical signal	✓	✗	✗	✓	✗	✓
		Ext. magnetic induction / Ext. mechanical signal	✓	✓	✗	✓	✗	✓
		Int. mechanical excitation / Ext. mechanical signal	✓	✗	✗	✓	✗	✓
	Cemented	Ext. mechanical excitation / Ext. mechanical signal	✓	✗	✗	✓	✗	✓
		Ext. mechanical excitation / Int. mechanical signal	✓	✓	✗	✓	✗	✓
Acoustic	Cementless	Ext. mechanical excitation / Ext. acoustic signal	✓	✗	✗	✓	✗	✓
		Int. mechanical excitation / Ext. acoustic signal	✓	✗	✗	✓	✗	✓
		Ext. magnetic induction / Ext. acoustic signal	✓	✓	✗	✓	✗	✓
	Cemented	Ext. mechanical excitation / Ext. acoustic signal	✓	✗	✗	✓	✗	✓
		Int. mechanical excitation / Ext. acoustic signal	✓	✗	✗	✓	✗	✓
		Int. mechanical excitation / Int. acoustic signal	✓	✓	✗	✓	✗	✓
		Ext. acoustic emission / Ext. acoustic signal	✓	✗	✗	✓	✗	✗
Bioelectrical Impedance	Cementless	Ext. electrical current / Ext. electric potential difference	✓	✗	✗	✓	✗	✓
Magnetic Induction	Cementless	Ext. magnetic induction / Ext. magnetic induction	✓	✓	✗	✓	✗	✓
Strain	Cementless	Int. mechanical loads / Int. bone deformation	✗	✓	✓	✓	✗	✓
		Int. mechanical loads / Int. fixation plate deformation	✓	✓	✗	✓	✗	✓
Capacitive	Cementless	Intracorporeal dielectric alteration / Intracorporeal capacitance change	✓	✓	✓	✓	✓	✓

[a]Terminology: Int.- Intracorporeal; Ext. - Extracorporeal

[b]Description:

(1) Operate non-invasively regarding peri-implants tissues;

(2) Allow the integration inside implants;

(3) Allow stretchable and flexible integration inside implants;

(4) Allow their design with different topological structures and for different geometries of the bone-implant interface;

(5) Enable controllable and personalized monitoring of target regions on the tissues;

(6) Allow to follow-up the bone-implant interface state throughout the daily life of patients.

capacitive architecture) into biological specimens. As demonstrated, this sensing system is able to detect small changes in the sensor-bone interface by variations in the dielectric structure. In the first carried tests, the capacitance changes were observed according to the type of cycle (compression and decompression). The compression cycle, provided a decreasing trend in the electric capacitance, indicating that the bone is getting further away from the sensing technology; and differently, during the decompression cycle, the trend expresses that the capacitance increases with the implant displacement, suggesting the bone-sensor approximation. To further corroborate the results obtained in the compression and decompression tests, implant rotation tests were also carried out. By testing different orientations, one could assess the differences in the measured results, as it should be expected to obtain differing results according to the orientation. Indeed, by observing the resulting data, one can highlight the different trends observed for orientations of up to 180°, agreeing with the expected results. Moreover, for the loading considering position 2 (90° rotation), small capacitance changes were anticipated as the interface was not expected to present significant changes, which was experimentally observed.

The proposed implant design can have further applications, namely to improve technologies already used for electrical stimulation. For example, it can be used to incorporate sensors, having a similar effect as a technology used for bone growth promotion called BISS (bipolar screw induction system) [88–90]. Despite the current implant having a bigger diameter, the potential of miniaturization can overcome this limitation. Additionally, by integrating the capacitive sensing technology, the instrumented implant is not limited to the prevention of bone necrosis (through stimulation), but also being able to monitor its healing progress.

When comparing the obtained values to the ones provided by Henriques [36], one can notice the smaller growth rate of the planar capacitive system here tested. This can be explained due to the press-fitting fixation, which established a *quasi*-zero distance between the bone and the sensing technology at the start of the experiment. Furthermore, the design used by Henriques [36] was slightly different, both in area and number of electrodes, causing differing performance results in capacitive change. Although one cannot accurately predict the displacement in the proximity of the sensor area, the capacitance change allows us to assume not large displacements were imposed. The *quasi*-linear behavior of the capacitance might be indicative of a progressive change in the distance between the sensor and the bone tissue. All these facts suggest that the comparison with the results obtained by Henriques [36] must be carefully conducted. It is more accurate to compare the final stages of his experiments with the ones here reported, as a non-parallel bone-sensor displacement occurs. Figures 7.1 and 7.2 represent the comparison between the results achieved by Henriques [36] and the ones obtained using the new design during the compression and decompression tests. Comparison between tests highlights similar trends either during increasing or decreasing capacitive changes: the compression cycle of the new sensing technology and the decompression tests from Henriques; and similarly, the decompression cycle from the new sensing technology and the approximation and contact tests from Henriques [36]. From Figure 7.1 one can observe the similar trend and the percentage of capacitance change: as shown in the previous section the mean percentage variation from the compression cycle was 3.67%, as for the decompression data from Henriques [36] the mean percentage change was 3.95%. The non-linear zone in Figure 7.1 b is explained in Henriques' work by the trabecular adaption along the decompression. Regarding Figure 7.2, the mean percentage change of the new sensing technology was 5.06%, while for approximation and contact tests performed by Henriques [36] was 5.44%. Furthermore, both curves present a very similar trend.

Although the obtained results are promising, some limitations regarding the *in vitro* experiment were detected. One of the greater difficulties in the setup preparation was the minimization of the bending observed in the specimens. This caused a decrease in displacement in the implant, diminishing the changes in the bone-sensor interface, although after the setup preparation this was nearly completely attenuated. In addition, the flexible structure of the femur resulted in bone readjustment in response to the applied load. This phenomena was observed during the experiments, as the load did not stabilize and would continually decrease until equilibrium was reached. For these reasons, controlling the *in vitro* experiment by using the applied force was found unreliable and so the machine displacement was used. It was further observed that the sensor only demonstrated significant capacitance changes for input displacements of around 0.2 mm. As Henriques showed in his work, and as it was shown during the validation tests in Section 5.1.2, capacitive technologies have the ability to detect small capacitive changes

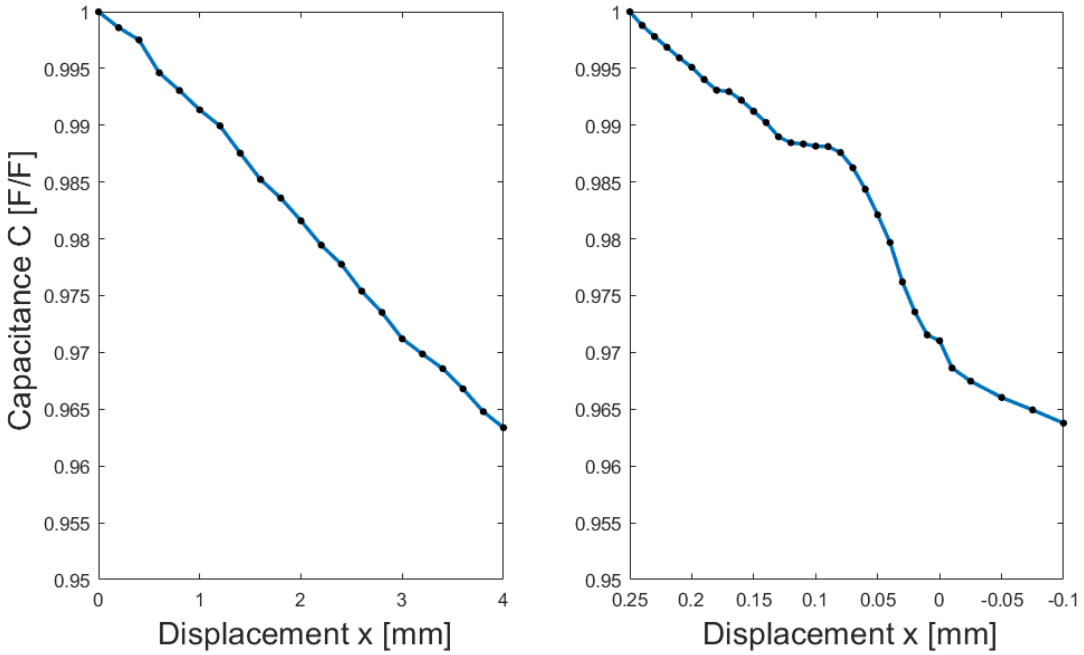

Figure 7.1: (a) Compression cycle of the new sensing technology. (b) Decompression test performed by Henriques [36].

for bone-sensor displacement in the order of micrometers. Hence, at a first stage, the step increments were of 0.05 mm, but the capacitance changes were not significant enough to assuredly state these were not caused by external factors. This might be due to the bone's flexible structure, as the applied stimuli could not be sufficient to exceed its adaptability. Under loading, the bone structure adapts to the applied force, which decreases under the adjustment process, either through its flexion, load distribution or trabecular adaptation.

Other challenge was to ensure similar environment conditions. It was attempted to perform laboratorial tests under similar temperature and humidity, as these highly influence the performance of the planar capacitive sensor. It was observed that even with the same bone sample, different external conditions would yield significantly dissimilar values of capacitance, thus reaffirming the usefulness of analyzing normalized data.

Throughout the decompression cycle, starting around the 0.4 mm step, the capacitance presented a convergence pattern. By observing the load behavior during the experiment, it was possible to notice that when the cycle reached this stage, the load was nearly null, due to the constant adaptation of the specimen. This may lead us to the conclusion that the bone-implant interface is also in a non-stop adaptation process.

As a result of the variation in the capacitance values, a correlation between the capacitance and the absolute value of the bone-sensor distance was not feasible. Furthermore, due to the flexibility of the bone structure it was difficult to predict the behavior of the implant under the loading scenario. Therefore, one can only estimate the distance variation by analyzing the percentage difference of the capacitance. Up to date, only the data provided in the validation tests (Section 5.1.2) is reliable to use in predicting

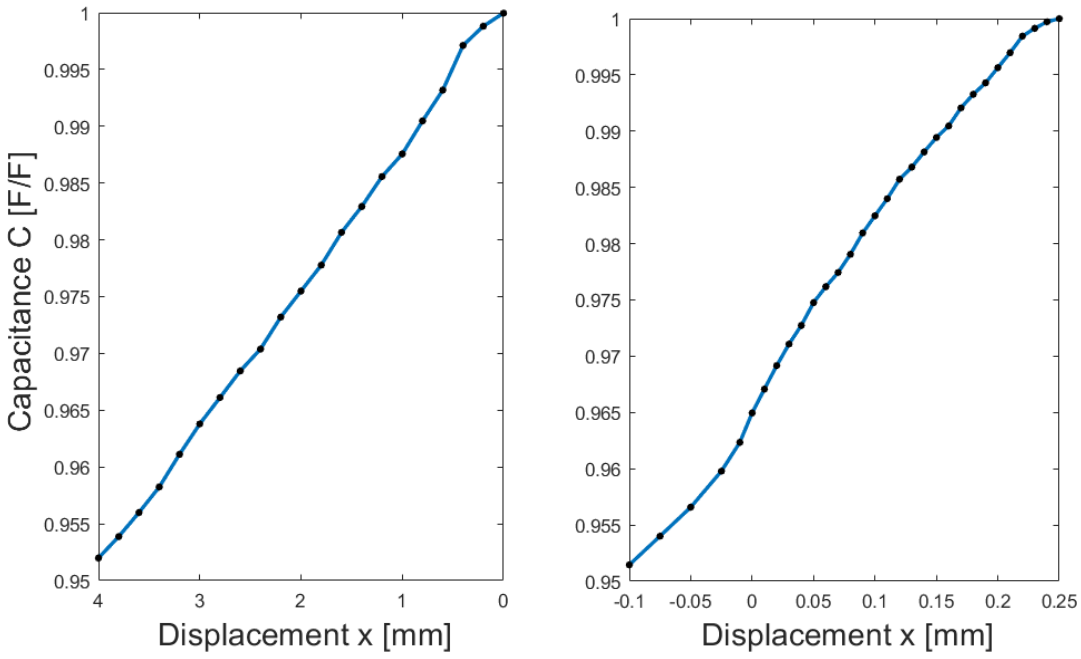

Figure 7.2: (a) Decompression cycle of the new sensing technology. (b) Approximation and contact tests performed by Henriques [36].

the capacitance behavior in terms of the bone-sensor distance.

It is worth referring that the implant was developed intended to house two distinct sensors. Having two sensors in the implant would allow for a comparison between them, as they would be subjected to different bone-sensor displacements. Despite the prototype was manufactured, the incorporation of the second sensor was not successfully achieved due to difficulties during the insertion process in the bone.

Part IV

Conclusion and Future Works

Chapter 8

Conclusion

Currently, one can say there is not an effective monitoring method or technology for assessing the state of bone-implant interfaces and although a lot of effort has already been conducted in this field, further technological development is required.

This research work aimed for further scientific breakthroughs on the development of a solution for assessing the implant-bone interface state, ultimately leading to the possibility for preventive and personalized treatments. As such, the ultimate objective of the current work was to evaluate the behavior of planar capacitive technologies when completely implanted in a biological organism. The following conclusions were achieved:

- A systematic analysis and review of the current methods and technologies present in the literature let conclude there is a total of thirty-nine technologies for implant stability assessment, divided into six different methodologies, namely: vibrometric, acoustic, bioelectric impedance, magnetic induction, strain and capacitive;
- The developed planar capacitive sensing technology is possible to be integrated inside bone implants (e.g. joint implants) and also to measure variations in the bone-implant interface according to capacitive change;
- The implant's design and geometry are suitable for implantation inside biological specimens, as well as the material choice proved to be electrically neutral;
- The developed *in vitro* experimental setup was suitable to fixate the biological specimens as well as to integrate the bone-implant-sensor components;
- The two distinct *in vitro* tests allowed to demonstrate the potential of the capacitive technology to monitor a constantly changing interface by variations in the capacitance; furthermore, the effect of different sensor orientations (and interfaces) in the measured capacitance corroborated the obtained values;
- From the obtained results it was possible to notice the different trends in the measured capacitance according to the type of loading.

As demonstrated, capacitive technologies show potential in detecting changes in its adjacent tissues. Hence, this is a promising technology for effective monitoring of the bone-implant interface state. The implantation of the technology into biological specimens is a step forward in the evolution of capacitive systems, as one can have a more

accurate prediction of the influence of surrounding tissues. This work further contributed to the understanding of the potential of capacitive technologies when applied into biological real-world monitoring applications.

Chapter 9

Future works

The possibility to develop instrumented implants increases with evidences of their potential, and more specifically, the present work showed the potential of capacitive technologies in assessing the bone-implant interface. Although this was a step towards a better and novel solution, a great effort and research are still needed. As such, the following future developments are suggested:

- Improve over the experimental methodology in order to achieve a realistic bone-implant interface;
- Improve the fixation of the specimens (e.g. cement);
- Control the environment aspects: humidity, temperature of the laboratory and air drafts;
- Develop different geometries and disposition of the capacitive sensor pads as well as the development of a more flexible and adaptable printed circuit (eg. polyimide material as used by Burton *et al.* [85]), adequate to several topological geometries;
- Develop implants with the ability of energy harvesting systems, to avoid the need of having external power links or finite life systems like batteries;
- Develop computational models of the bone structure and fluids to predict its behavior under the influence of external loads;
- Analyze the temperature influence on the capacitive change;
- Study of the influence of different excitation frequencies in the capacitance values;
- Study of the relation between bone displacement and capacitance change;
- Publish of a scientific paper with the obtained results.

Intentionally blank page.

Bibliography

[1] R. A. Brand, M. A. Mont, and M. M. Manring, "Biographical sketch: Themistocles Gluck (1853-1942),'' *Clinical Orthopaedics and Related Research*, vol. 469, no. 6, pp. 1525–1527, 2011.

[2] R. Trebše, "Infected total joint arthroplasty: The algorithmic approach,'' *Springer*, pp. 7–11, 2012.

[3] S. R. Knight, R. Aujla, and S. P. Biswas, "Total Hip Arthroplasty - over 100 Years of Operative History,'' *Orthopedic Reviews*, vol. 3, no. 16, pp. 72–74, 2011.

[4] S. Comitini, D. Tigani, D. Leonetti, M. Commessatti, F. Cuoghi, P. Barca, A. Martucci, C. Bettuzzi, and L. Amendola, "Evolution in Knee Replacement Implant,'' *Single Cell Biology*, vol. 4, no. 42, 2014.

[5] B. Bashinskaya, R. M. Zimmerman, B. P. Walcott, and V. Antoci, "Arthroplasty Utilization in the United States is Predicted by Age-Specific Population Groups,'' *ISRN Orthopedics*, vol. 2012, pp. 1–8, 2012.

[6] S. Kurtz, K. Ong, E. Lau, F. Mowat, and M. Halpern, "Projections of primary and revision hip and knee arthroplasty in the United States from 2005 to 2030,'' *The Journal of Bone & Joint Surgery*, vol. 89, no. 4, pp. 780–785., 2007.

[7] J.-Y. Reginster, "The prevalence and burden of arthritis,'' *Rheumatology*, vol. 41, pp. 3–6, 2002.

[8] P. M. Brooks, "Impact of osteoarthritis on individuals and society: how much disability? Social consequences and health economic implications.,'' *Current opinion in rheumatology*, vol. 14, no. 5 PG - 573-7, pp. 573–577, 2002.

[9] C. Palazzo, C. Nguyen, M. M. Lefevre-Colau, F. Rannou, and S. Poiraudeau, "Risk factors and burden of osteoarthritis,'' *Annals of Physical and Rehabilitation Medicine*, vol. 59, no. 3, pp. 134–138, 2016.

[10] K. Zhao, E. Lau, K. J. Bozic, M. Kelly, K. Ong, and S. M. Kurtz, "Future Young Patient Demand for Primary and Revision Joint Replacement: National Projections from 2010 to 2030,'' *Clinical Orthopaedics and Related Research®*, vol. 467, no. 10, pp. 2606–2612, 2009.

[11] M. Khan, K. Osman, G. Green, and F. S. Haddad, "The epidemiology of failure in total knee arthroplasty,'' *The Bone & Joint Journal*, vol. 98-B, no. 1_Supple_A, pp. 105–112, 2016.

[12] B. J. McGrory, C. D. Etkin, and D. G. Lewallen, "Comparing contemporary revision burden among hip and knee joint replacement registries,'' *Arthroplasty Today*, vol. 2, no. 2, pp. 83–86., 2016.

[13] Australian Orthopaedic Association National Joint Replacement Registry, "Hip, knee & shoulder arthroplasty - Annual Report 2018,'' pp. 1–444, 2018.

[14] R. Brittain, E. Young, V. Mccormack, and M. Swanson, "National Joint Registry 16th Annual Report,'' no. December 2018, 2019.

[15] J. Kärrholm, M. Mohaddes, D. Odin, J. Vinblad, C. Rogmark, and O. Rolfson, *Swedish Hip Arthroplasty Register Annual Report 2017*. No. September, 2017.

[16] Y. Zhang, A. W. Putnam, A. D. Heiner, J. J. Callaghan, and T. D. Brown, "Reliability of detecting prosthesis/cement interface radiolucencies in total hip arthroplasty,'' *Journal of Orthopaedic Research*, vol. 20, no. 4, pp. 683–687, 2002.

[17] O. S. Hoekstra, G. J. J. Teule, J. Berkhof, O. P. P. Temmerman, I. C. Heyligers, and P. G. H. M. Raijmakers, "Accuracy of diagnostic imaging techniques in the diagnosis of aseptic loosening of the femoral component of a hip prosthesis,'' *The Journal of Bone and Joint Surgery. British volume*, vol. 87-B, no. 6, pp. 781–785, 2005.

[18] H. J. Cooper, A. S. Ranawat, H. G. Potter, L. F. Foo, S. T. Jawetz, and C. S. Ranawat, "Magnetic Resonance Imaging in the Diagnosis and Management of Hip Pain After Total Hip Arthroplasty,'' *Journal of Arthroplasty*, vol. 24, no. 5, pp. 661–667, 2009.

[19] J.-B. Meyer, A. Blum, A. Chanson, A. Raymond, P. Gondim-Teixeira, O. Bakour, M. Louis, and R. Kechidi, "CT of hip prosthesis: New techniques and new paradigms,'' *Diagnostic and Interventional Imaging*, vol. 97, no. 7-8, pp. 725–733, 2016.

[20] O. Awan, L. Chen, and C. S. Resnik, "Imaging evaluation of complications of hip arthroplasty: Review of current concepts and imaging findings,'' *Canadian Association of Radiologists Journal*, vol. 64, no. 4, pp. 306–313, 2013.

[21] O. Roche, M. Louis, A. Blum, J.-B. Meyer, D. Molé, H. Coudane, F. Sirveaux, A. Raymond, E. Gabiache, P. Olivier, D. Mainard, P. Gondim-Teixeira, and M. Grandhaye, "Developments in imaging methods used in hip arthroplasty: A diagnostic algorithm,'' *Diagnostic and Interventional Imaging*, vol. 97, no. 7-8, pp. 735–747, 2016.

[22] O. P. Temmerman, P. G. Raijmakers, W. L. Deville, J. Berkhof, L. Hooft, and I. C. Heyligers, "The Use of Plain Radiography, Subtraction Arthrography, Nuclear Arthrography, and Bone Scintigraphy in the Diagnosis of a Loose Acetabular Component of a Total Hip Prosthesis. A Systematic Review,'' *Journal of Arthroplasty*, vol. 22, no. 6, pp. 818–827, 2007.

[23] L. Claassen, M. Ettinger, C. Plaass, K. Daniilidis, T. Calliess, and M. Ezechieli, "Diagnostic value of bone scintigraphy for aseptic loosening after total knee arthroplasty,'' *Technology and Health Care*, vol. 22, no. 5, pp. 767–773, 2014.

[24] W. J. Oyen, J. A. Lemmens, R. A. Claessens, J. R. van Horn, T. J. Slooff, and F. H. Corstens, "Nuclear arthrography: combined scintigraphic and radiographic procedure for diagnosis of total hip prosthesis loosening,'' *Journal of Nuclear Medicine*, vol. 37, no. 1, pp. 62–70, 1996.

[25] V. Goriainov, R. Cook, J. M. Latham, D. G. Dunlop, and R. O. Oreffo, "Bone and metal: an orthopaedic perspective on osseointegration of metals,'' *Acta Biomaterialia*, vol. 10, no. 10, pp. 4043–4057., 2014.

[26] A. Troelsen, E. Malchau, N. Sillesen, and H. Malchau, "A review of current fixation use and registry outcomes in total hip arthroplasty: the uncemented paradox,'' *Clinical Orthopaedics and related research*, vol. 471, no. 1, pp. 2052–2059, 2013.

[27] N. W. Rydell, *Forces Acting on the Femoral Head-prosthesis - A Study on Strain gauge Supplied Prostheses in Living Persons*. Department of Orthopaedic Surgery, University of Göteborg, 1966.

[28] G. Bergmann, G. N. Duda, J. Dymke, F. Graichen, A. Rohlmann, and P. Damm, "High-Tech Hip Implant for Wireless Temperature Measurements In Vivo,'' *PLoS ONE*, vol. 7, no. 8, pp. 1–7, 2012.

[29] A. Arami, M. Simoncini, O. Atasoy, W. Hasenkamp, S. Ali, A. Bertsch, E. Meurville, S. Tanner, H. Dejnabadi, V. Leclercq, P. Renaud, C. Dehollain, P. A. Farine, B. M. Jolles, K. Aminian, and P. Ryser, "Instrumented prosthesis for knee implants monitoring,'' *IEEE International Conference on Automation Science and Engineering*, pp. 828–835, 2011.

[30] G. Bergmann, F. Graichen, and A. Rohlmann, "Hip joint forces in sheep,'' *Journal of Biomechanics*, vol. 32, no. 8, pp. 769–777., 1999.

[31] F. Graichen, G. Bergmann, and A. Rohlmann, "Hip endoprosthesis for in vivo measurement of joint force and temperature,'' *Journal of Biomechanics*, vol. 32, no. 10, pp. 1113–1117., 1999.

[32] P. Damm, F. Graichen, A. Rohlmann, A. Bendera, and G. Bergmann, "Total hip joint prosthesis for in vivo measurement of forces and moments,'' *Medical Engineering & Physics*, vol. 32, no. 1, pp. 95–100., 2010.

[33] C. Ruther, U. Timm, H. Ewald, W. Mittelmeier, R. Bader, R. Schmelter, A. Lohrengel, and D. Kluess, *Current Possibilities for Detection of Loosening of Total Hip Replacements and How Intelligent Implants Could Improve Diagnostic Accuracy*, pp. 363–386. 2012.

[34] R. Puers, M. Catrysse, G. Vandevoorde, R. J. Collier, E. Louridas, F. Burny, M. Donkerwolcke, and F. Moulart, "Telemetry system for the detection of hip prosthesis loosening by vibration analysis,'' *Sensors and Actuators A: Physical*, vol. 85, no. 1-3, pp. 42–47., 2000.

[35] M. P. Soares dos Santos, J. A. F. Ferreira, A. Ramos, and J. A. O. Simões, "Active orthopaedic implants: towards optimality,'' *Journal of the Franklin Institute*, vol. 352, no. 3, pp. 813–834., 2015.

[36] L. M. Henriques, *Sistema de monitorização capacitivo para implantes ósseos instrumentados*. Master thesis, University of Aveiro, 2018.

[37] M. P. Soares dos Santos, J. Coutinho, A. Marote, B. Sousa, A. Ramos, J. A. F. Ferreira, R. Bernardo, A. Rodrigues, A. T. Marques, O. A. B. da Cruz e Silva, E. P. Furlani, J. A. O. Simões, and S. I. Vieira, "Capacitive technologies for highly controlled and personalized electrical stimulation by implantable biomedical systems,'' *Scientific Reports*, vol. 9, no. 5001, pp. 1–20., 2019.

[38] C. Ruther, H. Nierath, H. Ewald, J. L. Cunningham, W. Mittelmeier, R. Bader, and D. Kluess, "Investigation of an acoustic-mechanical method to detect implant loosening,'' *Medical Engineering & Physics*, vol. 35, no. 11, pp. 1669–1675., 2013.

[39] F. Completo, A. Fonseca, *Fundamentos de Biomecânica Músculo-Esquelética e Ortopédica*. Publindústria, 2011.

[40] S. C. Cowin, *Bone Mechanics Handbook*. CRC Press, 2^{nd} ed., 2001.

[41] T. Bellido, "Osteocyte-Driven Bone Remodeling,'' *Calcified Tissue International*, vol. 94, no. 1, pp. 25–34, 2014.

[42] D. R. Sumner, "Long-term implant fixation and stress-shielding in total hip replacement,'' *Journal of Biomechanics*, vol. 48, no. 5, pp. 797–800., 2015.

[43] G. Henry, *1918. Anatomy of the Human Body*.

[44] C. Gabriel, S. Gabriel, and E. Corthout, "The dielectric properties of biological tissues: III. Parametric models for the dielectric spectrum of tissues,'' *Physics in Medicine and Biology*, vol. 41, no. 11, pp. 2271–2294, 2000.

[45] J. H. Cachão, M. P. Soares, R. Bernardo, A. Ramos, R. Bader, J. A. F. Ferreira, A. T. Marques, and J. A. O. Simões, "Altering the course of technologies to monitor loosening states of endoprosthetic implants,'' *Sensors*, pp. 1–36, 2019.

[46] A. P. Georgiou and J. L. Cunningham, "Accurate diagnosis of hip prosthesis loosening using a vibrational technique,'' *Clinical Biomechanics*, vol. 16, no. 4, pp. 315–323., 2001.

[47] A. A. Alshuhri, T. P. Holsgrove, A. W. Miles, and J. L. Cunningham, "Development of a non-invasive diagnostic technique for acetabular component loosening in total hip replacements,'' *Medical Engineering & Physics*, vol. 37, no. 8, p. 739–745., 2015.

[48] A. A. Alshuhri, T. P. Holsgrove, A. W.Miles, and J. L.Cunningham, "Non-invasive vibrometry-based diagnostic detection of acetabular cup loosening in total hip replacement (THR),'' *Medical Engineering & Physics*, vol. 48, pp. 188–195., 2017.

[49] J. S. Rieger, S. Jaeger, C. Schuld, J. P. Kretzer, and R. G. Bitsch, "A vibrational technique for diagnosing loosened total hip endoprostheses: An experimental saw-bone study,'' *Medical Engineering & Physics*, vol. 35, no. 3, pp. 329–337., 2013.

[50] J. S. Rieger, S. Jaeger, J. P. Kretzer, R. Rupp, and R. G. Bitsch, "Loosening detection of the femoral component of hip prostheses with extracorporeal shockwaves: A pilot study,'' *Medical Engineering & Physics*, vol. 37, no. 2, pp. 157–164., 2015.

[51] M. Lannocca, E. Varini, A. Cappello, L. Cristofolini, and E. Bialoblocka, "Intra-operative evaluation of cementless hip implant stability:a prototype device based on vibration analysis,'' *Medical Engineering & Physics*, vol. 29, no. 8, pp. 886–894., 2007.

[52] E. Varini, E. Bialoblocka-Juszczyk, M. Lannocca, A. Cappello, and L. Cristofolini, "Assessment of implant stability of cementless hip prostheses through the frequency response function of the stem–bone system,'' *Sensors and Actuators A: Physical*, vol. 163, no. 2, p. ., 2010.

[53] L. C. Pastrav, S. V. N. Jaecques, I. Jonkers, G. V. der Perre1, and M. Mulier, "In vivo evaluation of a vibration analysis technique for the per-operative monitoring of the fixation of hip prostheses,'' *Journal of Orthopaedic Surgery and Research*, vol. 4, no. 10, pp. 1–10., 2009.

[54] C.-C. Jiang, J.-H. Lee, and T.-T. Yuan, "Vibration arthrometry in the patients with failed total knee replacement,'' *IEEE Transactions on Biomedical Engineering*, vol. 47, no. 2, pp. 219–227., 2000.

[55] C. Ruther, U. Timm, A. Fritsche, H. Ewald, W. Mittelmeier, R. Bader, and D. Kluess, *A New Approach for Diagnostic Investigation of Total Hip Replacement Loosening*, pp. 74–79. 2013.

[56] D. Glaser, R. D. Komistek, H. E. Cates, and M. R. Mahfouz, "A non-invasive acoustic and vibration analysis technique for evaluation of hip joint conditions,'' *Journal of Biomechanics*, vol. 43, no. 3, pp. 426–432, 2010.

[57] C. Ruther, C. Schulze, A. Boehme, H. Nierath, H. Ewald, W. Mittelmeier, R. Bader, and D. Kluess, "Investigation of a passive sensor array for diagnosis of loosening of endoprosthetic implants,'' *Sensors*, vol. 13, no. 1, pp. 1–20., 2013.

[58] G. Qi, W. P. Mouchon, and T. E. Tan, "How much can a vibrational diagnostic tool reveal in total hip arthroplasty loosening?,'' *Clinical Biomechanics*, vol. 18, no. 5, pp. 444–458., 2003.

[59] P. L. S. Li, N. B. Jones, and P. J. Gregg, "Vibration analysis in the detection of total hip prosthetic loosening,'' *Medical Engineering & Physics*, vol. 18, no. 7, pp. 596–600., 1996.

[60] A. D. Rosenstein, G. F. McCoy, C. J. Bulstrode, P. D. McLardy-Smith, J. L. Cunningham, and A. R. Turner-Smith, "The differentiation of loose and secure femoral implants in total hip replacement using a vibrational technique: an anatomical and pilot clinical study,'' *Proceedings of the Institution of Mechanical Engineers, Part H: Journal of Engineering in Medicine*, vol. 203, no. 2, pp. 77–81., 1989.

[61] A. Rowlands, F. A. Duck, and J. L. Cunningham, "Bone vibration measurement using ultrasound: Application to detection of hip prosthesis loosening,'' *Medical Engineering & Physics*, vol. 30, no. 3, pp. 278–284., 2008.

[62] S. Leuridan, Q. Goossens, T. V. Sloten, K. D. Landsheer, H. Delport, L. Pastrav, K. Denis, W. Desmet, and J. V. Sloten, "Vibration-based fixation assessment of

tibial knee implants: A combined in vitro and in silico feasibility study,'' *Medical Engineering & Physics*, vol. 49, pp. 109–120., 2017.

[63] A. Arami, J.-R. Delaloye, H. Rouhani, B. M. Jolles, and K. Aminian, "Knee implant loosening detection: A vibration analysis investigation,'' *Annals of Biomedical Engineering*, vol. 46, no. 1, pp. 97–107., 2018.

[64] U. Marschner, H. Grätz, B. Jettkant, D. Ruwisch, G. Woldt, W. J. Fischer, and B. Clasbrummel, "Integration of a wireless lock-in measurement of hip prosthesis vibrations for loosening detection,'' *Sensors and Actuators A: Physical*, vol. 156, no. 1, pp. 145–154., 2009.

[65] S. Sauer, U. Marschner, H. Gratz, and W.-J. Fischer, "Medical wireless vibration measurement system for hip prosthesis loosening detection,'' in *Proceedings of the Third International Conference on Sensor Device Technologies and Applications Applications (SENSORDEVICES 2012)*, pp. 9–13., 2012.

[66] M. A. Pérez and B. Seral-Garcia, "A finite element analysis of the vibration behaviour of a cementless hip system,'' *Computer Methods in Biomechanics and Biomedical Engineering*, vol. 16, 2013.

[67] M. P. Soares dos Santos, A. Marote, T. Santos, J. Torrão, A. Ramos, J. A. O. Simões, O. A. B. da Cruz e Silva, E. P. Furlani, S. I. Vieira, and J. A. F. Ferreira, "New cosurface capacitive stimulators for the development of active osseointegrative implantable devices,'' *Scientific Reports*, vol. 6, no. 30231, pp. 1–15., 2016.

[68] A. C. Unger, H. Cabrera-Palacios, A. P. Schulz, C. Jürgens, and A. Paech, "Acoustic monitoring (rfm) of total hip arthroplasty results of a cadaver study,'' pp. 264–271, 1998.

[69] Q. Goossens, S. Leuridan, P. Henyš, J. Roosen, L. Pastrav, M. Mulier, W. Desmet, K. Denis, and J. Vander Sloten, "Development of an acoustic measurement protocol to monitor acetabular implant fixation in cementless total hip Arthroplasty: A preliminary study,'' *Medical Engineering and Physics*, vol. 49, pp. 28–38, 2017.

[70] D. Glaser, R. D. Komistek, H. E. Cates, and M. R. Mahfouz, "Clicking and squeaking: In vivo correlation of sound and separation for different bearing surfaces,'' *Journal of Bone and Joint Surgery - Series A*, vol. 90, no. SUPPL. 4, pp. 112–120, 2008.

[71] H. Ewald, U. Timm, R. Bader, and D. Kluess, "Acoustic sensor system for loosening detection of hip implants,'' *2011 Fifth International Conference on Sensing Technology*, pp. 494–497, 2011.

[72] H. Ewald, C. Ruther, W. Mittelmeier, and R. Bader, "A novel in vivo Sensor for Loosening Diagnostics in Total Hip Replacement,'' *2011 IEEE SENSORS Proceedings*, pp. 89–92, 2011.

[73] P. G. Reinhall, S. K. Benirschke, M. C. Dahl, R. P. Ching, P. A. Kramer, and S. T. Hansen, "The efficacy of using vibrometry to detect osteointegration of the Agility total ankle,'' *Journal of Biomechanics*, vol. 43, no. 9, pp. 1840–1843, 2010.

[74] J. P. Davies, M. K. Tse, and W. H. Harris, "Monitoring the integrity of the cement-metal interface of total joint components in vitro using acoustic emission and ultrasound,'' *Journal of Arthroplasty*, vol. 11, no. 5, pp. 594–601, 1996.

[75] A. Roques, M. Browne, J. Thompson, C. Rowland, and A. Taylor, "Investigation of fatigue crack growth in acrylic bone cement using the acoustic emission technique,'' *Biomaterials*, vol. 25, no. 5, pp. 769–778, 2004.

[76] G. Qi, J. Li, K. A. Mann, W. P. Mouchon, M. A. Hamstad, A. Salehi, and S. A. Whitten, "3D real time methodology monitoring cement failures in THA,'' 2004.

[77] N. Gueiral and E. Nogueira, "Acoustic Emission Studies in Hip Arthroplasty – Peak Stress Impact In Vitro Cemented Prosthesis,'' 2005.

[78] M. Mavrogordato, M. Taylor, A. Taylor, and M. Browne, "Medical Engineering & Physics Real time monitoring of progressive damage during loading of a simplified total hip stem construct using embedded acoustic emission sensors,'' *Medical Engineering and Physics*, vol. 33, no. 4, pp. 395–406, 2011.

[79] J. P. Davies, M. K. Tse, and W. H. Harris, "In vitro evaluation of bonding of the cement-metal interface of a total hip femoral component using ultrasound,'' *Journal of Orthopaedic Research*, vol. 13, no. 3, pp. 335–338, 1995.

[80] W. Rodgers, R. Welsh, L. J. King, A. J. Fitzpatrick, T. B. F. Wood, and G. J. Hooper, "Signal processing and event detection of hip implant acoustic emissions,'' *Control Engineering Practice*, vol. 58, no. May 2016, pp. 287–297, 2017.

[81] A. J. Fitzpatrick, G. W. Rodgers, G. J. Hooper, and T. B. F. Woodfield, "Biomedical Signal Processing and Control Development and validation of an acoustic emission device to measure wear in total hip replacements in-vitro and in-vivo,'' *Biomedical Signal Processing and Control*, vol. 33, pp. 281–288, 2017.

[82] P. Arpaia, F. Clemente, and A. Zanesco, "Low-invasive diagnosis of metallic prosthesis osseointegration by electrical impedance spectroscopy,'' *IEEE Transactions on Instrumentation and Measurement*, vol. 56, no. 3, pp. 784–789, 2007.

[83] P. Arpaia, F. Clemente, and C. Romanucci, "In-vivo test procedure and instrument characterization for eis-based diagnosis of prosthesis osseointegration,'' in *2007 IEEE Instrumentation & Measurement Technology Conference IMTC 2007*, pp. 1–6, IEEE, 2007.

[84] C. Ruther, H. Ewald, W. Mittelmeier, A. Fritsche, R. Bader, and D. Kluess, "A novel sensor concept for optimization of loosening diagnostics in total hip replacement,'' *Journal of biomechanical engineering*, vol. 133, no. 10, p. 104503, 2011.

[85] A. R. Burton, P. Sun, and J. P. Lynch, "Bio-compatible wireless inductive thin-film strain sensor for monitoring the growth and strain response of bone in osseointegrated prostheses,'' *Structural Health Monitoring*, pp. 1 – 19, 2019.

[86] K. C. McGilvray, E. Unal, K. L. Troyer, B. G. Santoni, R. H. Palmer, J. T. Easley, H. V. Demir, and C. M. Puttlitz, "Implantable microelectromechanical sensors for

diagnostic monitoring and post-surgical prediction of bone fracture healing,'' *Journal of Orthopaedic Research*, vol. 33, no. 10, pp. 1439–1446, 2015.

[87] Analog Devices. 24-Bit Capacitance-to-Digital Converterwith Temperature Sensor, 2005. Available at: `https://docs-emea.rs-online.com/webdocs/0e38/0900766b80e38fa6.pdf`.

[88] W. Mittelmeier, S. Lehner, W. Kraus, H. P. Matter, L. Gerdesmeyer, and E. Steinhauser, "BISS: Concept and biomechanical investigations of a new screw system for electromagnetically induced internal osteostimulation,'' *Archives of Orthopaedic and Trauma Surgery*, vol. 124, no. 2, pp. 86–91, 2004.

[89] Y. Su, R. Souffrant, D. Kluess, M. Ellenrieder, U. van Rienen, W. Mittelmeier, and R. Bader, "Changes of the electric field distribution in the femoral head due to position and design of an electro-stimulating implant,'' *Biomed Tech*, vol. 58, pp. 177–178, 2013.

[90] P. C. Grunert, A. Jonitz-Heincke, Y. Su, R. Souffrant, D. Hansmann, H. Ewald, A. Krüger, W. Mittelmeier, and R. Bader, "Establishment of a Novel In Vitro Test Setup for Electric and Magnetic Stimulation of Human Osteoblasts,'' *Cell Biochemistry and Biophysics*, vol. 70, no. 2, pp. 805–817, 2014.

Appendices

Appendix A

Monitoring technologies analysis tables

Table A.1: ***Technology features based on the vibrometric approach for cementless fixations.***[a]

	Refs.	Input	Output	Components and location	Detection algorithm	Monitoring ability	*In vitro* validation	*In vivo* validation	Periodicity
Method 1	Georgiou and Cunningham [46]	Mechanical vibration (<1 kHz)	Mechanical vibration	Shaker: knee; accelerometer: hip	Number of harmonics and amplitudes	Location: ND; States: loose or secure	—	23 patients	Limited to laboratory
	Alshuri *et al.* [47,48]	Mechanical vibration (100-1500 Hz)	Mechanical vibration	Shaker: femoral lateral condyle; 2 accelerometers: iliac crest and greater trochanter	Harmonic ratios	Location: ND; States: secure and 2 loosening states	3 composite hemi-pelvis; a Sawbones femur	—	Limited to laboratory
	Rieger *et al.* [49]	Mechanical vibration (100-2000 Hz)	Mechanical vibration	Shaker: knee; 3 accelerometers: medial condyle, greater trochanter, ilium's crest	Frequency shifts	Location: ND; States: loose or secure	Sawbone femur and hip	—	Limited to laboratory
	Rieger *et al.* [50]	Mechanical shockwaves	Mechanical vibration	piezoelectric atuators: lateral knee condyle, greater trochanter, ilium crest; 3 accelerometers: same locations	Frequency shifts	Location: ND; States: loose or secure	3 human hip specimens	—	Limited to laboratory
	Lannocca *et al.* [51]; Varini *et al.* [52]	Mechanical vibration (1.2-2 kHz)	Mechanical vibration	Piezoelectric actuator: device; accelerometer: greater trochanter	Frequency shifts	Location: ND; States: stable or unstable	5 femurs[b]	—	Intra-operatively
	Lannocca *et al.* [51]; Varini *et al.* [52]	Mechanical vibration (1.2-2 kHz)	Mechanical vibration	Piezoelectric actuator: device; LVDT: greater trochanter	Micro-motions	Location: ND; States: stable or unstable	9 femurs[b]	—	Intra-operatively
	Pastrav *et al.* [53]	Mechanical vibration (<10 kHz)	Mechanical vibration	Shaker: prosthesis neck; mechanical impedance head: prosthesis neck	Frequency shifts	Location: ND; States: stable or unstable	—	30 patients	Intra-operatively
	Jiang, Lee and Yuan [54]	Flexion-extension motion	Mechanical vibration	isokinetic dynamometer: leg (tibia); accelerometer: patella;	Spectral power ratios	Location: ND; States: loose or secure	—	14 patients	Limited to laboratory
Method 2	Ruther *et al.* [38,55]	Magnetic induction (70Hz)	Mechanical vibration	Magnetic oscilator: inside the implant (porcine ulna); Coil: 30 mm apart of the implant; accelerometer: porcine foreleg	Frequency shifts; central frequencies; transient periods	Location: ND; States: secure and 2 loosening states	7 porcine foreleg	—	Limited to laboratory
Method 3	Glaser *et al.* [56]	Implat motion	Mechanical vibration	Two accelerometers: greater trochanter and iliac spine	Output signal high frequency and amplitude	Location: ND; States: different loosening states	—	5 patients	Limited to laboratory

[a] Terminology: ND - not described;

[b] Lannocca *et al.* [51] provided experimental results using four composite femurs; Varini *et al.* [52] presented validations results using 5 femurs (4 cadaveric and 1 composite).

Table A.2: ***Technology features based on the vibrometric approach for cemented fixations.***[a]

	Refs.	Input	Output	Components and location	Detection algorithm	Monitoring ability	*In vitro* validation	*In vivo* validation	Periodicity
Method 1	Li, Jones and Gregg [59]	Mechanical vibration (100-1200 Hz)	Mechanical vibration	Shaker: distal femur; two accelerometers: distal and proximal femur	Frequency shifts and number of harmonics	Location: ND; State: secure or loose	54 models[b]	—	Limited to laboratory
	Rosenstein *et al.* [60]	Mechanical vibration (100-1000 Hz)	Mechanical vibration	Shaker: lateral condyle; accelerometer: greater trochanter	Number of harmonics	Location: ND; State: Secure or loose	5 femurs	11 patients[c]	Limited to laboratory
	Rowlands, Duck and Cunningham [61]	Mechanical vibration (100-1500 Hz)	Mechanical vibration	Vibrator: distal femur; accelerometer: greater trochanter	Harmonic ratios	Location: ND; States: secure or loose	Sawbone femur and Tufnol tubing	—	Limited to laboratory
	Leuridan *et al.* [62]	Mechanical vibration	Mechanical vibration	Impact hammer: tibial plate; accelerometers: femur's surface and tibial plate	Frequency response function of the output signal	Location: ND; States: secure and 3 loosening stages	5 artificial femurs	—	Limited to laboratory
	Arami *et al.* [63]	Mechanical vibration (30-3000 Hz)	Mechanical vibration	Accelerometer and vibrator: 10 cm below the patella; two accelerometers: fixed to the tibial plate	Appearance of a new peak in the output signal[d]	Location: ND; State: Secure or loose	14 lower limbs specimens and 14 cadavers	—	Limited to laboratory
Method 2	Puers *et al.* [34]	Mechanical vibration (100-200 Hz)	Mechanical vibration	Shaker: distal femur; accelerometer: implant's femoral head	Non-similarity between the input and output signal	Location: ND; State: Secure or loose	1 cadaver	—	Limited to laboratory
	Marschner *et al.* [64]	Mechanical vibration (500-2500 Hz)	Mechanical vibration	Shaker: distal femur; 2 accelerometers: distal end of stem	Shifts in the output resonance frequency (≈300 Hz)	Location: ND; State: proximally loose and proximally secure	1 artificial femur	—	Limited to laboratory
	Sauer *et al.* [65]	Mechanical vibration (500-2500 Hz)	Mechanical vibration	Shaker: central femur; accelerometer: implant's femoral head	Shifts in the output resonance frequency (20-100 Hz)	Location: ND; State: three loosening states	Artificial femur	—	Limited to laboratory

[a] Terminology: ND - not described;

[b] Twenty-one of the secure specimens, seventeen of loose and 16 of early loosening;

[c] Seven of these were admitted to a revision surgery and four had done a primary total hip replacement two weeks previously;

[d] In the 750-900 Hz range

Table A.3: ***Technology features based on the acoustic approach for cementless fixations.*** [a]

	Refs.	Input	Output	Components and location	Detection algorithm	Monitoring ability	*In vitro* validation	*In vivo* validation	Periodicity
Method 1	Alshuri *et al.* [47, 48]	Mechanical vibration (100-1500 Hz)	Acoustic waves	Shaker: femoral lateral condyle; ultrasound probe: iliac crest	Harmonic ratios	Location: ND; States: secure and 2 loosening states	3 composite hemi-pelvis; a Sawbones femur	—	Limited to laboratory
	Ünger *et al.* [68]	Mechanical vibration	Acoustic waves	Metallic object: implant surface; microphone: lateral femoral condyle	Shifts in the output frequency	Location: ND; States: different loosening stages	1 cadaver	—	Limited to laboratory
	Goosens *et al.* [69]	Mechanical vibration	Acoustic waves	Hammer; microphone: 20 cm above the experimental setup	Shifts in the output frequency	Location: ND; States: Different loosening stages	Artificial bone block; artificial pelvis; and cadaveric pelvis	—	Limited to laboratory
Method 2	Glaser *et al.* [56, 70]	Implant's motion	Acoustic waves	Acoustic transducer: hip's skin surface	Output signal high frequency and amplitude	Location: ND; States: different loosening stages	—	29 patients[b]	Limited to laboratory
Method 3	Ewald *et al.* [71, 72]	Magnetic induction	Acoustic waves	Extracorporeal coil; microphone; oscillators: stem walls	Shifts in the output frequency	Location: ND; States: secure and 3 loosening stages	Bench top test simulating different tissues layers	—	Limited to laboratory

[a]Terminology: ND - not described; [b]24 patients in one study [70], 5 in the other [56] ;

Table A.4: ***Technology features based on the acoustic approach for cemented fixations.***[a]

	Refs.	Input	Output	Components and location	Detection algorithm	Monitoring ability	*In vitro* validation	*In vivo* validation	Periodicity
Method 1	Rowlands, Duck and Cunningham [61]	Mechanical vibration (100-1500 Hz)	Acoustic waves	Vibrator: distal femur; ultrasound probe: proximal femur	Harmonic ratios	Location: ND; States: different loosening stages	Sawbone femur and tufnol tubing	—	Limited to laboratory
	Unger *et al.* [68]	Mechanical vibration	Acoustic waves	Hammer: femoral condyle; microphone: hip	Shifts in the resonance frequency	Location: ND; States: loose or secure	1 cadaver	—	Limited to laboratory
	Dahl *et al.* [73]	Mechanical vibration	Acoustic waves	Electromagnetic actuator: extracorporeal; Ultrasound probe: surface	Presence of harmonics and shifts in the output frequency	Location: ND; States: loose or secure	Cadaver ankle	—	Limited to laboratory
Method 2	Davies *et al.* [74]	Cement degradation and debonding	Acoustic waves	Acoustic emission transducer: femur's surface	Acoustic emission intensity and output signal waveform	Location: ND; States: several loosening stages	Artificial femur (fatigue test - 4 MPa at 2 Hz)	—	Limited to laboratory
	Roques *et al.* [75]	Cement cracks	Acoustic waves	Two accelerometers: material's surface	Acoustic emissions energy and signal duration	Location: could detect; States: different interface states	Cement blocks specimens (fatigue and 4 point bending tests)	—	Limited to laboratory
	Qi *et al.* [76]	Cement cracks	Acoustic waves	Eight acoustic sensors: femur's surface	Acoustic events character-istics	Location: could detect; States: different interface states	Sawbones femur (fatigue test)	—	Limited to laboratory
	Gueiral and Nogueira [77]	Cement cracks	Acoustic waves	Three acoustic sensors: femur's surface	Bursts of acoustic emissions	Location: could detect; States: different interface states	Sawbones femur (fatigue test)	—	Limited to laboratory
	Mavrogordato *et al.* [78]	Cement cracks	Acoustic waves	Acoustic sensors: externally placed	Output signal's high energy and short rise time	Location: could detect; States: different interface states	Tufnol tubing	—	Limited to laboratory
Method 3	Mavrogordato *et al.* [78]	Cement cracks	Acoustic waves	Acoustic sensors: embedded in the stem	Output signal's high energy and short rise time	Location: could detect; States: different interface states	Tufnol tubing	—	Limited to laboratory
Method 4	Davies, Tse and Harris [79]	Acoustic emission	Acoustic waves	Specimen surface[b]	Amplitude and time of arrival of the reflected wave	Location: ND; States: bonded or debonded	Cement slab, artificial and cadaver femurs	—	Limited to laboratory

[a] Terminology: ND - not described;

[b] Cement slab, artificial and cadaver femur;

Table A.5: *Technology features based on the biolectrical impedance approach for cementless fixations.*[a]

	Refs.	Input	Output	Components and location	Detection algorithm	Monitoring ability	*In vitro* validation	*In vivo* validation	Periodicity
Method 1	Arpaia *et al.* [82, 83]	Voltage (Sinusoidal: 10-100 mV)	Biolectrical impedance	Location: skin surface, near the implant	Variation of impedance	Location: ND; Secure or loose	Cow long bone	3 patients with percutaneous implants	Limited to laboratory

[a] Terminology: ND - not described;

Table A.6: *Technology features based on the magnetic induction approach for cementless fixations.* [a]

	Refs.	Input	Output	Components and location	Detection algorithm	Monitoring ability	*In vitro* validation	*In vivo* validation	Periodicity
Method 1	Ewald *et al.* [71]	Magnetic induction	Magnetic induction	Coil: extracorporeally; piezo-crystal: inside the implant	Difference in the output signal amplitude	Location: ND; States: Secure and different states of loosening	Artificial bone	—	Limited to Laboratory
	Rüther *et al.* [84]	Magnetic induction	Magnetic induction	Coils: extracorporeally; oscillators: inside the implant	Different oscillator velocity[b]	Location: ND; Secure and different states of loose	Test bench apparatus	—	Limited to laboratory

[a] Terminology: ND - not described;

[b] Translated into an induced voltage;

Table A.7: *Technology features based on the strain approach for cementless fixations.*[a]

	Refs.	Input	Output	Components and location	Detection algorithm	Monitoring ability	*In vitro* validation	*In vivo* validation	Periodicity
Method 1	Burton, Sun and Lynch [85]	Mechanical load	Strain	Circuit: Wrapped around the bone surface	Shifts in the output resonance frequency	Location: ND; States: Several deformation stages (axial and radial)	Polyurethane femur model	—	Limited to laboratory
Method 2	McGilvray *et al.* [86]	Mechanical load	Strain	Fixation plate: along the femur; sensor: center of the fixation plate	Shifts in the output resonance frequency	Location: ND; States: Secure and different loosening stages	Ovine osteotomy	14 Sheep (ovine)	Limited to Laboratory

[a]Terminology: ND - not described;

Table A.8: *Technology features based on the capacitive approach for cementless fixations.* [a]

	Refs.	Input	Output	Components and location	Detection algorithm	Monitoring ability	*In vitro* validation	*In vivo* validation	Periodicity
Method 1	Henriques [36]	Dielectric alterations	Capacitance	Inside the implant	Changes in capacitance	Location: ND; Secure or loose	Porcine, bovine and lamb bone samples	—	Limited to laboratory

[a] Terminology: ND - not described;

Intentionally blank page.

Appendix B

Additional results

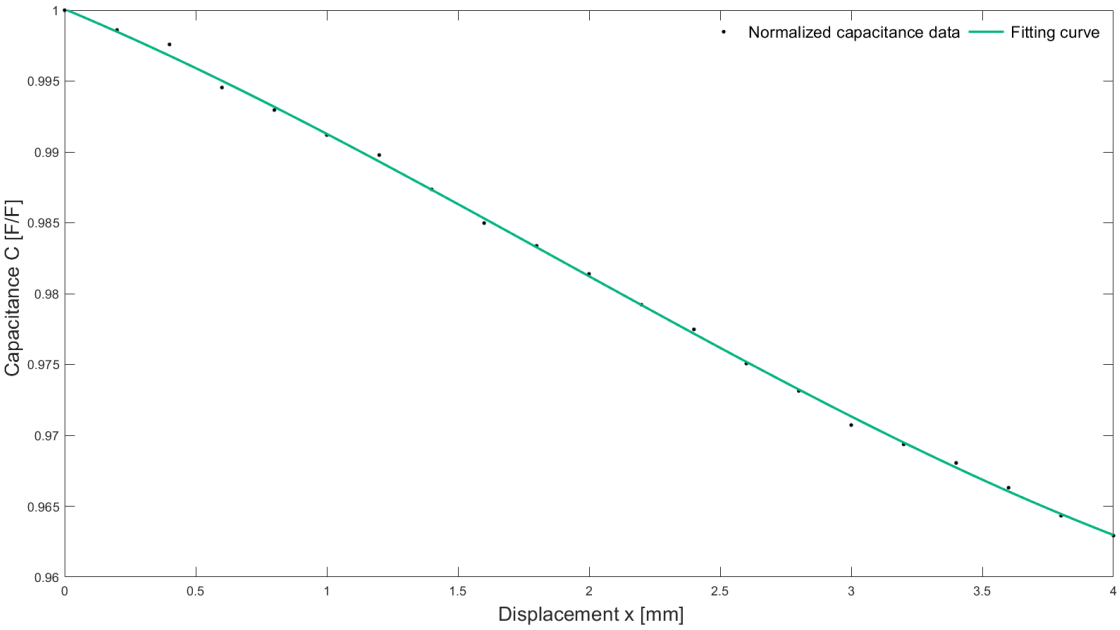

Figure B.1: Curve fitting regarding the normalized mean of the compression cycle. The curve expression and parameters are given in Equation 6.1.

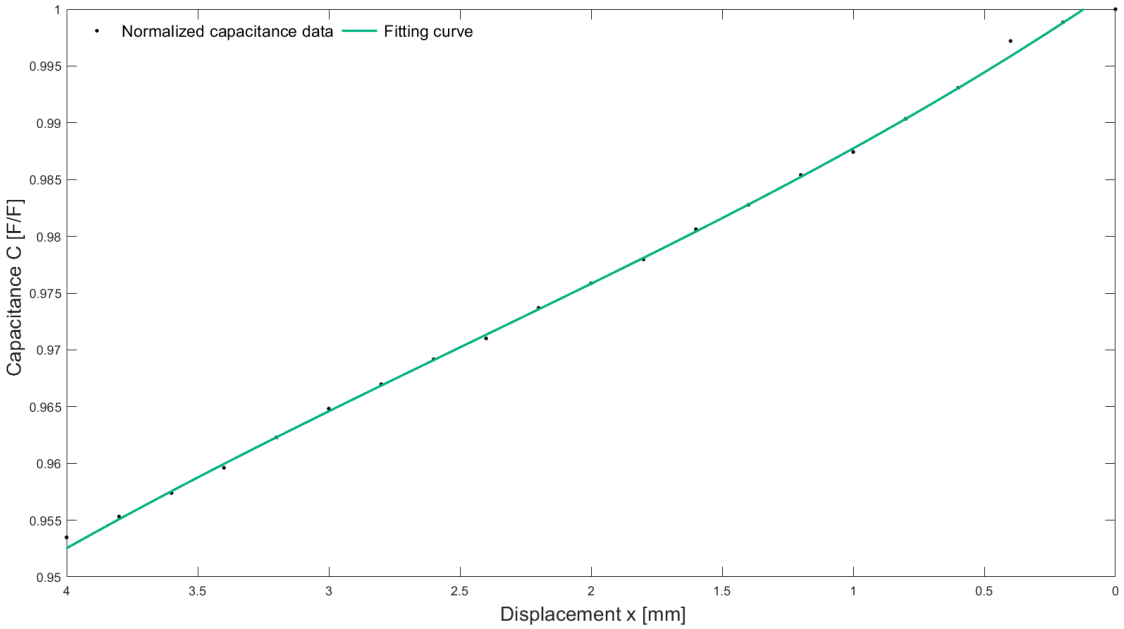

Figure B.2: Curve fitting regarding the normalized mean of the decompression cycle. The curve expression and parameters are given in Equation 6.1.

Appendix C

Technical drawings

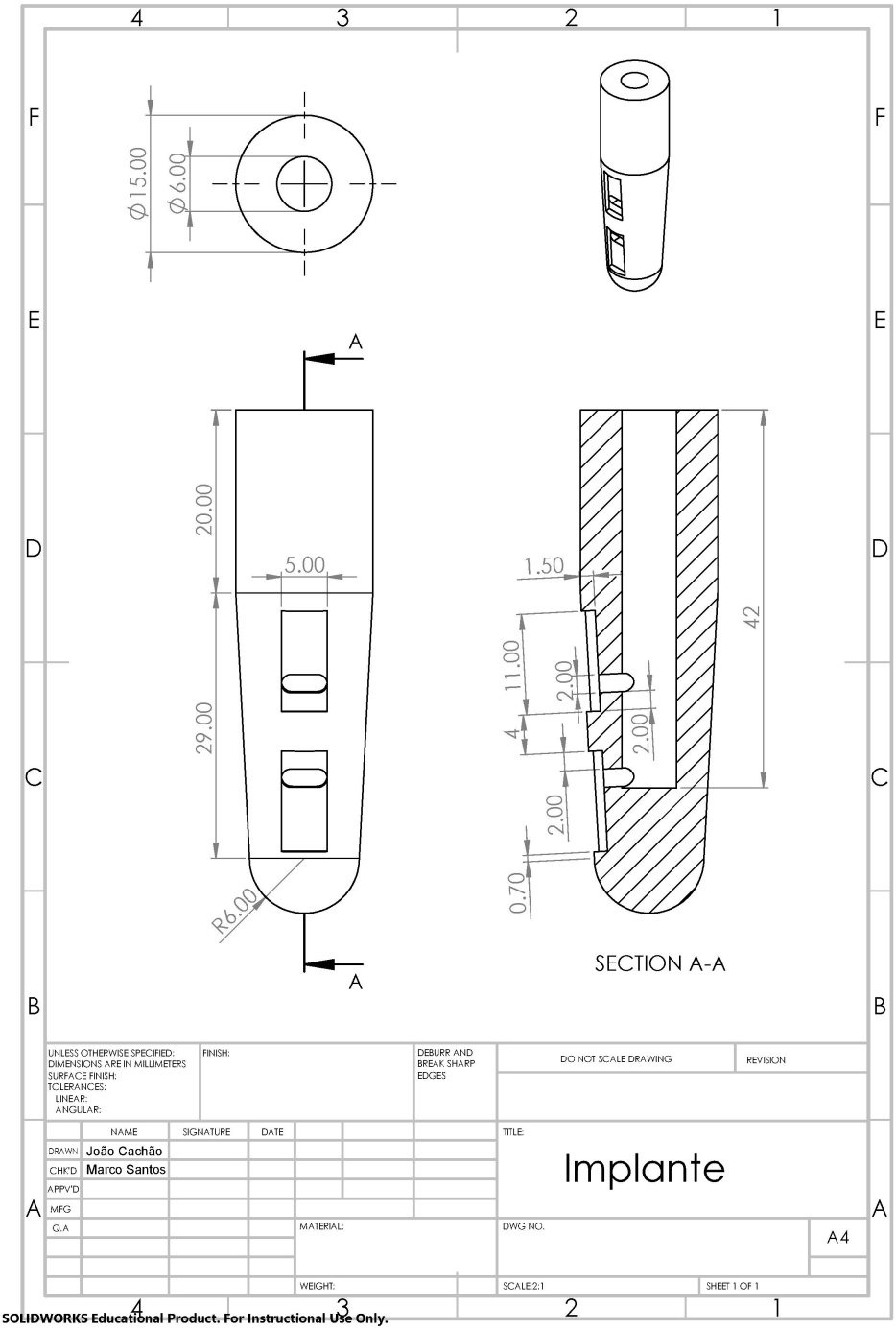

Figure C.1: Technical drawing of the implant used for implantation in the porcine specimens, housing the two sensors.

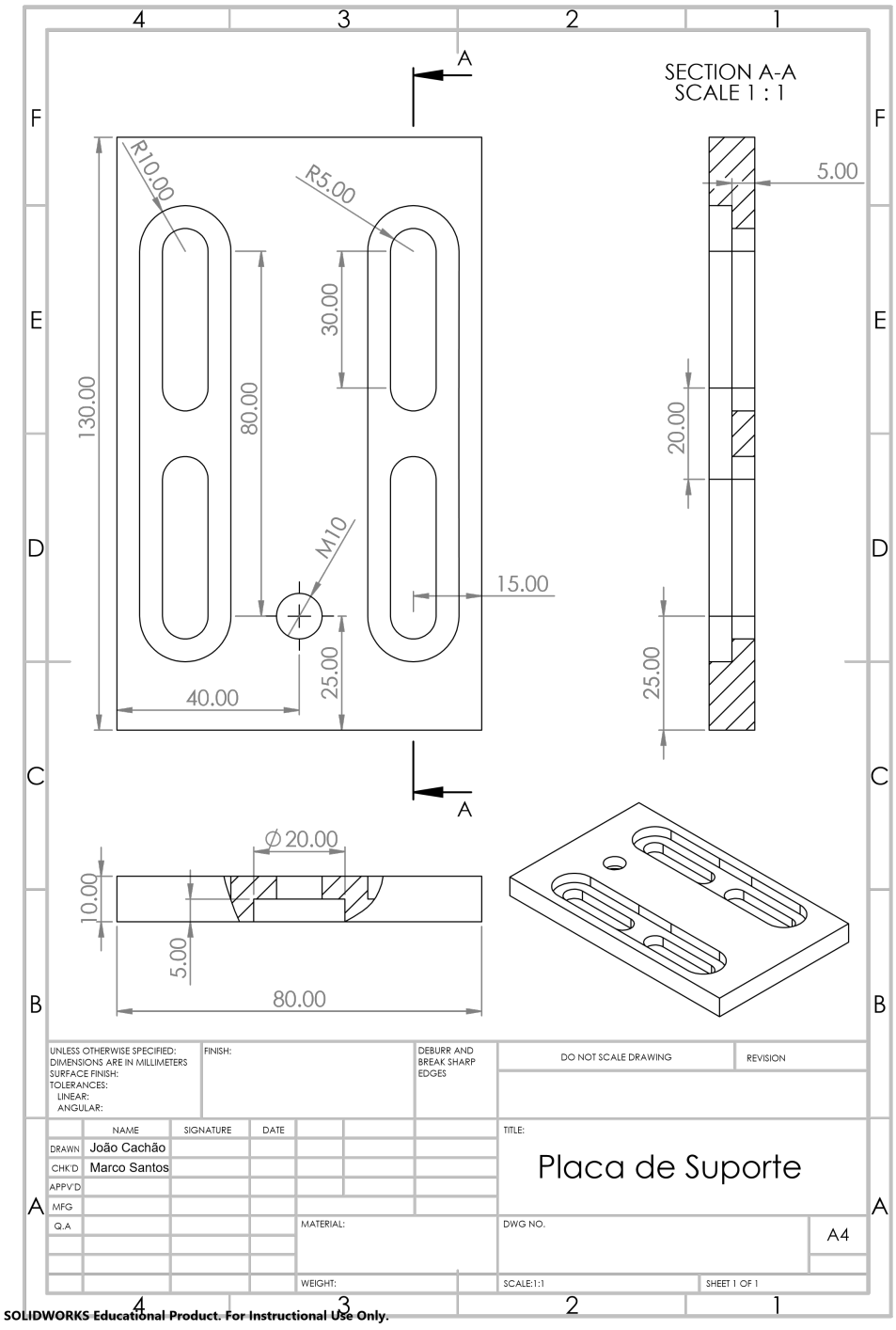

Figure C.2: Technical drawing of the support plate for holding the porcine specimens during the loading test. Note: the second hole meant to fixate the U shaped plate was added post-fabrication of the support plate and thus is not featured in this technical drawing.

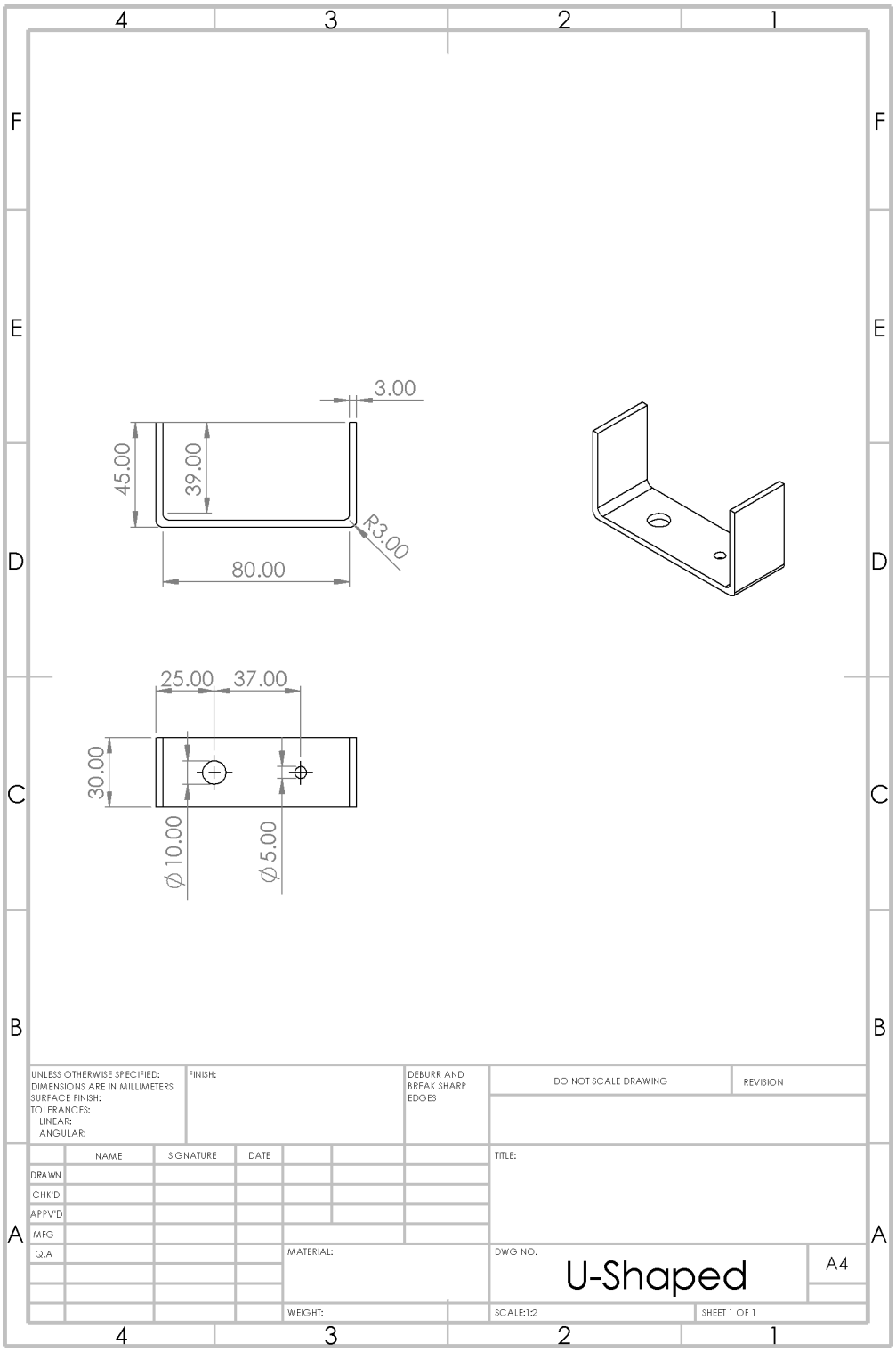

Figure C.3: Technical drawing of the U-shaped plate used in the experimental setup with the support platform.

Annex A

Tissues electrical properties

Tissue type	ε_∞	$\Delta\varepsilon_1$	τ_1 (ps)	α_1	$\Delta\varepsilon_2$	τ_2 (ns)	α_2	$\Delta\varepsilon_3$	τ_3 (μs)	α_3	$\Delta\varepsilon_4$	τ_4 (ms)	α_4	σ
Blood	4.0	56.0	8.38	0.10	5200	132.63	0.10	0.0			0.0			0.7000
Bone (cancellous)	2.5	18.0	13.26	0.22	300	79.58	0.25	2.0×10^4	159.15	0.20	2.0×10^7	15.915	0.00	0.0700
Bone (cortical)	2.5	10.0	13.26	0.20	180	79.58	0.20	5.0×10^3	159.15	0.20	1.0×10^5	15.915	0.00	0.0200

(a)

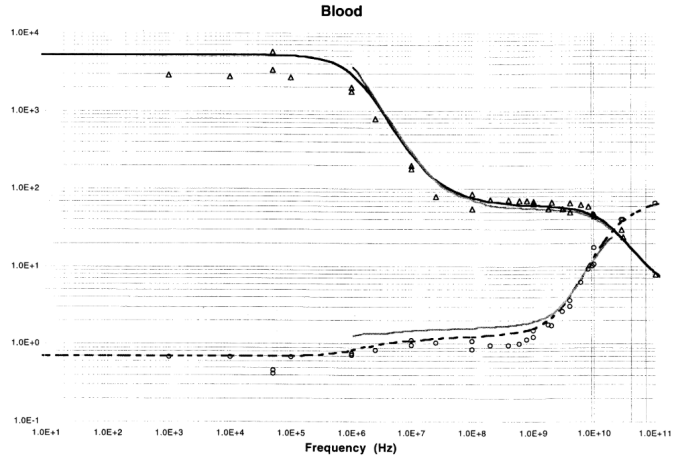

(b)

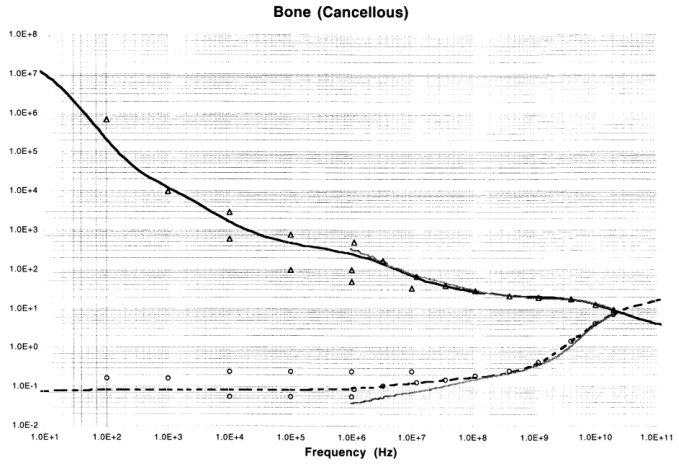

(c)

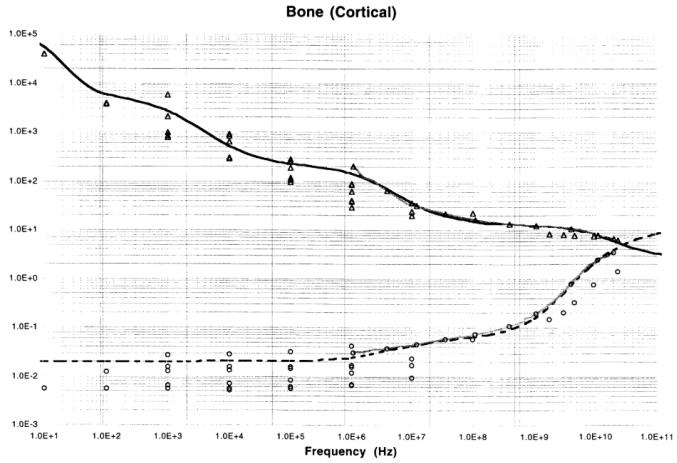

(d)

Figure A.1: Electrical properties of blood, cancellous and cortical bone, taken from Gabriel, Lau and Gabriel [44]. By referring to Equation 2.2 and using the values provided on Table (a) one can obtain the values from permittivity and conductivity. Graphics (b,c,d) refer to the permittivity (filled lines) and conductivity (dotted lines) in function of the applied frequency for blood, cancellous and cortical bone, respectively.